

THE STRUCTURE DETERMINATION OF
SOME DI-(TERTIARY ARSINE) DERIVATIVES
OF METAL CARBONYLS

by

PAUL J. ROBERTS

B.Sc. (Hon.), University of British Columbia, 1967

A THESIS SUBMITTED IN PARTIAL FULFILLMENT OF
THE REQUIREMENTS FOR THE DEGREE OF
DOCTOR OF PHILOSOPHY

in the Department

of

Chemistry

We accept this thesis as conforming to the
required standard

THE UNIVERSITY OF BRITISH COLUMBIA

November, 1970

In presenting this thesis in partial fulfilment of the requirements for an advanced degree at the University of British Columbia, I agree that the Library shall make it freely available for reference and study. I further agree that permission for extensive copying of this thesis for scholarly purposes may be granted by the Head of my Department or by his representatives. It is understood that copying or publication of this thesis for financial gain shall not be allowed without my written permission.

Department of Chemistry

The University of British Columbia
Vancouver 8, Canada

Date November 16, 1970

ABSTRACT

Supervisor: Professor James Trotter

The structures of four di-(tertiary arsine) derivatives of metal carbonyls have been determined by a selection of direct, Patterson, and Fourier methods, applied to Mo-K_α diffractometer data.

1,2- bis(dimethylarsino)tetrafluorocyclobutene-tri-iron decacarbonyl, $\text{Me}_2\text{AsC}=\text{C}(\text{AsMe}_2)\text{CF}_2\text{CF}_2 \cdot \text{Fe}_3(\text{CO})_{10}$, crystallizes in the monoclinic space group $P2_1/c$, with $a = 11.60$, $b = 20.04$, $c = 22.11 \text{ \AA}$, $\beta = 93.7^\circ$, $Z = 8$ (two molecules per asymmetric unit). The structure was refined by least-squares procedures (a total of 74 atoms) to a final R of 0.09 for 2524 observed (of a total of 3234) reflections. The molecule is best described as a derivative of $\text{Fe}_3(\text{CO})_{12}$, in which one terminal carbonyl group on each of the two equivalent iron atoms is replaced by an arsenic atom of the di-(tertiary arsine) ligand. The central Fe_3As_2 cluster is significantly bent in one of the molecules of the asymmetric unit, but is more nearly planar in the other molecule. The Fe-Fe bond distances in the iron triangle ($2.53, 2.65, 2.65 \text{ \AA}$) do not differ significantly from those in the parent compound.

Crystals of bis(1,2- bis(dimethylarsino)tetrafluorocyclobutene)triruthenium octacarbonyl, $(\text{Me}_2\text{AsC}=\text{C}(\text{AsMe}_2)\text{CF}_2\text{CF}_2)_2 \cdot \text{Ru}_3(\text{CO})_8$, are orthorhombic, space group $Pbcn$, $a = 9.07$,

b = 18.53, c = 21.81 Å, z = 4 (one-half molecule per asymmetric unit). The structure was refined by least-squares procedures to a final R of 0.078 for 1507 observed (of a total of 1712) reflections. The molecule lies on a crystallographic two-fold axis, and is best described as a derivative of Ru₃(CO)₁₂ in which two carbonyls on one ruthenium and one carbonyl on each of the other ruthenium atoms are replaced by the arsenic atoms of the bidentate di-(tertiary arsine) ligands, in such a way that each ligand bridges two ruthenium atoms, and one Ru-Ru bond remains unbridged. This unbridged Ru-Ru bond (2.785 Å) is significantly shorter than the bridged ones (2.853 Å) and than those of the parent Ru₃(CO)₁₂ (average 2.848 Å). The skeletons of the di-(tertiary arsine) ligands do not deviate significantly from exact planarity, the plane of each ligand being twisted 18° with respect to the plane of the ruthenium triangle. The mean Ru-As bond length is 2.407 Å.

1,2- bis(dimethylarsino)tetrafluoroclobutene-triruthenium decacarbonyl, Me₂AsC=C(AsMe₂)CF₂CF₂.Ru₃(CO)₁₀, crystallizes in orthorhombic space group P2₁2₁2₁, a = 8.594, b = 18.795, c = 16.69 Å, z = 4. The structure was refined by least-squares procedures to a final R of 0.076 for 1828 observed (of a total of 2028) reflections. The compound is a derivative of Ru₃(CO)₁₂ in which one equatorial carbonyl group on each of two ruthenium atoms

is replaced by an arsenic atom of the di-(tertiary arsine) ligand in such a way that the plane of the ligand is twisted 18° with respect to the plane of the ruthenium triangle. Ru-Ru bond distances are 2.831, 2.831, and 2.858 Å, the difference between the short and long bond lengths being statistically significant and explicable in terms of the bonding characteristics of the ligand.

1,2- bis(dimethylarsino)hexafluoropropanemolybdenum tetracarbonyl, $\text{Me}_2\text{AsCF}(\text{CF}_3)\text{CF}_2\text{AsMe}_2 \cdot \text{Mo}(\text{CO})_4$, crystallizes in the monoclinic space group $\text{C}2/\text{c}$, $a = 25.06$, $b = 13.27$, $c = 11.56$ Å, $\beta = 102.8^\circ$, $z = 8$. The structure was refined by least squares methods to a final R of 0.073 for 1510 observed (of a total of 1750) reflections. The molecule is derived from $\text{Mo}(\text{CO})_6$ by replacing two carbonyl groups with the arsenic atoms of the chelating di-(tertiary arsine) ligand. Two of the carbon-fluorine bond distances (mean 1.505 Å) are significantly longer than the others (mean 1.30 Å) and the distance between the carbon atoms of the ligand skeleton is remarkably short (1.40 Å). The weighted mean Mo-As bond length is 2.572 Å.

TABLE OF CONTENTS

	PAGE
TITLE PAGE	i
ABSTRACT	ii
TABLE OF CONTENTS	v
LIST OF TABLES	vii
LIST OF FIGURES	x
ACKNOWLEDGEMENTS	xii
I. INTRODUCTION	1
A. THE TECHNIQUE OF X-RAY CRYSTAL ANALYSIS	2
B. CHARACTERISTICS OF METAL CARBONYLS AND THEIR DERIVATIVES	8
C. RESULTS OF PRELIMINARY EXPERIMENTS	11
II. EXPERIMENTAL SECTION	16
III. THE STRUCTURE DETERMINATION OF $\text{Me}_2\text{As}\overline{\text{C}}=\text{C}(\text{AsMe}_2)\text{CF}_2\text{CF}_2 \cdot \text{Fe}_3(\text{CO})_{10}$.	21
STRUCTURE ANALYSIS	22
DISCUSSION	36
IV. THE STRUCTURE DETERMINATION OF $(\text{Me}_2\text{As}\overline{\text{C}}=\text{C}(\text{AsMe}_2)\text{CF}_2\text{CF}_2)_2 \cdot \text{Ru}_3(\text{CO})_8$.	46
STRUCTURE ANALYSIS	47
DISCUSSION	56
V. THE STRUCTURE DETERMINATION OF $\text{Me}_2\text{As}\overline{\text{C}}=\text{C}(\text{AsMe}_2)\text{CF}_2\text{CF}_2 \cdot \text{Ru}_3(\text{CO})_{10}$.	64
STRUCTURE ANALYSIS	65
DISCUSSION	74
VI. THE STRUCTURE DETERMINATION OF $\text{Me}_2\text{AsCF}_2\text{CF}(\text{CF}_3)\text{AsMe}_2 \cdot \text{Mo}(\text{CO})_4$.	79
STRUCTURE ANALYSIS	80

DISCUSSION	86
VII. COMPUTER PROGRAMMING	97
A. THE WEIGHTING SCHEME PROGRAM "UPDATE".	98
B. IMPLEMENTATION OF THE THERMAL PLOT PROGRAM "ORTEP".	103
VIII. REFERENCES	106

LIST OF TABLES

	PAGE
I. INTRODUCTION	
II. EXPERIMENTAL SECTION	
II.I Crystal and experimental data for all structures.	19
III. THE STRUCTURE DETERMINATION OF $\text{Me}_2\text{AsC}=\text{C}(\text{AsMe}_2)\text{CF}_2\text{CF}_2 \cdot$ $\text{Fe}_3(\text{CO})_{10}$.	
III.I Comparison of 51 possible solutions generated by Hoge's sign determination program.	25
III.II Final measured and calculated structure factors.	29
III.III Final positional and thermal parameters with their standard deviations.	31
III.IV Equations of weighted mean planes for iron triangle and di-(tertiary arsine).	33
III.V Bond distances and valency angles.	34
III.VI Magnitudes of the principal axes of thermal vibration ellipsoids of iron and arsenic atoms.	42
IV. THE STRUCTURE DETERMINATION OF $(\text{Me}_2\text{AsC}=\text{C}(\text{AsMe}_2)\text{CF}_2\text{CF}_2)_2 \cdot$ $\text{Ru}_3(\text{CO})_8$.	
IV.I Comparison of 16 possible solutions generated by Long's sign determination program.	49
IV.II Final measured and calculated structure factors.	51
IV.III Final positional and thermal parameters with their standard deviations.	53

IV.IV	Bond distances and valence angles.	54
IV.V	Equations of weighted mean planes for ruthenium triangle and di-(tertiary arsine).	55
IV.VI	Magnitudes of principal axes of thermal vibration for atoms refined anisotropically.	55
V.	THE STRUCTURE DETERMINATION OF $\text{Me}_2\text{AsC}=\text{C}(\text{AsMe}_2)\text{CF}_2\text{CF}_2 \cdot \text{Ru}_3(\text{CO})_{10}$.	
V.I	Final measured and calculated structure factors.	67
V.II	Final positional and thermal parameters with their standard deviations.	69
V.III	Bond distances and valence angles.	71
V.IV	Equations of weighted mean planes for ruthenium triangle and di-(tertiary arsine).	73
V.V	Magnitudes of principal axes of thermal vibration for ruthenium and arsenic atoms.	73
VI.	THE STRUCTURE DETERMINATION OF $\text{Me}_2\text{AsCF}_2\text{CF}(\text{CF}_3)\text{AsMe}_2 \cdot \text{Mo}(\text{CO})_4$.	
VI.I	Final measured and calculated structure factors.	82
VI.II	Final positional and thermal parameters with their standard deviations.	83
VI.III	Bond distances and valence angles.	84
VI.IV	Magnitudes of principal axes of thermal vibration of atoms refined anisotropically.	85
VI.V	Equations of weighted mean plane of molybdenum octahedron and direction cosines of vector C(5)-C(6).	88

VII. COMPUTER PROGRAMMING**VII.I Fortran listing of program "UPDATE".****101**

LIST OF FIGURES

	PAGE
I. INTRODUCTION	
I.1 Expected structure for $\text{Me}_2\text{As}\overline{\text{C}}=\text{C}(\text{AsMe}_2)\text{CF}_2\overline{\text{C}}\text{F}_2 \cdot \text{Fe}_3(\text{CO})_{10}$.	12
I.2 Two possible structures for $(\text{Me}_2\text{As}\overline{\text{C}}=\text{C}(\text{AsMe}_2)\text{CF}_2\overline{\text{C}}\text{F}_2)_2\text{Ru}_3(\text{CO})_8$.	14
I.3 Two possible structures for $\text{Me}_2\text{As}\overline{\text{C}}=\text{C}(\text{AsMe}_2)\text{CF}_2\overline{\text{C}}\text{F}_2 \cdot \text{Ru}_3(\text{CO})_{10}$.	15
II. EXPERIMENTAL SECTION	
III. THE STRUCTURE DETERMINATION OF $\text{Me}_2\text{As}\overline{\text{C}}=\text{C}(\text{AsMe}_2)\text{CF}_2\overline{\text{C}}\text{F}_2 \cdot \text{Fe}_3(\text{CO})_{10}$.	
III.1 E-map with heavy atom positions superimposed.	27
III.2 Molecular structure of $\text{Me}_2\text{As}\overline{\text{C}}=\text{C}(\text{AsMe}_2)\text{CF}_2\overline{\text{C}}\text{F}_2 \cdot \text{Fe}_3(\text{CO})_{10}$.	37
III.3 View of asymmetric carbonyl bridges.	39
III.4 Co-ordination about arsenic atoms, showing angles averaged over the four arsenic atoms in the asymmetric unit.	41
III.5 Intermolecular contacts in general view.	43
III.6 Projection of unit cell down <u>a</u> -axis.	45
IV. THE STRUCTURE DETERMINATION OF $(\text{Me}_2\text{As}\overline{\text{C}}=\text{C}(\text{AsMe}_2)\text{CF}_2\overline{\text{C}}\text{F}_2)_2 \cdot \text{Ru}_3(\text{CO})_8$.	
IV.1 Molecular structure of $(\text{Me}_2\text{As}\overline{\text{C}}=\text{C}(\text{AsMe}_2)\text{CF}_2\overline{\text{C}}\text{F}_2)_2 \cdot \text{Ru}_3(\text{CO})_8$.	57
IV.2 Comparison of $(\text{Me}_2\text{As}\overline{\text{C}}=\text{C}(\text{AsMe}_2)\text{CF}_2\overline{\text{C}}\text{F}_2)_2\text{Ru}_3(\text{CO})_8$ and $(\text{C}_6\text{H}_8)_2\text{Ru}_3(\text{CO})_4$.	59
IV.3 Distortion of co-ordination about ruthenium.	60

IV.4	Projection of the unit cell down <u>a</u> -axis.	63
V.	THE STRUCTURE DETERMINATION OF $\text{Me}_2\text{AsC}=\text{C}(\text{AsMe}_2)\text{CF}_2\text{CF}_2 \cdot \text{Ru}_3(\text{CO})_{10}$.	
V.1	Molecular structure of $\text{Me}_2\text{AsC}=\text{C}(\text{AsMe}_2)\text{CF}_2\text{CF}_2 \cdot \text{Ru}_3(\text{CO})_{10}$.	75
V.2	Distortion of co-ordination about ruthenium.	77
V.3	Projection of unit cell down <u>a</u> -axis.	78
VI.	THE STRUCTURE DETERMINATION OF $\text{Me}_2\text{AsCF}_2\text{CF}(\text{CF}_3)\text{AsMe}_2 \cdot \text{Mo}(\text{CO})_4$.	
VI.1	Molecular structure of $\text{Me}_2\text{AsCF}_2\text{CF}(\text{CF}_3)\text{AsMe}_2 \cdot \text{Mo}(\text{CO})_4$.	87
VI.2	View of bond distances and dihedral angles around C(5)-C(6) bond.	90
VI.3	Postulated bonding scheme to account for anomalous observations.	92
VI.4	Projection of unit cell down <u>c</u> -axis.	96
VII.	COMPUTER PROGRAMMING	
VII.1	Stereo diagrams of all four di-(tertiary arsine) derivatives.	104

ACKNOWLEDGEMENTS

I wish to express my gratitude to Professor Trotter for his continuous guidance and to Professor B. R. Penfold and Dr. F. H. Allen for assistance with various aspects of crystallographic computing.

I would like to thank Professors W. R. Cullen and N. L. Paddock for reading the preliminary draft of this thesis and for making many helpful suggestions. Professor Cullen also supplied the crystal samples used in this work.

The co-operation of Mr. T. V. Taylor of the University of British Columbia Computing Centre in preparing tables of structure factors and listings of programs is also greatly appreciated.

I am indebted to the National Research Council of Canada for financial support during the entire term of this work.

I. INTRODUCTION

A. THE TECHNIQUE OF X-RAY CRYSTAL ANALYSIS

As revealed by the innumerable organic and inorganic compounds, natural products, biologically important molecules, and alloys which have been examined in the sixty years since its discovery, the technique of x-ray crystal analysis has become an extremely powerful method of structure determination for chemists, biochemists, physicists and metallurgists. The application of the technique has been tremendously facilitated by the advent of electronic computers and mechanized data collection. However, there remains one obstacle in the way of completely universal applicability of the method. Although the amplitude of the wave diffracted by the crystal lattice can be measured, its phase cannot. To overcome this difficulty, several methods have been devised, of which the Patterson function, which uses the squares of the amplitudes (F 's) of the diffracted waves, and direct methods, in which the phases are determined from the magnitudes of normalized structure factors (E 's), are two of the most important, and ought to be discussed here in sufficient detail to clarify the ensuing descriptions of structure determination.

Since the structure amplitudes are Fourier transforms of the periodic electron density of the crystal lattice, (eq. 1.1), it follows that the electron density must therefore be the Fourier transform of the

structure amplitudes and can be written in terms of a Fourier series of which the structure amplitudes are coefficients (eq. 1.2).

$$F_{\underline{h}\underline{k}\underline{\ell}} = \frac{1}{V} \int_V \rho(\underline{x}, \underline{y}, \underline{z}) \exp\{2\pi i(\underline{h}\underline{x} + \underline{k}\underline{y} + \underline{\ell}\underline{z})\} dV. \quad (1.1)$$

$$\rho(\underline{x}, \underline{y}, \underline{z}) = \frac{1}{V} \sum_{\underline{h}\underline{k}\underline{\ell}} F_{\underline{h}\underline{k}\underline{\ell}} \exp\{-2\pi i(\underline{h}\underline{x} + \underline{k}\underline{y} + \underline{\ell}\underline{z})\} \quad (1.2)$$

However, each structure amplitude has an associated unknown phase, and the electron density cannot be calculated directly from experimentally observed quantities. However, if part of the structure is known, structure factors based on the positions of these known atoms can be calculated and the phases of these calculated structure factors can be assumed to be approximations to the correct phases. An electron density map calculated using these approximate phases is expected to reveal additional elements of the structure and new structure factors, whose phases will be closer to the correct values, can be calculated. The iterative application of this process results in a complete structure, the approximate atomic positions of which are then refined by least-squares methods to yield final refined parameters with a final set of phases. This method is particularly successful if the atoms of the known portion of the molecule constitute a large fraction of the scattering matter in the unit cell. Apparently the sole obstacle of structure determination is the inability to locate a starting

segment in the unit cell and it is to this problem that we now turn our attention.

Early in the history of x-ray crystallography¹, it was shown that a Fourier series (eq. 1.3) of which the coefficients were the phaseless squares of the amplitudes of the diffracted waves, produced a map which contained peaks at positions corresponding to the ends of vectors between atomic positions.

$$P(x, y, z) = \frac{1}{v} \sum_{hkl} |F_{hkl}|^2 \cos 2\pi (\underline{hx} + \underline{ky} + \underline{\ell z}) \quad (1.3)$$

By considering the symmetry requirements of the space group of crystallization, it would then seem a straightforward matter to locate the molecule in the unit cell. There are, however, several drawbacks to the method. Peaks in the vector distribution tend to be very much broader than in the electron distribution and the vector map can become diffuse and complicated if the molecule contains more than a few atoms. Since the intensity of the vector peak is proportional to the product of the atomic numbers of the atoms to which it corresponds, it is obvious that vectors between relatively heavy atoms will appear much more intense than vectors between the lighter atoms. Provided that the structure is dominated by a relatively small number of heavy atoms, the vector map can usually be unravelled and atomic positions assigned to these atoms.

We have seen that the presence of a large number

of atoms of similar atomic number is detrimental to the ease with which a solution can be extracted from the Patterson map, but that a small number of relatively heavy atoms makes this a powerful method. The reverse is true for direct methods, by which process phases are assigned from a statistical analysis of the structure amplitudes. The theory is formulated^{2,3} on a random arrangement of similar atoms but has been successfully applied to many crystal structures which contain atoms of extremely different atomic numbers.

The cornerstone of direct methods in centrosymmetric space groups is the relation

$$\underline{F}_{\underline{h}\underline{k}\underline{\ell}} = \Phi_{\underline{h}\underline{k}\underline{\ell}} \sum_{\underline{h}'} \sum_{\underline{k}'} \sum_{\underline{\ell}'} \underline{F}_{\underline{h}'\underline{k}'\underline{\ell}'} \cdot \underline{F}_{\underline{h}-\underline{h}'\underline{k}-\underline{k}'} \underline{\ell}-\underline{\ell}' \quad (1.4)$$

where $\Phi_{\underline{h}\underline{k}\underline{\ell}}$ is a simple scaling term. Although it appears that one \underline{F} can be determined only if the magnitudes and phases of all others are known, the series must tend strongly in one direction (+ or -) if $\underline{F}_{\underline{h}\underline{k}\underline{\ell}}$ is sufficiently large, and this direction is determined by the agreement in signs among products of large \underline{F} 's³. We can therefore write the following relation.

$$S(\underline{F}_{\underline{h}\underline{k}\underline{\ell}}) \sim S(\underline{F}_{\underline{h}'\underline{k}'\underline{\ell}'}) \cdot S(\underline{F}_{\underline{h}-\underline{h}'\underline{k}-\underline{k}'} \underline{\ell}-\underline{\ell}') \quad (1.5)$$

where S means "the sign of" and \sim means "is probably equal to".⁴ The probability with which this equation holds depends

on the magnitudes of the three reflections and is given by

$$P = \frac{1}{2} + \frac{1}{2} \tanh\left(\sigma_3/\sigma_2^3\right)^{1/2} |\underline{E}_{h\underline{k}\ell} \cdot \underline{E}_{\underline{h}' \underline{k}' \underline{\ell}'} \cdot \underline{E}_{\underline{h}-\underline{h}' \underline{k}-\underline{k}' \underline{\ell}-\underline{\ell}'}| \quad (1.6)$$

where $\sigma_3/\sigma_2^3/2$ is a parameter dependent on the contents of the unit cell and independent of their location and where \underline{E} 's are defined by

$$\underline{E}_{h\underline{k}\ell} = |F_{h\underline{k}\ell}|^2 / \epsilon \sum_i^N f_i^2 \quad (1.7)$$

where ϵ is an integer which takes on different values for different classes of reflections.

A slightly more rigorous treatment of eq. 1.4 results in the most commonly used form of Sayre's equation.

$$S(F_{h\underline{k}\ell}) \sim \sum_{\underline{h}' \underline{k}' \underline{\ell}'} S(F_{\underline{h}' \underline{k}' \underline{\ell}'}) \cdot S(F_{\underline{h}-\underline{h}' \underline{k}-\underline{k}' \underline{\ell}-\underline{\ell}'}) \quad (1.8)$$

with corresponding probability

$$P_+ (\underline{E}_{h\underline{k}\ell}) = \frac{1}{2} + \frac{1}{2} \tanh(\sigma_3/\sigma_2^3)^{1/2} |\underline{E}_{h\underline{k}\ell} \sum_{\underline{h}' \underline{k}' \underline{\ell}'} \underline{E}_{\underline{h}' \underline{k}' \underline{\ell}'} \cdot \underline{E}_{\underline{h}-\underline{h}' \underline{k}-\underline{k}' \underline{\ell}-\underline{\ell}'}| \quad (1.9)$$

where P_+ is the probability that the sign of $\underline{E}_{h\underline{k}\ell}$ is positive.

If the value of the summation in eq. 1.9 is negative, P_+ will be less than $\frac{1}{2}$ and will imply that the sign of $\underline{E}_{h\underline{k}\ell}$ is negative with a probability

$$P_- = 1 - P_+$$

In practice, phases are assigned to a small number of reflections and Sayre's equations are applied.

to determine others. This can be achieved in several ways.

An initial set of ten very large reflections can be allowed to take on all possible combinations of plus and minus signs. This would result in 2^{10} possibilities, of which several will be more consistent (i.e. have higher probabilities) than the others. Each of these highly probable combinations is then taken as a starting set and phases are generated for the remaining reflections by applying Sayre's equations.

An alternative approach arises as a consequence of the fact that the origin of a centrosymmetric unit cell can be arbitrarily located at any centre of symmetry. Three or sometimes fewer reflections, depending on the space group, can be assigned arbitrary phases, corresponding to the choice of origin. Three or four other reflections are allowed to take all possible combinations of plus and minus signs, resulting in 8 or 16 possible solutions.

Either method is completed by calculating an electron density map using the phases of those solutions of highest probability.

B. CHARACTERISTICS OF METAL CARBONYLS AND THEIR DERIVATIVES

Numerous reviews have appeared recently describing metal-carbon bonding,⁵⁻⁷ preparation, properties, and structure of metal carbonyls,^{8,9} metal atom clusters¹⁰ and Lewis base substituted carbonyl complexes.¹¹⁻¹⁴ The principal conclusions of these studies ought to be reviewed briefly as background to the material to be presented in following parts of this thesis.

The most regular feature of the metal carbonyls and their derivatives is the adherence of most of these compounds to the "effective atomic number" or "inert gas" law¹⁵ which requires that the central atom accept from the ligands sufficient electrons that the total number of electrons around the metal atom results in a closed shell configuration. For example, the compound $\text{Fe}(\text{CO})_2(\text{NO})_2$ can be considered to consist of $\text{Fe}(0)$ (26 electrons), two carbonyl groups (2×2 electrons) and two nitrosyl groups (2×3 electrons), for a total of 36 electrons, the krypton configuration. Since various ligands donate from one to a dozen electrons, the co-ordination number for a given metal atom will vary from one compound to another depending on the combination of ligands used to complete the inert gas configuration. For instance, inert gas configuration species exist for iron with co-ordination numbers of four (dicarbonyldinitrosyliron), five (pentacarbonyliron) and six (di-iodotetracarbonyliron).

It is obvious that an integral number of pair-donating ligands can complete the valence shell of a metal of even atomic number, whereas metal atoms of odd atomic number must receive an additional single electron. This requirement can be accommodated in several ways. A ligand which donates an odd number of electrons can be employed, resulting in compounds exemplified by $\text{Co}(\text{NO})(\text{CO})_3$ and $\text{HCo}(\text{CO})_4$, or the odd electron on each atom can be shared with another such atom, resulting in a metal-metal bond, as in $\text{Co}_2(\text{CO})_8$.

Besides this regularity in stoichiometry, metal carbonyls and their derivatives are characterized by the actual nature of the metal-ligand bond. The carbon atom of carbon monoxide possesses an sp hybridized lone pair of electrons which forms a σ -bond by overlap with a vacant transition metal orbital of the proper symmetry. The carbon monoxide group also has vacant π -antibonding orbitals which form a π -bond by overlap with filled non-bonding d orbitals on the metal atom. The metal-carbon bond order in these complexes must thereby be greater than unity, requiring a concurrent decrease in carbon-oxygen bond order. The presence of multiple bonding between metal and carbon atoms is reflected by the fact that x-ray studies show that the metal-carbon bond length is distinctly shorter than the sum of the single bond radii.¹⁶

Other ligands found in stable substitution complexes of metal carbonyls also possess both σ -donor and

π -acceptor properties. On ligands such as substituted phosphines and arsines, the acceptor properties arise from empty d orbitals on the phosphorus or arsenic atoms.

It has been found that most complexes of π -bonding ligands contain metals in low oxidation states. This can be explained in terms of the description of bonding presented above, since a positive charge on a metal atom enhances its acceptor properties but decreases its back-bonding capability whereas the presence of a negative charge produces the opposite effects. Since both σ - and π -bonding appear to be required for stable complexes, the presence of an electronic charge, either positive or negative, will inhibit this type of complex formation.

The four structures included in this thesis have been chosen since, as di-(tertiary arsine) derivatives of metal carbonyls, they represent a unified topic for study and discussion in terms of the principles established in this introduction. Because of the complexity of their systematic names, the ligands $\text{Me}_2\text{AsC}=\text{C}(\text{AsMe}_2)\text{CF}_2\text{CF}_2$ and $\text{Me}_2\text{AsCF}(\text{CF}_3)\text{CF}_2\text{AsMe}_2$ will often be denoted by the symbols L and L' respectively.

C. RESULTS OF PRELIMINARY EXPERIMENTS

Before an x-ray analysis is undertaken, several other experiments are often carried out, and the results of these experiments can lead to some idea of the structure of the compound under investigation. This is the case for three of the compounds in this thesis and these structural indications will now be discussed.

The infra-red, n.m.r. and Mössbauer spectra¹⁷ of LFe₃(CO)₁₀ suggest a structure in which two terminal carbonyl groups of the two equivalent iron atoms of Fe₃(CO)₁₂¹⁸ are replaced by the arsenics of the di-(tertiary arsine) ligand (Figure I.1). The presence of only one ¹⁹F resonance in the n.m.r. spectrum indicates that all the fluorine atoms are equivalent, so that the di-(tertiary arsine) ligand would be expected to be planar, in contrast to the previously determined structure of LFe₂(CO)₆, in which the ligand is bent as a result of the formation of a π-bond from the cyclobutene system to one of the iron atoms.¹⁹

The ¹H n.m.r. spectrum of L₂Ru₃(CO)₈ contains two singlets, indicating a moderately symmetrical structure for the ligand. The ¹⁹F n.m.r. spectrum²⁰ is a complex arrangement of fourteen peaks with some similarity to the spectrum of LFe(CO)₄, where only one arsenic atom of the ligand is bonded to the iron atom.²¹ These two pieces of evidence, and the observation that the ligand is normally reluctant to chelate, favour the structure shown in Figure

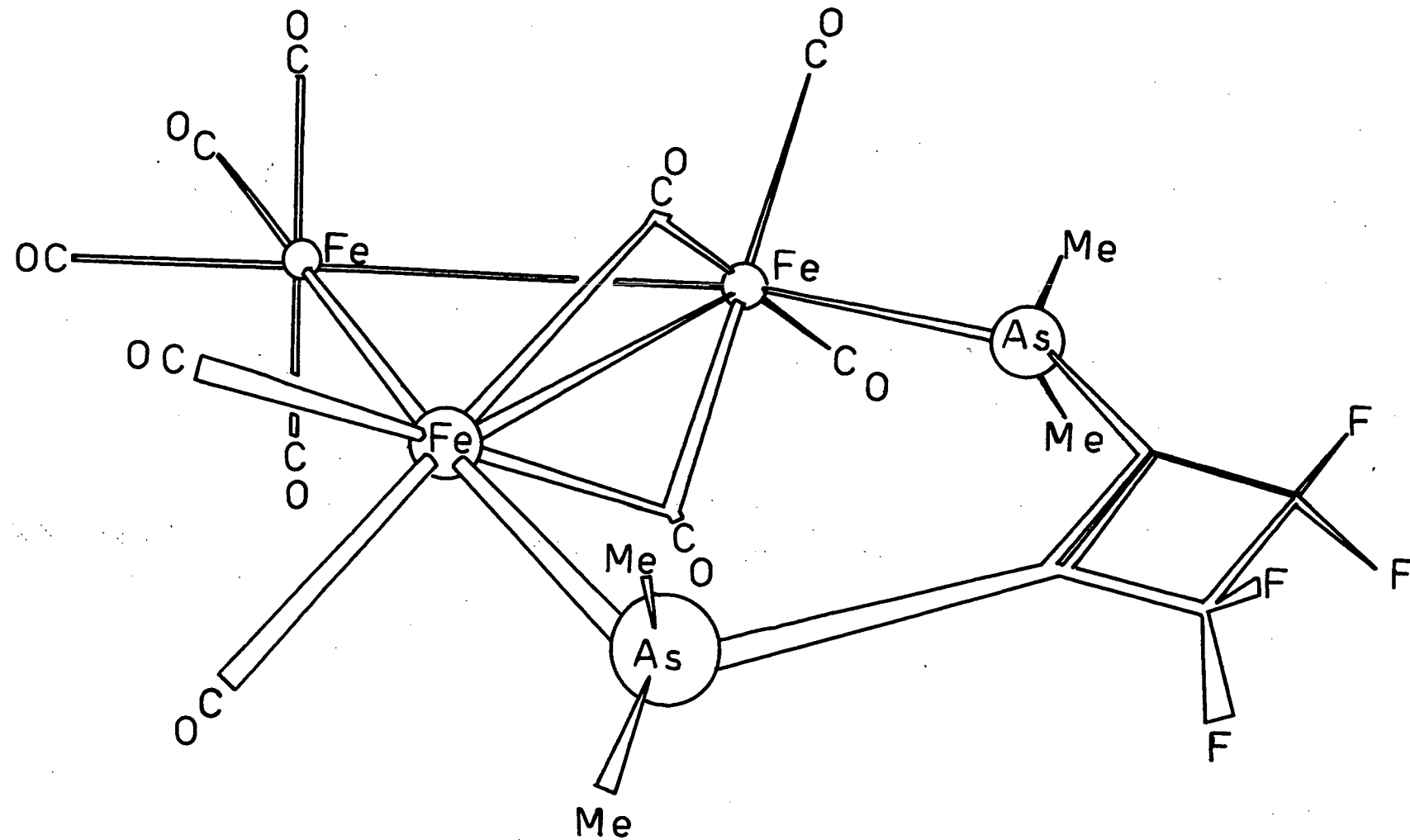
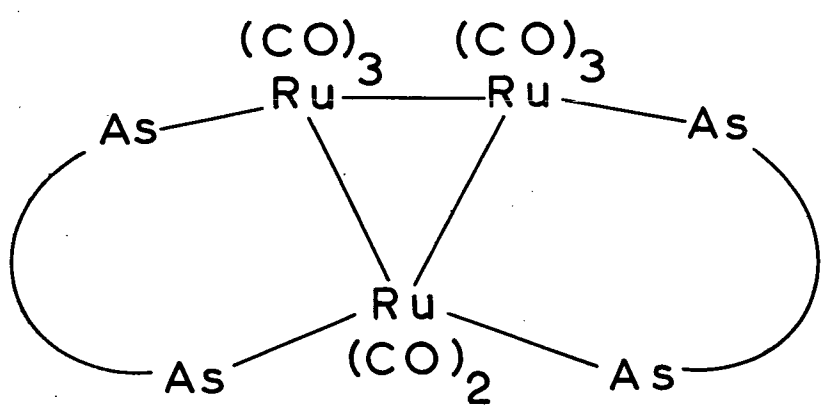


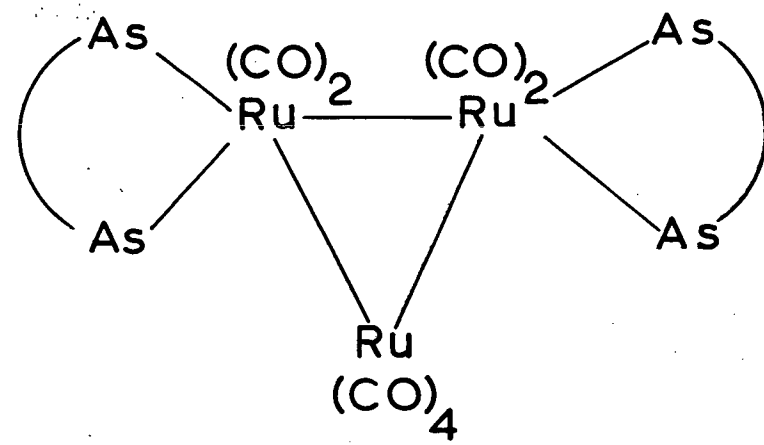
Figure I.1 Structure of $\text{Me}_2\text{AsC}=\text{C}(\text{AsMe}_2)\text{CF}_2\text{CF}_2 \cdot \text{Fe}_3(\text{CO})_{10}$
expected on the basis of preliminary experiments.

I.2a rather than that of Figure I.2b.

The ^{19}F and ^1H n.m.r. spectra²⁰ of $\text{LRu}_3(\text{CO})_{10}$ both consist of singlets, indicating a highly symmetrical structure for this complex. This could be accomplished by having the ligand either chelating (Figure I.3a) or bridging (Figure I.3b) in an equatorial position. The latter is favoured because of the similarity of the infra-red spectra of $\text{LFe}_3(\text{CO})_{10}$ and $\text{LRu}_3(\text{CO})_{10}$ in the terminal carbonyl region and because of the known reluctance of the ligand to chelate without also involving the double bond of the cyclobutene ring.

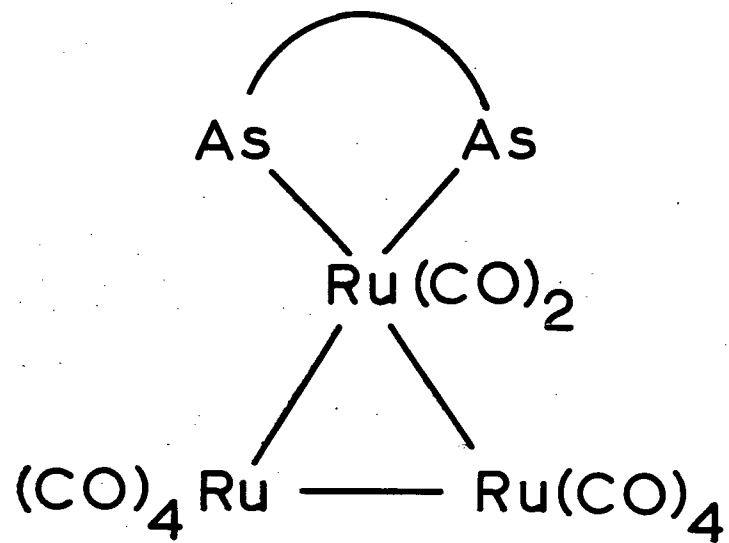


(a)

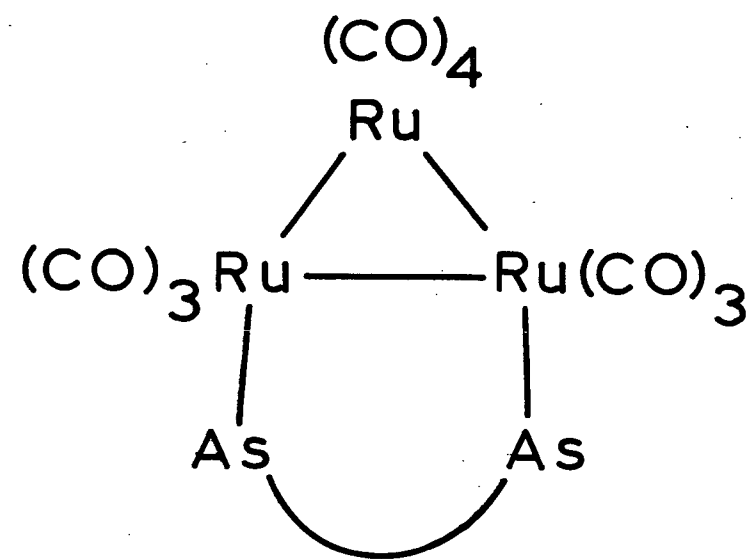


(b)

Figure I.2 Two possible structures for $(\text{Me}_2\text{As}\text{C}=\text{C}(\text{AsMe}_2)\text{CF}_2\text{CF}_2)_2 \cdot \text{Ru}_3(\text{CO})_8$.



(a)



(b)

Figure I.3 Two possible structures for $\text{Me}_2\text{AsC}=\text{C}(\text{AsMe}_2)\text{CF}_2\text{CF}_2 \cdot \text{Ru}_3(\text{CO})_{10}$.

II. EXPERIMENTAL SECTION

$LFe_3(CO)_{10}$ is obtained by chromatography of the mixture of products formed by ultraviolet irradiation of $Fe_3(CO)_{12}$ and the di-(tertiary arsine).¹⁷ The crystals are black needles elongated along a. The intensity data were collected using a sample of dimensions $0.3 \times 0.03 \times 0.04$ mm.

$L_2Ru_3(CO)_8$ is prepared by chromatography of the products of the reaction of $Ru_3(CO)_{12}$ with the ligand refluxed in hexane.²⁰ The crystal used to record the data was an irregular plate with {001} developed. Its dimensions were 0.05 mm. parallel to c and about 0.2 mm. across.

Ultraviolet irradiation of equimolar quantities of $Ru_3(CO)_{12}$ with the di-(tertiary arsine) results in the formation of $LRu_3(CO)_{10}$.²⁰ A single flake of the compound of dimensions $0.07 \times 0.44 \times 0.25$ mm. was recrystallized from diethyl ether for use in intensity measurements.

$L'Mo(CO)_4$ is prepared by recrystallization from petroleum ether-benzene of the products formed by refluxing $Mo(CO)_6$ with the ligand in toluene.²² The crystals are colourless needles elongated along c. Intensity data were recorded using a specimen of dimensions $0.16 \times 0.07 \times 0.57$ mm.

Unit cell and space group data for each compound were obtained by photographic methods and accurate lattice parameters for each were determined by least-squares treatment of $\sin^2\theta/\lambda^2$ values for thirty reflections measured on a diffractometer with Mo-K_α radiation.²³

Reflection intensities were measured on a Datex-automated General Electric XRD 6 diffractometer, with a scintillation counter, Mo- K_{α} radiation (Zr filter and pulse-height analyser), and a θ - 2θ scan. The scan range in 2θ was $(1.80 + 0.86 \tan\theta)$ degrees and backgrounds were measured at both ends of each scan.

The standard deviation of an intensity was calculated from the counting statistics using

$$\sigma^2(\underline{I}) = \underline{S} + \underline{B} + (\underline{dS})^2$$

where \underline{S} = scan count

\underline{B} = background, corrected to time of scan

$\underline{I} = \underline{S} - \underline{B}$

\underline{d} = an empirical constant which allows for unknown experimental errors; values used for each structure are given in Table II.I

Reflections whose intensities were less than 1σ were classified as unobserved. Lorentz and polarization factors were applied and the structure amplitudes were derived. Absorption corrections were not applied.

Crystal data and parameters of data collection are given in Table II.I.

Table II.I
Crystal and experimental data.

	$LFe_3(CO)_{10}$	$L_2Ru_3(CO)_8$	$LRu_3(CO)_{10}$	$L'Mo(CO)_4\ddagger$
formula	$C_{18}H_{12}As_2F_4Fe_3O_{10}$	$C_{24}H_{24}As_4F_8Ru_3O_8$	$C_{18}H_{12}As_2F_4Ru_3O_{10}$	$C_{11}H_{12}As_2F_6MoO_4$
molecular weight (gm.)	781.2	1195.3	917.3	567.7
crystal system	monoclinic	orthorhombic	orthorhombic	monoclinic
cell dimensions (\AA , deg.)	$a = 11.60(2)$ $b = 20.04(2)$ $c = 22.11(2)$ $\beta = 93.7(2)$	$a = 9.07(1)$ $b = 18.53(1)$ $c = 21.81(1)$	$a = 8.594(3)$ $b = 18.795(5)$ $c = 16.69(5)$	$a = 25.06(2)$ $b = 13.27(2)$ $c = 11.56(2)$ $\beta = 102.8(2)$
volume (\AA^3)	5129	3666	2696	3749
measured density (gm./cm. ³)	2.01 ± 0.02	2.14 ± 0.02	2.22 ± 0.02	2.04 ± 0.02
flotation in	CCl_4/CH_3I	$CCl_4/CHBr_3$	$CCl_4/CHBr_3$	$CCl_4/CHBr_3$
Z	8	4	4	8
calculated density (gm./cm. ³)	2.02	2.17	2.26	2.01
$F(000)$	3040	2272	1736	2096
absorption coefficient μ (cm. ⁻¹) (Mo-K α)	45	51	43	45
space group	$P2_1/c$ (C_{2h}^5)	$Pbcn$ (D_{2h}^{14})	$P2_12_12_1$ (D_2^4)	$C2/c$ (C_{2h}^6)

Table II.I (continued)

absent spectra	<u>h0l</u>	<u>l</u> = 2n+1	<u>0kl</u>	<u>k</u> = 2n+1	<u>h00</u>	<u>h</u> = 2n+1	<u>hkl</u>	<u>h+k</u> = 2n+1
	<u>0k0</u>	<u>k</u> = 2n+1	<u>h0l</u>	<u>l</u> = 2n+1	<u>0k0</u>	<u>k</u> = 2n+1	<u>h0l</u>	<u>l</u> = 2n+1
2θ (Mo-K _α) max. (deg.)		35		40		45		40
minimum interplanar spacing (Å)		1.18		1.04		0.93		1.04
number of reflections with 2θ < 2θ max.		3234		1712		2028		1750
number of unobserveds		710		205		200		240
d in σ ² expression		0.04		0.02		0.02		0.02
axis mounted parallel to φ axis of diffractometer		a*		a		c		c
scan speed (deg./min.)		4		2		2		2
time for background (sec.)		10		20		20		20

[†] L and L' represent the ligands $\text{Me}_2\text{AsC}=\text{C}(\text{AsMe}_2)\text{CF}_2\text{CF}_2$ and $\text{Me}_2\text{AsCF}(\text{CF}_3)\text{CF}_2\text{AsMe}_2$, respectively

III. THE STRUCTURE DETERMINATION

OF $\text{Me}_2\text{As}\overline{\text{C}=\text{C}(\text{AsMe}_2)\text{CF}_2\text{CF}_2}\cdot\text{Fe}_3(\text{CO})_{10}$

STRUCTURE ANALYSIS

The asymmetric unit contains two molecules, so that, with ten heavy atoms, the Patterson function was complicated. Two possible orientations appeared in the origin region, but as a result of the large number of peaks, it was not immediately possible to derive any further information.

An attempt was then made to solve the structure by direct methods using Hoge's series of four programs²⁴ which apply Sayre relationships in two dimensions in the Vand and Pepinsky^{25a} version of the Cochran and Douglas procedure.^{25b} The initial program first calculates a Wilson plot² for the data and outputs an overall scale and an overall temperature factor and then calculates and outputs normalized structure factors (\underline{E} 's). Average values of $|\underline{E}|$ and $|\underline{E}^2|$ are then calculated to indicate the presence or absence of a centrosymmetric electron distribution. The second program reads the tape output of the first and sorts the data into parity groups, including only those reflections for which $|\underline{E}|$ exceeds a specified value. The next stage of this program involves the determination of all Sayre relationships and the calculation of the probability with which each holds. The third program of the series uses these Sayre relationships to determine possible solutions, rejecting those for which, for any \vec{h}

$$S_{MAX} = \sum_{\vec{h}} |E_{\vec{h}}| \cdot |E_{\vec{k}}| \cdot |E_{\vec{h}-\vec{k}}| \quad (3.1)$$

(where \vec{h} is a reflection contained in a Sayre relationship which fails) exceeds a preset value.

Since the probability that the sign of $E_{\vec{h}}$ is correctly given by the Sayre relationships in which it is involved is calculated from the expression

$$P(\vec{h}) = \frac{1}{2} + \frac{1}{2}\tanh(\sigma_3/\sigma_2^3)^{1/2} \sum_{\vec{k}} |E_{\vec{h}}| \cdot |E_{\vec{k}}| \cdot |E_{\vec{h}-\vec{k}}| \quad (3.2)$$

then if only Sayre relationships which fail are included in the summation, eq. 3.2 becomes the probability that the sign of \vec{h} is opposite to that given in the solution. Hence by setting a value of SMAX corresponding to a probability of 0.985, all solutions for which any sign is incorrect to the extent of this probability can be rejected.

Those solutions which are within the limits of SMAX are printed out with the maximum value of this quantity attained for any reflection in each solution, as well as the number of plus signs in the solution and the value of the following expression

$$SEEE**2 = \sum_{\vec{h}} (\sum_{\vec{k}} |E_{\vec{h}}| \cdot |E_{\vec{k}}| \cdot |E_{\vec{h}-\vec{k}}|)^2 \quad (3.3)$$

where \vec{h} is a reflection contained in a Sayre relationship which fails.

The most probable solution would then be expected to be that which has approximately equal numbers of plus and minus signs and the minimum values for SMAX and SEEE**2.

The fourth program uses the \underline{E} 's from the first program and the signs from the third to produce a tape suitable for input to a Fourier calculation program containing up to six solutions at once, specified only by the number of the solution as it is generated.

In the present work, the a -axis projection was examined and the signs of 34 $\underline{0kl}$ reflections with normalized structure factor $|\underline{E}| > 1.4$ were determined. Table III.I contains a comparison of the 51 solutions which meet the acceptance criteria mentioned above. Sets 17, 18, 24, 26, 29, and 33 were used as input to a Fourier calculation. Set 29 was outstanding in having the lowest probability in the opposite-indication-of-sign test, and the \underline{E} -map (Figure III.1) computed with this set of signs revealed the positions, in projection, of the ten heavy atoms in the asymmetric unit.

With this information on the y - and z -parameters of the heavy atoms, attention was refocussed on the Patterson function, and the three-dimensional structure of the two heavy atom units was derived. Sixty-one of the sixty-four carbon, oxygen, and fluorine atoms were located from a Fourier summation with phases based on the iron and arsenic atoms, and the three remaining atoms were found on a subsequent electron density map.

Preliminary least-squares refinement of the parameters utilized the block-diagonal approximation, and re-

Table III.I
Comparison of 51 solutions from
Hoge's sign determination program

Set	Number of pluses	SMAX	SEEE**2	Set	Number of pluses	SMAX	SEEE**2
1	21	12.4	1026	22	18	12.4	1525
2	22	12.8	985	23	20	12.8	1449
3	20	12.4	992	24	16	12.3	710
4	21	12.8	951	25	17	12.3	1192
5	23	12.9	1450	26	16	12.0	587
6	20	12.4	1355	27	17	12.0	1005
7	21	12.8	1275	28	25	11.9	1269
8	20	12.4	1072	29	17	10.2	686
9	22	12.4	1200	30	21	12.8	1409
10	17	12.4	1196	31	22	12.9	1612
11	21	12.8	1159	32	20	12.8	1690
12	21	12.4	1213	33	20	12.8	878
13	16	12.4	1578	34	21	12.8	1380
14	20	12.8	1173	35	24	12.8	1437
15	19	12.3	1204	36	23	12.3	1239
16	22	12.3	1069	37	24	12.8	1342
17	21	11.8	541	38	19	11.3	1091
18	20	11.3	969	39	18	12.8	1194
19	23	12.8	1147	40	18	12.9	1254
20	22	12.9	1671	41	17	12.3	1080
21	21	12.4	1529	42	17	12.8	924

Table III.I (continued)

Set	Number of pluses	SMAX	SEEE**2	Set	Number of pluses	SMAX	SEEE**2
43	16	12.8	1416	48	19	12.8	1415
44	24	12.8	1606	49	16	12.0	1241
45	16	11.2	940	50	15	12.8	1275
46	22	12.8	1773	51	18	12.7	1084
47	18	12.3	1381				

duced R to 0.11. At this stage, a three-dimensional difference map showed electron density fluctuations around the iron and arsenic atoms which indicated anisotropic thermal motion. Refinement was continued using a modified full-matrix procedure. The function minimized was $\sum w(F_O - kF_C)^2$ with $w = \{A + B|F_O| + C|F_O|^2 + D|F_O|^3\}^{-1}$ for the observed reflections. Unobserved reflections were excluded from the refinement but included in the final structure factor calculation. The coefficients A , B , C , and D were adjusted by a short least-squares program written by the author (see Section VII) to achieve best constancy of local averages of $\sum w(F_O - kF_C)^2$ over the full range of $|F_O|$, the final values being 600, 0.3, -0.06, and 0.00027 respectively. Scattering factors were from ref. 26 and included the real part of the dispersion correction. The variables refined were the positional parameters, anisotropic thermal parameters for the ten heavy atoms, isotropic thermal parameters for the other atoms, and a single overall scale factor, a total of

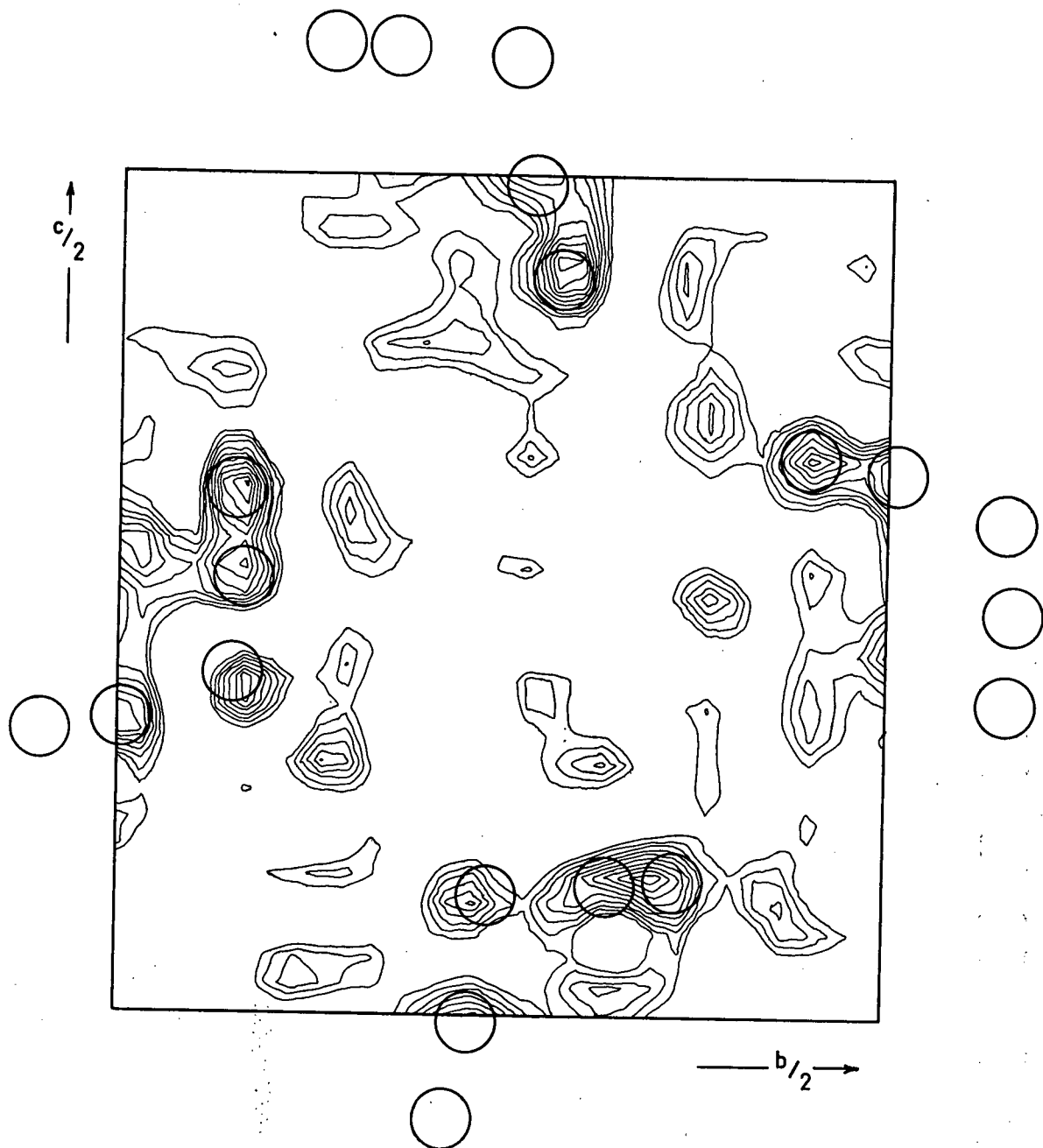


Figure III.1 E-map with final refined positions of heavy atoms superimposed.

347 variables. Since the dimensions of the computer program used were limited to 249 variables, it was necessary to vary different combinations of parameters in successive cycles. No parameter correlation coefficients greater than 0.35 were observed, and full convergence was reached after six cycles. Final values of \underline{R} and \underline{R}_w^+ were 0.090 and 0.096 respectively for the 2524 observed reflections and 0.131 and 0.117 respectively for all data. A final difference synthesis showed maximum fluctuations of ± 0.8 e/ \AA^3 . Final observed and calculated structure factors are given in Table III.III.

Final positional and thermal parameters are given in Table III.III, together with their standard deviations calculated from the inverse matrix of the last refinement cycle. The weighted mean planes of the iron triangle and di-(tertiary arsine) ligand of each molecule are given in Table III.IV, and the bond distances and valency angles are in Table III.V.

$$^+ \underline{R} = \sum |F_O - F_C| / \sum |F_O|; \underline{R}_w = \{ \sum w(F_O - F_C)^2 / \sum wF_O^2 \}^{1/2}$$

Table III.II

Final measured and calculated structure factors. Unobserved reflections have an asterisk after the $|F_{\text{O}}|$ value.

K	L	OBS CALC	K	L	OBS CALC	K	L	OBS CALC	K	L	OBS CALC	K	L	OBS CALC	K	L	OBS CALC	K	L	OBS CALC
**** H = 0****	9	13	36	16	-2	11	8*	11	7	3	95	80	12	8	106	101	2	13	46	35
0	2	179	4	9	16	77	22	-2	11	85	88	7	4	152	139	12	9	106	101	
0	4	177	183	0	10	55	32	2	12	95	113	12	-1	10	35	15	2	14	42	32
0	6	390	280	0	7	2	47	42	2	13	87	94	7	-6	21	21	2	14	52	46
0	10	0	54	0	9	131	136	2	14	23	19	7	6	82	101	2	16	53	57	
0	14	24	55	0	10	11	109	5	5	17	13	11	12	11	52	17	2	16	64	66
0	16	102	129	0	5	5	17	13	2	15	15	54	7	7	210	210	2	17	62	59
0	18	48	56	0	7	41	55	2	16	54	58	7	-8	27	64	12	17	63	59	
0	20	198	203	0	9	13	36	2	17	129	124	7	9	70	87	13	10	105	116	
1	2	198	203	0	10	10	0*	2	2	17	104	2	7	10	69	13	13	105	111	
1	4	171	171	0	11	13	82	0*	2	17	104	87	3	2	82	97	14	14	104	100
1	6	71	76	0	12	13	82	0*	2	17	104	91	7	11	13	82	14	14	104	100
1	8	108	105	0	12	13	81	26	1	9	10	104	11	3	207	210	3	9	11	104
1	10	282	280	0	12	13	81	26	3	1	11	12	12	12	12	12	12	12	12	
1	14	191	190	0	11	11	143	151	3	2	245	228	7	13	27	27	2	17	74	71
1	15	187	187	0	11	2	0*	0*	7	13	24	35	11	5	140	134	5	15	184	181
1	17	51	59	0	11	4	104	104	3	1	2	42	45	11	5	184	181	1	180	171
1	18	55	56	0	11	5	65	57	3	14	75	86	7	2	18	33	4	17	59	57
1	19	55	56	0	11	6	65	60	3	14	75	86	7	2	18	33	4	17	59	57
1	20	77	80	0	11	6	65	60	7	14	150	160	7	14	35	109	14	14	150	160
1	22	165	165	0	11	8	41	36	3	15	122	123	7	16	27	20	13	13	85	85
1	24	166	165	0	11	9	40	35	3	16	144	144	8	20	8	21	13	13	85	85
1	26	166	165	0	11	10	40	35	3	16	144	144	8	20	8	21	13	13	85	85
1	27	51	52	0	11	11	36	24	1	17	235	235	1	17	37	33	10	85	85	
1	28	161	165	0	11	12	70	70	3	17	50	56	8	-2	151	156	11	10	125	124
1	29	174	174	0	11	13	70	70	3	17	50	56	8	-2	151	156	11	10	125	124
1	30	174	174	0	11	14	70	70	3	17	50	56	8	-2	151	156	11	10	125	124
1	31	174	174	0	11	15	70	70	3	17	50	56	8	-2	151	156	11	10	125	124
1	32	174	174	0	11	16	70	70	3	17	50	56	8	-2	151	156	11	10	125	124
1	33	174	174	0	11	17	70	70	3	17	50	56	8	-2	151	156	11	10	125	124
1	34	174	174	0	11	18	70	70	3	17	50	56	8	-2	151	156	11	10	125	124
1	35	174	174	0	11	19	70	70	3	17	50	56	8	-2	151	156	11	10	125	124
1	36	174	174	0	11	20	70	70	3	17	50	56	8	-2	151	156	11	10	125	124
1	37	174	174	0	11	21	70	70	3	17	50	56	8	-2	151	156	11	10	125	124
1	38	174	174	0	11	22	70	70	3	17	50	56	8	-2	151	156	11	10	125	124
1	39	174	174	0	11	23	70	70	3	17	50	56	8	-2	151	156	11	10	125	124
1	40	174	174	0	11	24	70	70	3	17	50	56	8	-2	151	156	11	10	125	124
1	41	174	174	0	11	25	70	70	3	17	50	56	8	-2	151	156	11	10	125	124
1	42	174	174	0	11	26	70	70	3	17	50	56	8	-2	151	156	11	10	125	124
1	43	174	174	0	11	27	70	70	3	17	50	56	8	-2	151	156	11	10	125	124
1	44	174	174	0	11	28	70	70	3	17	50	56	8	-2	151	156	11	10	125	124
1	45	174	174	0	11	29	70	70	3	17	50	56	8	-2	151	156	11	10	125	124
1	46	174	174	0	11	30	70	70	3	17	50	56	8	-2	151	156	11	10	125	124
1	47	174	174	0	11	31	70	70	3	17	50	56	8	-2	151	156	11	10	125	124
1	48	174	174	0	11	32	70	70	3	17	50	56	8	-2	151	156	11	10	125	124
1	49	174	174	0	11	33	70	70	3	17	50	56	8	-2	151	156	11	10	125	124
1	50	174	174	0	11	34	70	70	3	17	50	56	8	-2	151	156	11	10	125	124
1	51	174	174	0	11	35	70	70	3	17	50	56	8	-2	151	156	11	10	125	124
1	52	174	174	0	11	36	70	70	3	17	50	56	8	-2	151	156	11	10	125	124
1	53	174	174	0	11	37	70	70	3	17	50	56	8	-2	151	156	11	10	125	124
1	54	174	174	0	11	38	70	70	3	17	50	56	8	-2	151	156	11	10	125	124
1	55	174	174	0	11	39	70	70	3	17	50	56	8	-2	151	156	11	10	125	124
1	56	174	174	0	11	40	70	70	3	17	50	56	8	-2	151	156	11	10	125	124
1	57	174	174	0	11	41	70	70	3	17	50	56	8	-2	151	156	11	10	125	124
1	58	174	174	0	11	42	70	70	3	17	50	56	8	-2	151	156	11	10	125	124
1	59	174	174	0	11	43	70	70	3	17	50	56	8	-2	151	156	11	10	125	124
1	60	204	193	0	11	44	70	70	3	17	50	56	8	-2	151	156	11	10	125	124
1	61	193	193	0	11	45	70	70	3	17	50	56	8	-2	151	156	11	10	125	124
1	62	174	174	0	11	46	70	70	3	17	50	56	8	-2	151	156	11	10	125	124
1	63	174	174	0	11	47	70	70	3	17	50	56	8	-2	151	156	11	10	125	124
1	64	174	174	0	11	48	70	70	3	17	50	56	8	-2	151	156	11	10	125	124
1	65	174	174	0	11	49	70	70	3	17	50	56	8	-2	151	156	11	10	125	124
1	66	174	174	0	11	50	70	70	3	17	50	56	8	-2	151	156	11	10	125	124
1	67	174	174	0	11	51	70	70	3	17	50	56	8	-2	151	156	11	10	125	124
1	68	174	174	0	11	52	70	70	3	17	50	56	8	-2	151	156	11	10	125	124
1	69	174	174	0	11	53	70	70	3	17	50	56	8	-2	151	156	11	10	125	124
1	70	174	174	0	11	54	70	70	3	17	50	56	8	-2	151	156	11	10	125	124
1	71	174	174	0	11	55	70	70	3	17	50	56	8	-2	151	156	11	10	125	124
1	72	174	174	0	11	56	70	70	3	17	50	56	8	-2	151	156	11	10	125	124
1	73	174	174	0	11	57	70	70	3	17	50	56	8	-2	151	156	11	10	125	124
1	74	174	174	0	11	58	70	70	3	17	50	56	8	-2	151	156	11	10	125	124
1	75	174	174	0	11	59	70	70	3	17	50	56	8	-2	151	156	11	10	125	124
1	76	174	174	0	11	60	70	70	3	17	50	56	8	-2	151	156	11	10	125	124
1	77	174	174	0	11	61	70													

Table III.II (continued)

K	L	OBS CALC	K	L	OBS CALC	K	L	OBS CALC	K	L	OBS CALC	K	L	OBS CALC	K	L	OBS CALC	K	L	OBS CALC	K	L	OBS CALC				
16	-5	289	36	4	-9	73	68	9	-13	56	51	3	-5	80	38	0	-8	78	32	6	-5	56	49	8	-5	63	55
16	-6	81	72	4	-10	76	74	10	-9	50	54	2	-7	178	193	7	-6	111	120	6	-9	52	46	8	-5	149	139
16	-7	95	54	4	-10	74	72	10	-10	51	48	2	-7	178	186	7	-6	109	108	6	-10	109	102	8	-6	12	63
16	-8	204	19	4	-11	63	60	10	-2	35	29	2	-2	22	24	7	-8	138	131	0	-16	61	61	1	-7	124	126
16	-9	41	69	4	-12	142	167	10	-2	51	56	2	-3	91	95	7	-8	35	38	0	-16	70	62	1	-7	19	21
16	-10	40	60	4	-13	52	50	10	-1	50	47	2	-4	29	32	7	-9	103	107	1	-20	293	279	0	-16	64	64
15	-1	59	9	4	-13	18	11	10	-4	62	192	2	-4	29	12	7	-10	0	17	1	-16	196	185	6	-10	14	14
15	-2	59	31	4	-14	84	76	10	-4	53	60	2	-5	103	106	7	-10	56	67	1	-2	214	222	7	-9	94	86
15	-3	59	31	4	-14	84	76	10	-4	53	60	2	-5	103	106	7	-10	56	67	1	-2	214	222	7	-9	94	86
15	-4	15	14	4	-15	40	21	10	-5	47	53	2	-6	68	59	7	-11	245	245	3	-5	58	41	7	-11	122	123
15	-5	33	10	4	-15	76	77	10	-6	52	58	2	-6	159	147	7	-12	21	21	3	-14	14	16	1	-13	153	147
15	-6	55	5	4	-16	44	46	10	-5	55	58	2	-7	100	102	7	-12	104	106	2	-4	106	108	7	-7	23	24
15	-7	55	5	4	-16	31	22	10	-5	55	58	2	-7	116	107	7	-13	113	113	2	-4	106	108	7	-7	23	24
15	-8	46	5	4	-17	78	86	10	-7	108	6	2	-8	15	25	7	-13	104	47	1	-5	60	50	7	-8	195	158
15	-9	59	64	4	-17	149	189	8	-7	17	21	2	-7	213	279	7	-14	45	46	1	-5	32	30	7	-6	24	24
15	-10	59	34	4	-17	149	189	8	-7	17	21	2	-8	147	152	7	-14	45	46	1	-5	32	30	7	-6	24	24
15	-11	59	3	4	-17	149	189	8	-7	17	21	2	-8	147	152	7	-14	45	46	1	-5	32	30	7	-6	24	24
15	-12	59	3	4	-17	137	134	11	-1	125	137	2	-9	105	320	7	-17	176	168	1	-5	140	130	2	-9	50	63
15	-13	65	64	4	-10	6	6	3	182	182	1	-1	142	154	8	-10	110	109	7	-14	54	54	2	-6	245	245	
15	-14	65	64	4	-10	21	20	11	-4	160	159	3	-2	17	16	8	-10	235	235	7	-7	105	107	2	-7	151	151
15	-15	64	64	4	-10	21	20	11	-4	160	159	3	-2	17	16	8	-10	235	235	7	-7	151	151	2	-7	151	151
15	-16	64	64	4	-11	17	17	11	-5	164	145	2	-3	127	141	8	-10	71	67	2	-13	20	25	9	-10	107	107
15	-17	64	64	4	-11	17	17	11	-5	164	145	2	-3	127	141	8	-10	71	67	2	-13	20	25	9	-10	107	107
15	-18	64	64	4	-11	17	17	11	-5	164	145	2	-3	127	141	8	-10	71	67	2	-13	20	25	9	-10	107	107
15	-19	64	64	4	-11	17	17	11	-5	164	145	2	-3	127	141	8	-10	71	67	2	-13	20	25	9	-10	107	107
15	-20	64	64	4	-11	17	17	11	-5	164	145	2	-3	127	141	8	-10	71	67	2	-13	20	25	9	-10	107	107
15	-21	64	64	4	-11	17	17	11	-5	164	145	2	-3	127	141	8	-10	71	67	2	-13	20	25	9	-10	107	107
15	-22	64	64	4	-11	17	17	11	-5	164	145	2	-3	127	141	8	-10	71	67	2	-13	20	25	9	-10	107	107
15	-23	64	64	4	-11	17	17	11	-5	164	145	2	-3	127	141	8	-10	71	67	2	-13	20	25	9	-10	107	107
15	-24	64	64	4	-11	17	17	11	-5	164	145	2	-3	127	141	8	-10	71	67	2	-13	20	25	9	-10	107	107
15	-25	64	64	4	-11	17	17	11	-5	164	145	2	-3	127	141	8	-10	71	67	2	-13	20	25	9	-10	107	107
15	-26	64	64	4	-11	17	17	11	-5	164	145	2	-3	127	141	8	-10	71	67	2	-13	20	25	9	-10	107	107
15	-27	64	64	4	-11	17	17	11	-5	164	145	2	-3	127	141	8	-10	71	67	2	-13	20	25	9	-10	107	107
15	-28	64	64	4	-11	17	17	11	-5	164	145	2	-3	127	141	8	-10	71	67	2	-13	20	25	9	-10	107	107
15	-29	64	64	4	-11	17	17	11	-5	164	145	2	-3	127	141	8	-10	71	67	2	-13	20	25	9	-10	107	107
15	-30	64	64	4	-11	17	17	11	-5	164	145	2	-3	127	141	8	-10	71	67	2	-13	20	25	9	-10	107	107
15	-31	64	64	4	-11	17	17	11	-5	164	145	2	-3	127	141	8	-10	71	67	2	-13	20	25	9	-10	107	107
15	-32	64	64	4	-11	17	17	11	-5	164	145	2	-3	127	141	8	-10	71	67	2	-13	20	25	9	-10	107	107
15	-33	64	64	4	-11	17	17	11	-5	164	145	2	-3	127	141	8	-10	71	67	2	-13	20	25	9	-10	107	107
15	-34	64	64	4	-11	17	17	11	-5	164	145	2	-3	127	141	8	-10	71	67	2	-13	20	25	9	-10	107	107
15	-35	64	64	4	-11	17	17	11	-5	164	145	2	-3	127	141	8	-10	71	67	2	-13	20	25	9	-10	107	107
15	-36	64	64	4	-11	17	17	11	-5	164	145	2	-3	127	141	8	-10	71	67	2	-13	20	25	9	-10	107	107
15	-37	64	64	4	-11	17	17	11	-5	164	145	2	-3	127	141	8	-10	71	67	2	-13	20	25	9	-10	107	107
15	-38	64	64	4	-11	17	17	11	-5	164	145	2	-3	127	141	8	-10	71	67	2	-13	20	25	9	-10	107	107
15	-39	64	64	4	-11	17	17	11	-5	164	145	2	-3	127	141	8	-10	71	67	2	-13	20	25	9	-10	107	107
15	-40	64	64	4	-11	17	17	11	-5	164	145	2	-3	127	141	8	-10	71	67	2	-13	20	25	9	-10	107	107
15	-41	64	64	4	-11	17	17	11	-5	164	145	2	-3	127	141	8	-10	71	67	2	-13	20	25	9	-10	107	107
15	-42	64	64	4	-11	17	17	11	-5	164	145	2	-3	127	141	8	-10	71	67	2	-13	20	25	9	-10	107	107
15	-43	64	64	4	-11	17	17	11	-5	164	145	2	-3	127	141	8	-10	71	67	2	-13	20	25	9	-10	107	107
15	-44	64	64	4	-11	17	17	11	-5	164	145	2	-3	127	141	8	-10	71	67	2	-13	20	25	9	-10	107	107
15	-45	64	64	4	-11	17	17	11	-5	164	145	2	-3	127	141	8	-10	71	67	2	-13	20	25	9	-10	107	107
15	-46	64	64	4	-11	17	17	11	-5	164	145	2	-3	127	141	8	-10	71	67	2	-13	20	25	9	-10	107	107
15	-47	64	64	4	-11	17	17	11	-5	164	145	2	-3	127	141	8	-10	71	67	2	-13	20	25	9	-10	107	107
15	-48	64	64	4	-11	17	17	11	-5	164	145	2	-3	127	141	8	-10	71	67	2	-13	20	25	9	-10	107	107
15	-49	64	64	4	-11	17	17	11	-5	164	145	2	-3	127	141	8	-10	71	67	2	-13	20	25	9	-10	107	107
15	-50	64	64	4	-11	17	17	11	-5	164	145	2	-3	127	141	8	-10	71									

Table III.III

Final positional (fractional, $\times 10^4$) and thermal parameters. Standard deviations are given in parentheses.

ATOM	<u>Molecule 1</u>				<u>Molecule 2</u>			
	<u>X</u>	<u>Y</u>	<u>Z</u>	<u>B</u> (\AA^2)	<u>X</u>	<u>Y</u>	<u>Z</u>	<u>B</u> (\AA^2)
Fe(1)	3759(3)	0773(2)	1986(2)		8370(4)	2441(3)	0695(2)	
Fe(2)	1932(3)	0822(2)	2646(2)		6462(4)	3155(2)	0738(2)	
Fe(3)	1871(4)	0053(2)	1738(2)		6492(4)	2248(2)	-0048(2)	
As(4)	0196(3)	0762(2)	3092(1)		4616(3)	3527(2)	0792(1)	
As(5)	0123(3)	-0490(2)	1633(1)		4683(3)	2109(2)	-0529(1)	
C(6)	4694(31)	1330(18)	2313(16)	5.7(8)	9362(36)	2764(20)	1247(19)	7.5(10)
C(7)	4249(33)	0122(20)	2501(18)	6.7(10)	7881(31)	1830(19)	1184(17)	6.3(9)
C(8)	3046(30)	1380(19)	1537(17)	6.2(9)	8602(28)	3035(18)	0172(16)	5.4(8)
C(9)	4546(25)	0498(15)	1421(14)	4.0(7)	9233(33)	1892(20)	0354(17)	6.7(10)
C(10)	1994(27)	1685(17)	2609(14)	4.5(8)	7087(25)	3905(16)	0714(13)	3.9(7)
C(11)	2881(25)	0779(15)	3292(14)	4.1(7)	6759(29)	3031(18)	1546(18)	6.3(9)
C(12)	2732(26)	-0627(15)	1691(13)	3.6(7)	6756(29)	1425(20)	0014(15)	5.6(9)
C(13)	1908(27)	0271(16)	0975(16)	4.9(8)	7265(34)	2323(20)	-0694(19)	7.4(10)
C(14)	1945(29)	-0133(18)	2620(16)	5.2(8)	5772(27)	2228(16)	0699(15)	4.7(8)
C(15)	0999(27)	0868(16)	1849(14)	4.6(7)	6281(27)	3266(17)	-0138(15)	4.6(8)
C(16)	0063(31)	-1445(19)	1706(17)	7.1(10)	3993(31)	1239(18)	-0461(16)	6.6(9)
C(17)	-0819(30)	-0300(18)	0884(16)	6.4(9)	4406(33)	2319(19)	-1404(17)	7.2(10)
C(18)	0165(29)	0405(17)	3903(16)	5.8(9)	3900(27)	3356(16)	1546(14)	5.1(8)
C(19)	-0710(32)	1564(19)	3118(17)	7.3(10)	4256(29)	4471(17)	0625(15)	5.7(9)
C(20)	-0903(21)	0172(12)	2681(12)	2.3(6)	3474(29)	3127(18)	0239(16)	5.9(9)
C(21)	-0919(25)	-0222(14)	2224(13)	3.9(7)	3508(24)	2691(15)	-0202(13)	3.7(7)
C(22)	-2184(29)	-0009(18)	2810(16)	5.3(8)	2143(31)	3240(19)	0099(17)	6.1(9)
C(23)	-2172(35)	-0456(21)	2266(18)	7.2(10)	2195(28)	2755(18)	-0377(16)	5.1(8)
F(24)	-2237(19)	-0284(11)	3355(11)	8.5(6)	1544(17)	3078(10)	0555(9)	7.6(5)
F(25)	-2908(19)	0507(11)	2770(10)	8.6(6)	1874(18)	3854(11)	-0066(10)	8.1(6)
F(26)	-2951(19)	-0304(11)	1840(10)	8.5(6)	1897(17)	2950(10)	-0961(10)	7.6(5)
F(27)	-2341(17)	-1098(11)	2398(9)	7.7(5)	1612(18)	2176(11)	-0322(10)	8.2(6)

Table III.III (continued)

ATOM	<u>Molecule 1</u>				<u>Molecule 2</u>			
	<u>x</u>	<u>y</u>	<u>z</u>	<u>B</u> (\AA^2)	<u>x</u>	<u>y</u>	<u>z</u>	<u>B</u> (\AA^2)
O(28)	5359(21)	1724(12)	2543(11)	6.9(6)	9953(25)	3063(15)	1584(13)	9.3(8)
O(29)	4592(21)	-0263(13)	2820(12)	7.1(6)	7668(22)	1444(14)	1560(12)	8.2(7)
O(30)	2664(19)	1789(12)	1218(10)	5.8(5)	8924(22)	3447(14)	-0155(12)	8.0(7)
O(31)	5040(20)	0279(11)	1018(11)	6.2(6)	9753(21)	1455(14)	0158(11)	7.5(6)
O(32)	3328(21)	-1087(13)	1590(11)	7.1(6)	6905(21)	0838(14)	0083(11)	7.4(6)
O(33)	1875(20)	0403(12)	0464(12)	6.8(6)	7665(25)	2401(14)	-1167(14)	9.2(8)
O(34)	3426(20)	0789(12)	3745(11)	6.6(6)	6826(20)	2973(12)	2062(12)	7.2(6)
O(35)	1945(20)	2253(13)	2615(10)	6.6(6)	7446(21)	4475(13)	0667(11)	7.1(6)
O(36)	1916(19)	-0608(12)	2926(10)	6.1(6)	5238(18)	1911(11)	1023(10)	5.3(5)
O(37)	0301(18)	1215(9)	1602(9)	4.8(5)	6110(19)	3625(12)	-0531(11)	6.3(6)

	<u>b</u> ₁₁	<u>b</u> ₂₂	<u>b</u> ₃₃	<u>b</u> ₁₂	<u>b</u> ₁₃	<u>b</u> ₂₃ *
<u>Molecule 1</u>						
Fe(1)	53	26	22	-4	4	0
Fe(2)	44	27	21	-6	4	-10
Fe(3)	56	30	17	-6	4	-5
As(4)	48	21	20	-4	5	-6
As(5)	59	24	21	-10	0	-7
<u>Molecule 2</u>						
Fe(1)	48	41	26	0	-1	3
Fe(2)	66	27	31	-1	-6	-8
Fe(3)	54	30	26	3	2	-6
As(4)	65	21	23	1	5	-3
As(5)	71	26	19	-2	-4	-3
Mean σ	4	1	1	2	2	1

* COEFFICIENTS IN THE TEMPERATURE EXPRESSION:
$$\exp -10^{-4} (\underline{b}_{11}\underline{h}^2 + \underline{b}_{22}\underline{k}^2 + \underline{b}_{33}\underline{\ell}^2 + 2\underline{b}_{12}\underline{hk} + 2\underline{b}_{13}\underline{h\ell} + 2\underline{b}_{23}\underline{k\ell})$$

Table III.IV
Equations of weighted mean planes

Equations of planes in the form $\underline{\ell}X' + \underline{m}Y' + \underline{n}Z' = p$, where
 X' , Y' , Z' are coordinates in Å, referred to orthogonal
axes $\underline{a}, \underline{b}, \underline{c}^*$

	$\underline{\ell}$	\underline{m}	\underline{n}	p	Maximum displacement (Å)
Iron triangle (3 Fe atoms)					
Molecule 1	0.3477	-0.7384	0.5778	2.8059	0
Molecule 2	0.3921	0.6513	-0.6497	5.9574	0
Di-(tertiary arsine) (2 As and 4 C atoms)					
Molecule 1	0.2872	-0.7502	0.5956	2.8559	0.009
Molecule 2	0.2296	0.7076	-0.6683	5.0354	0.037

Table III.V

Bond distances (\AA) and valency angles (degrees). Unless otherwise specified, standard deviations of bond lengths are 0.03-0.04 \AA ; of angles at Fe and As, 0.7-1.8 $^\circ$; and of angles at C, 2.2-3.4 $^\circ$.

	<u>Molecule 1</u>	<u>Molecule 2</u>	<u>Molecule 1</u>	<u>Molecule 2</u>
Fe(1)-Fe(2)	2.652(8)	2.643(7)	As(4)-C(20)	1.92
Fe(1)-Fe(3)	2.651(7)	2.671(9)	As(5)-C(21)	1.91
Fe(2)-Fe(3)	2.527(6)	2.517(7)	C(20)-C(21)	1.28
Fe(2)-As(4)	2.301(7)	2.278(6)	C(20)-C(22)	1.58
Fe(3)-As(5)	2.300(6)	2.307(7)	C(21)-C(23)	1.54
Fe(1)-C(6)	1.69	1.75	C(22)-C(23)	1.50
Fe(1)-C(7)	1.80	1.75		
Fe(1)-C(8)	1.74	1.69	C(22)-F(24)	1.33
Fe(1)-C(9)	1.69	1.70	C(22)-F(25)	1.33
Fe(2)-C(10)	1.73	1.67	C(23)-F(26)	1.30
Fe(2)-C(11)	1.75	1.81	C(23)-F(27)	1.34
Fe(3)-C(12)	1.70	1.68	AVERAGE C-F	1.33
Fe(3)-C(13)	1.75	1.74		
AVERAGE Fe-C _{term}	1.73		C(6)-O(28)	1.19
			C(7)-O(29)	1.10
Fe(2)-C(14)	1.91	2.02	C(8)-O(30)	1.15
Fe(2)-C(15)	2.01	1.95	C(9)-O(31)	1.18
Fe(3)-C(14)	1.98	1.90	C(10)-O(35)	1.14
Fe(3)-C(15)	1.94	2.06	C(11)-O(34)	1.15
			C(12)-O(32)	1.18
As(4)-C(18)	1.93	1.94	C(13)-O(33)	1.16
As(4)-C(19)	1.92	1.97	C(14)-O(36)	1.17
As(5)-C(16)	1.92	1.93	C(15)-O(37)	1.18
As(5)-C(17)	1.96	1.98	AVERAGE C-O	1.16
AVERAGE As-Me	1.94			

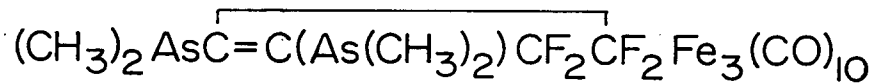
Table III.V (continued)

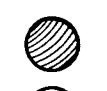
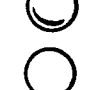
	<u>Molecule</u>			<u>Molecule</u>	
	<u>1</u>	<u>2</u>		<u>1</u>	<u>2</u>
C(6)-Fe(1)-C(7)	92	93	Fe(2)-As(4)-C(18)	119	116
C(6)-Fe(1)-C(8)	93	95	Fe(2)-As(4)-C(19)	118	120
C(6)-Fe(1)-C(9)	100	100	Fe(2)-As(4)-C(20)	114	116
C(6)-Fe(1)-Fe(2)	105	107	C(18)-As(4)-C(19)	104	104
C(7)-Fe(1)-C(9)	94	93	C(18)-As(4)-C(20)	99	99
C(7)-Fe(1)-Fe(2)	85	93	C(19)-As(4)-C(20)	100	99
C(7)-Fe(1)-Fe(3)	88	90	Fe(3)-As(5)-C(16)	120	116
C(8)-Fe(1)-C(9)	94	92	Fe(3)-As(5)-C(17)	116	121
C(8)-Fe(1)-Fe(2)	86	79	Fe(3)-As(5)-C(21)	113	113
C(8)-Fe(1)-Fe(3)	85	81	C(16)-As(5)-C(17)	104	103
C(9)-Fe(1)-Fe(3)	96	97	C(16)-As(5)-C(21)	101	99
Fe(2)-Fe(1)-Fe(3)	56.9(2)	56.5(2)	C(17)-As(5)-C(21)	100	102
C(10)-Fe(2)-C(11)	94	96	As(4)-C(20)-C(21)	137	134
C(10)-Fe(2)-C(15)	86	83	As(4)-C(20)-C(22)	131	134
C(10)-Fe(2)-As(4)	97	97	C(21)-C(20)-C(22)	92	92
C(11)-Fe(2)-C(14)	88	88	As(5)-C(21)-C(20)	137	136
C(11)-Fe(2)-As(4)	100	96	As(5)-C(21)-C(23)	127	130
C(14)-Fe(2)-Fe(3)	51	48	C(20)-C(21)-C(23)	96	93
C(14)-Fe(2)-As(4)	88	86			
C(15)-Fe(2)-Fe(3)	49	53	C(20)-C(22)-F(24)	111	112
C(15)-Fe(2)-As(4)	87	89	C(20)-C(22)-F(25)	114	114
Fe(1)-Fe(2)-C(10)	89	97	C(20)-C(22)-C(23)	86	88
Fe(1)-Fe(2)-C(11)	88	82	F(24)-C(22)-C(23)	119	117
Fe(1)-Fe(2)-C(14)	87	80	F(24)-C(22)-F(25)	109	109
Fe(1)-Fe(2)-C(15)	86	94	F(25)-C(22)-C(23)	117	117
Fe(1)-Fe(2)-Fe(3)	61.5(2)	62.3(2)			
Fe(3)-Fe(2)-As(4)	109.1(2)	109.1(2)	C(21)-C(23)-F(26)	120	116
C(12)-Fe(3)-C(13)	95	93	C(21)-C(23)-F(27)	118	113
C(12)-Fe(3)-C(14)	86	90	C(21)-C(23)-C(22)	86	88
C(12)-Fe(3)-As(5)	97	94	F(26)-C(23)-C(22)	114	119
C(13)-Fe(3)-C(15)	88	84	F(26)-C(23)-F(27)	106	103
C(13)-Fe(3)-As(5)	96	98	F(27)-C(23)-C(22)	113	118
C(14)-Fe(3)-Fe(2)	48	52	Fe(1)-C(6)-O(28)	180	170
C(14)-Fe(3)-As(5)	90	88	Fe(1)-C(7)-O(29)	177	172
C(15)-Fe(3)-Fe(2)	51	49	Fe(1)-C(8)-O(30)	174	170
C(15)-Fe(3)-As(5)	87	89	Fe(1)-C(9)-O(31)	176	171
Fe(1)-Fe(3)-C(12)	88	87	Fe(2)-C(10)-O(35)	174	174
Fe(1)-Fe(3)-C(13)	90	93	Fe(2)-C(11)-O(34)	173	173
Fe(1)-Fe(3)-C(14)	85	82	Fe(3)-C(12)-O(32)	173	177
Fe(1)-Fe(3)-C(15)	87	90	Fe(3)-C(13)-O(33)	176	172
Fe(1)-Fe(3)-Fe(2)	61.6(2)	61.2(2)	Fe(2)-C(14)-O(36)	143	134
Fe(2)-Fe(3)-As(5)	110.4(3)	110.7(2)	Fe(3)-C(14)-O(36)	136	146
			Fe(2)-C(15)-O(37)	139	147
			Fe(3)-C(15)-O(37)	142	136

DISCUSSION

The molecule (Figure III.2) is best described as a derivative of $\text{Fe}_3(\text{CO})_{12}$ ¹⁸, with one equatorial carbonyl group on each of the two equivalent iron atoms replaced by the arsenic atoms of the di-(tertiary arsine) ligand. In each of the two molecules in the asymmetric unit, the arsenic and carbon atoms of the ligand are coplanar (Table III.IV) in contrast to the non-planarity in $\text{LFe}_2(\text{CO})_6$.¹⁹ Presumably the deviation from planarity in the latter compound is associated with the involvement of the cyclo-butene π -electrons in bonding to one of the iron atoms; this bonding is not present in $\text{LFe}_3(\text{CO})_{10}$, so that planarity of the ligand is not unexpected. The difference in bonding in the two compounds is further indicated by the C=C bond lengths; the distance (Table III.V) in $\text{LFe}_3(\text{CO})_{10}$ is 1.30(3) Å (standard deviation in parentheses), indicating retention of double-bond character, while the corresponding length in $\text{LFe}_2(\text{CO})_6$ is 1.51(4) Å, consistent with the involvement of the π -electrons in bonding to an iron atom.

In each of the two $\text{LFe}_3(\text{CO})_{10}$ molecules in the asymmetric unit, the ligand is not quite coplanar with the iron triangle, and the amount of bending is slightly different in the two molecules. In molecule 1 the angle between the triangle and ligand planes is only 3.7°, but molecule 2 is more significantly bent, the angle being 9.9°. Since the angle is different in the two molecules, the



-  As
-  Fe
-  F
-  O
-  C

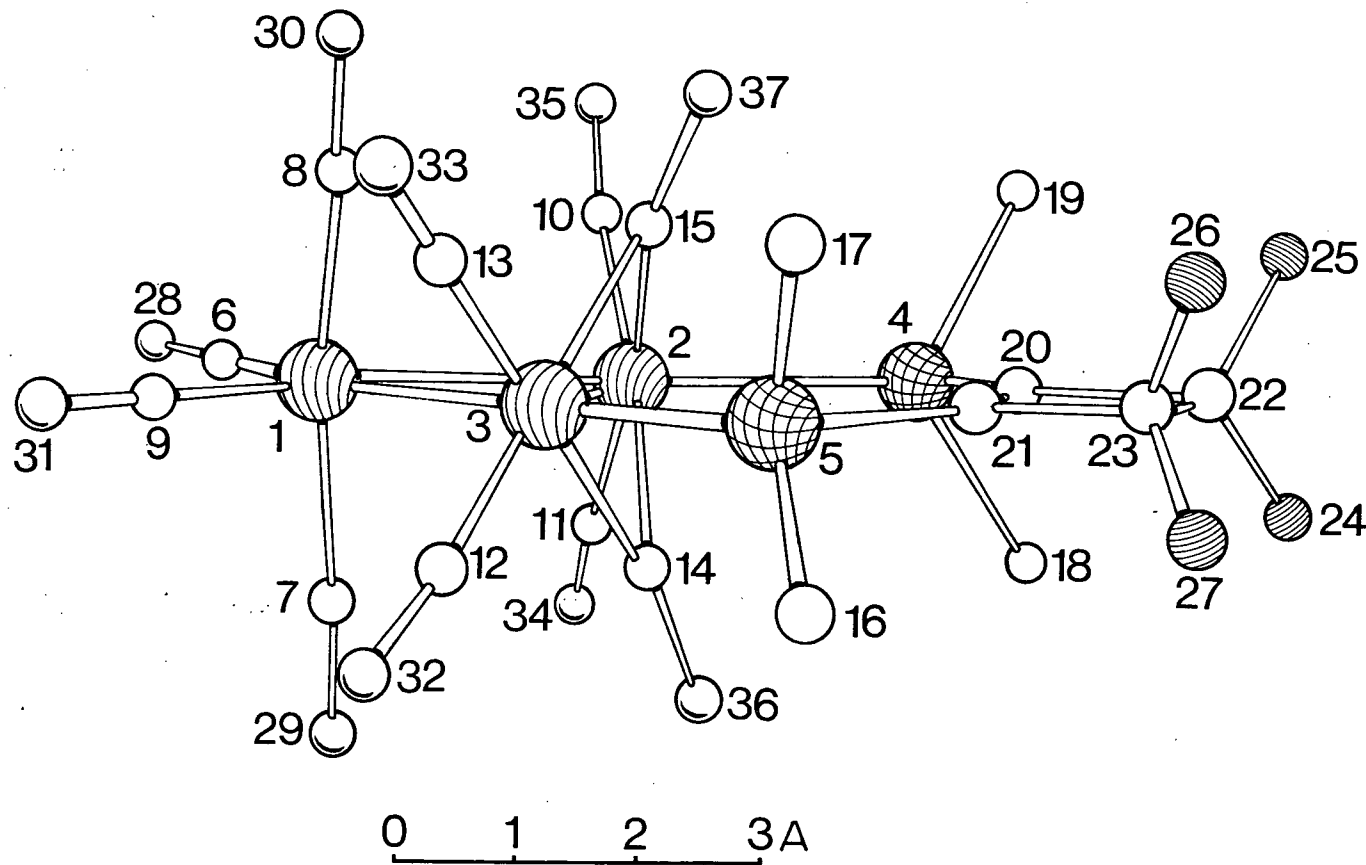
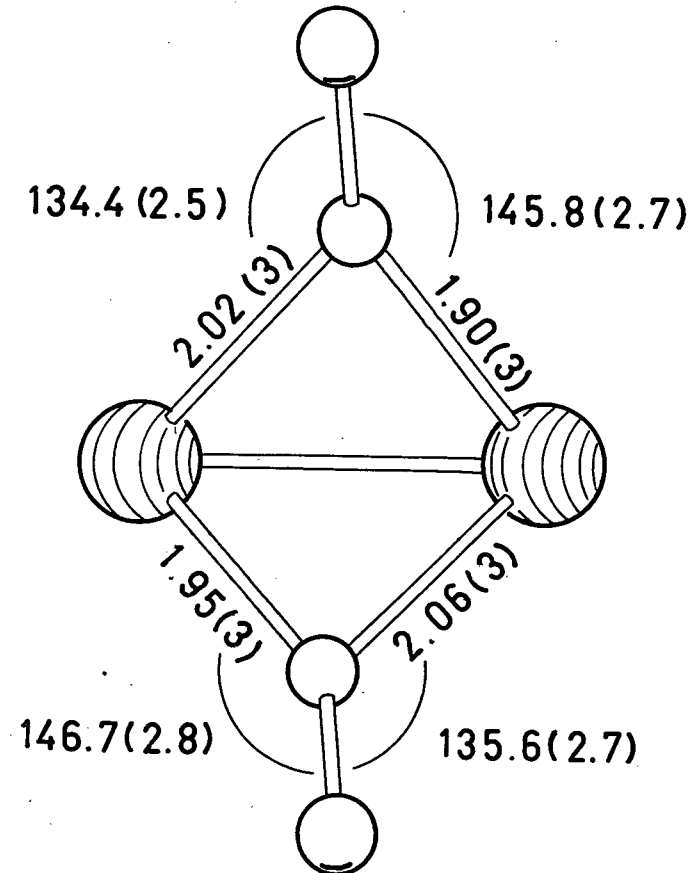
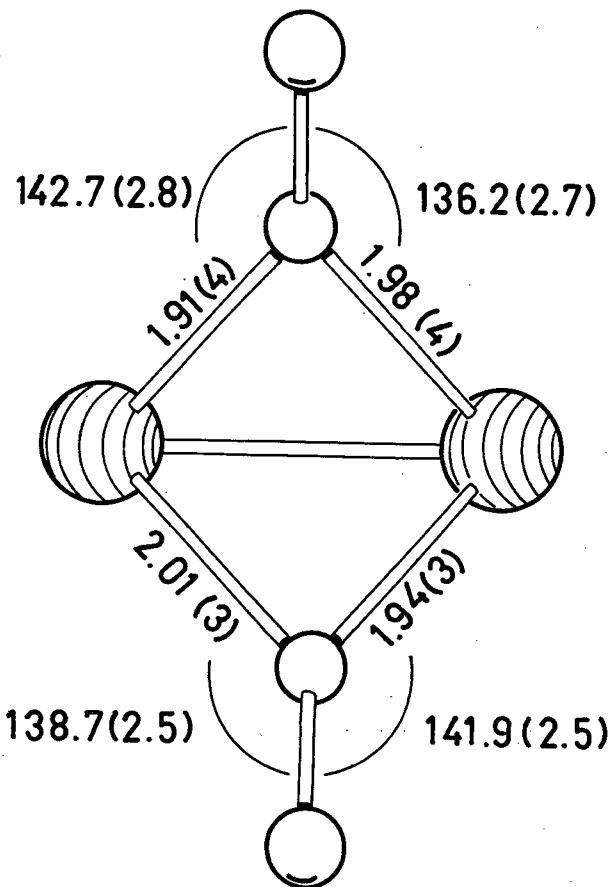


Figure III.2 Molecular structure of $\text{LFe}_3(\text{CO})_{10}$.

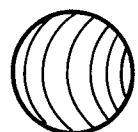
small deviations from planarity are probably a result of crystal packing forces.

The bond lengths and valency angles in the two $LFe_3(CO)_{10}$ molecules in the asymmetric unit are not significantly different (Table III.V). The Fe-Fe distances in the isosceles iron triangle are $2.65(1)$ Å for the equivalent bonds, and $2.53(1)$ Å for the carbonyl-bridged bond. These lengths are close to the distances of $2.67(1)$ Å and $2.56(1)$ Å for the parent $Fe_3(CO)_{12}$ molecule,¹⁸ so that replacement of two terminal carbonyl groups by the di-(tertiary arsine) ligand has apparently proceeded with little disturbance of the bonding in the iron triangle.

The mean Fe-C(terminal) distance is 1.73 Å, close to the distance found in related compounds,²⁷⁻³⁰ and all the Fe-C-O are close to linear, as expected.³¹ The Fe-C(bridging) distances are considerably longer, and the bridges appear to be slightly asymmetric (Figure III.3). The mean of the four longer Fe-C(bridging) bonds (with standard deviation of the mean) is $2.02(2)$ Å, while the average of the shorter bonds is $1.93(2)$ Å, the difference being greater than 3σ and probably significant. This asymmetry is similar to, although not as pronounced as that found in $Ph_3PFe_3(CO)_{11}$ (average Fe-C(bridging), 2.04 and 1.87 Å).²⁷ As Dahm and Jacobson point out,²⁷ this asymmetry need not be the result of crystal packing forces, but could be inherent in the bonding of the parent $Fe_3(CO)_{12}$,



MOLECULE 1



Fe



O



C

MOLECULE 2

Figure III.3 View of asymmetric carbonyl bridges.

in which there is some evidence for unsymmetrical bridging carbonyl groups.¹⁸ The C-O bond lengths average 1.17 Å, and the distances in the bridging carbonyls are not significantly longer than the average.

All the other bond lengths and valency angles (Table III.V) are quite similar to those in related compounds. The angles in the $\text{Fe}_3(\text{CO})_{10}$ moiety are similar to those in $\text{Ph}_3\text{PFe}_3(\text{CO})_{11}$ ²⁷ and the dimensions of the di-(tertiary arsine) ligand are close to those in $\text{LCo}_2(\text{CO})_6$ ³² and $\text{LFe}_2(\text{CO})_6$ ¹⁹ apart from the differences caused by the non-planarity of the ligand in the latter compound. The valency angles at arsenic show deviations from the exact tetrahedral value (Figure III.4), the Fe-As-C angles (113-121°) being larger than the C-As-C angles (99-104°). Fe-As bond lengths (mean 2.297 Å) correspond to those found in $\text{LFe}_2(\text{CO})_6$ ¹⁹ and $\{\text{Fe}(\text{CO})_3\}_2(\text{AsMe}_3)_4$.³³

The magnitudes of the principal axes of the thermal vibration ellipsoids of the iron and arsenic atoms are given in Table III.VI. The largest vibrations are approximately perpendicular to the plane of the iron triangle.

All the intermolecular distances correspond to normal van der Waals interactions, the closest approaches being about 3.1 Å. The molecules are arranged (Figure III.5) so that an oxygen atom of a bridging carbonyl group of each molecule in the asymmetric unit is approximately equidistant

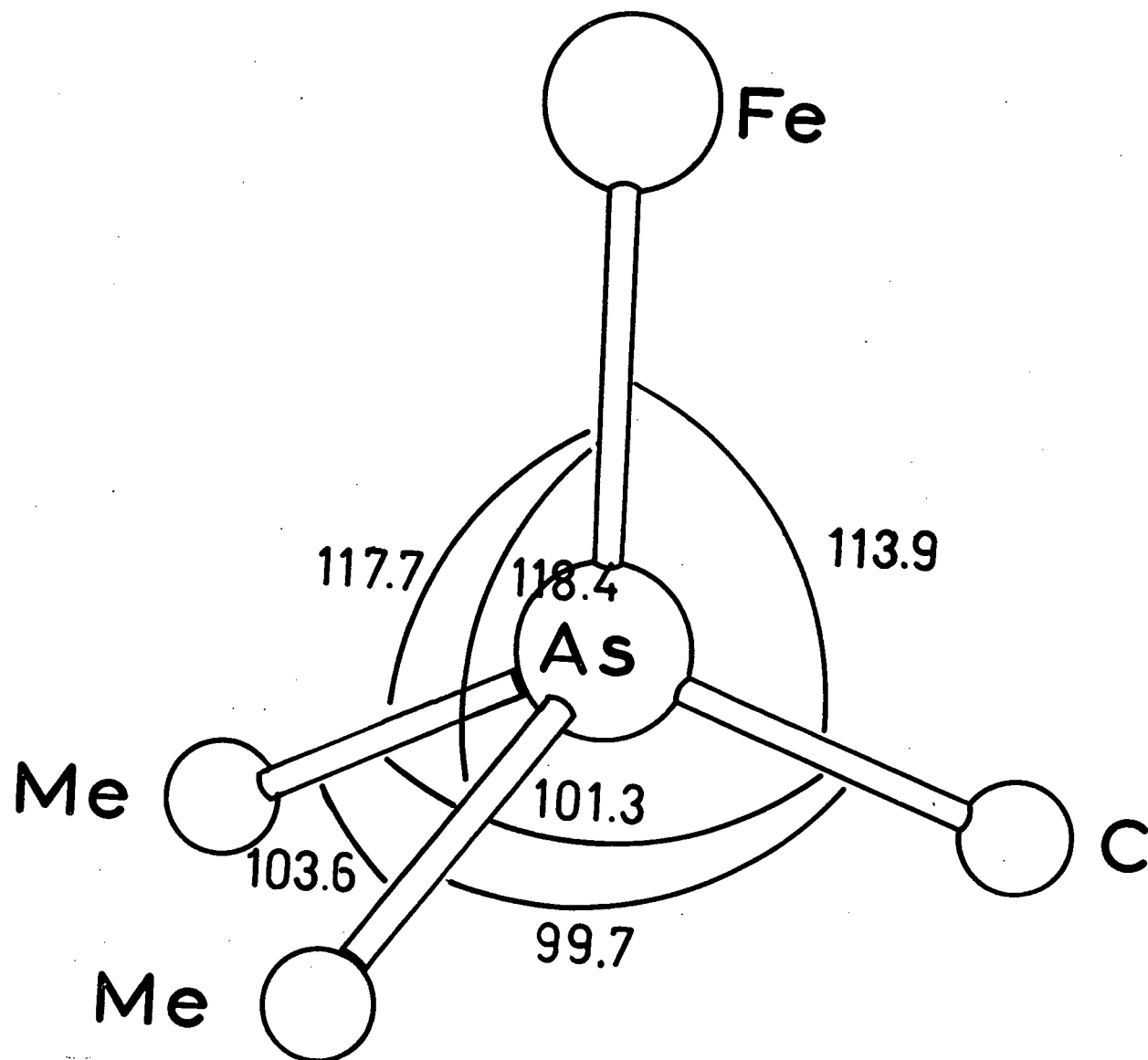


Figure III.4 Co-ordination about arsenic atoms, showing angles averaged over the four arsenic atoms in the asymmetric unit.

Table III.VI

Magnitudes (\AA , $\sigma = 0.005\text{--}0.008 \text{\AA}$) of the principal axes of the thermal vibration ellipsoids of the iron and arsenic atoms

	<u>Molecule 1</u>			<u>Molecule 2</u>		
	Axis 1	Axis 2	Axis 3	Axis 1	Axis 2	Axis 3
Fe(1)	0.186	0.233	0.235	0.179	0.249	0.292
Fe(2)	0.165	0.175	0.277	0.195	0.223	0.298
Fe(3)	0.190	0.192	0.261	0.190	0.222	0.273
As(4)	0.177	0.179	0.249	0.194	0.212	0.243
As(5)	0.166	0.218	0.260	0.193	0.232	0.240

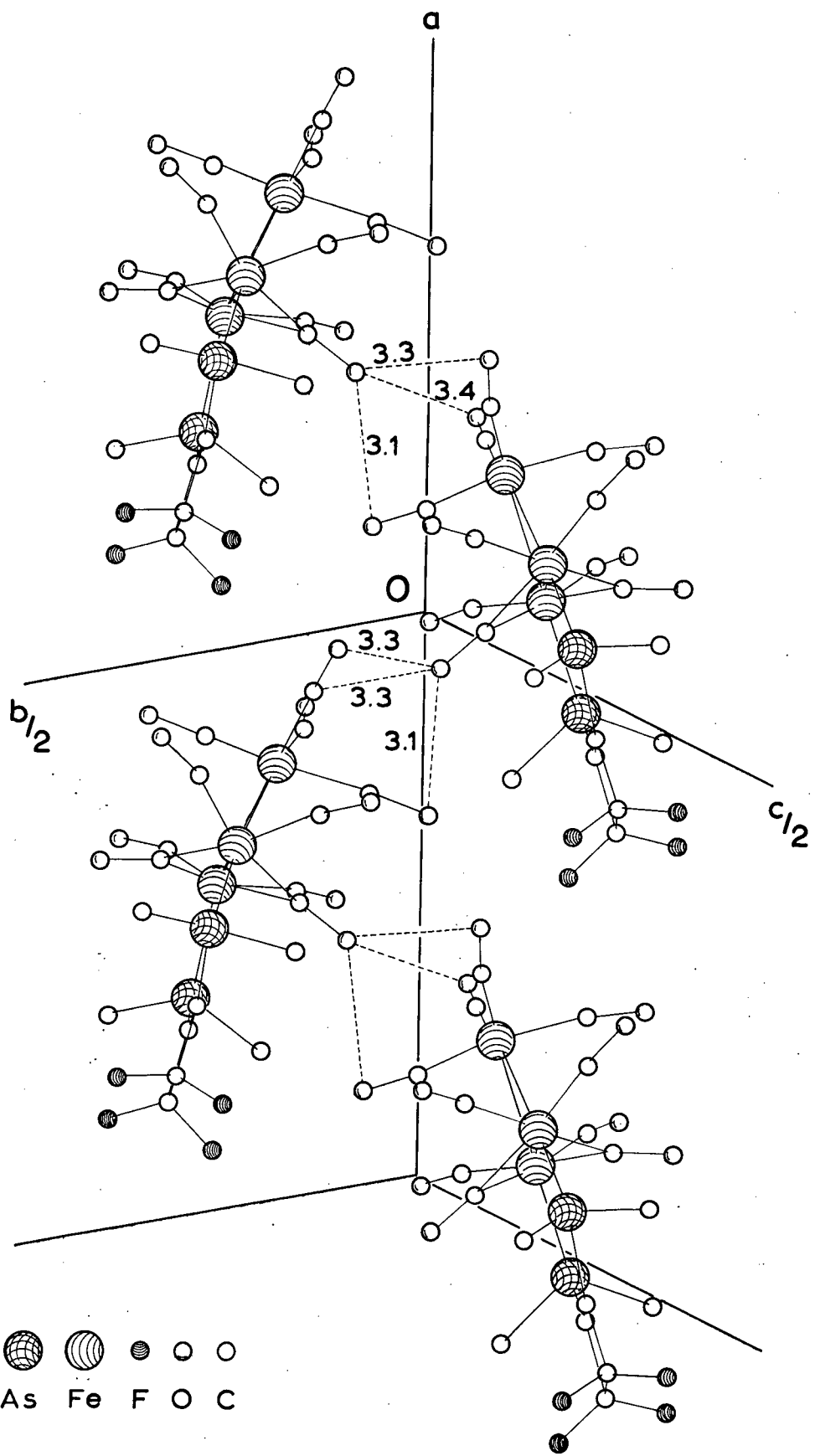


Figure III.5 Intermolecular contacts in general view.

from three of the four terminal carbonyl groups of the unique iron atom of the other molecule. Another, simplified view of the molecular packing is shown in Figure III.6.

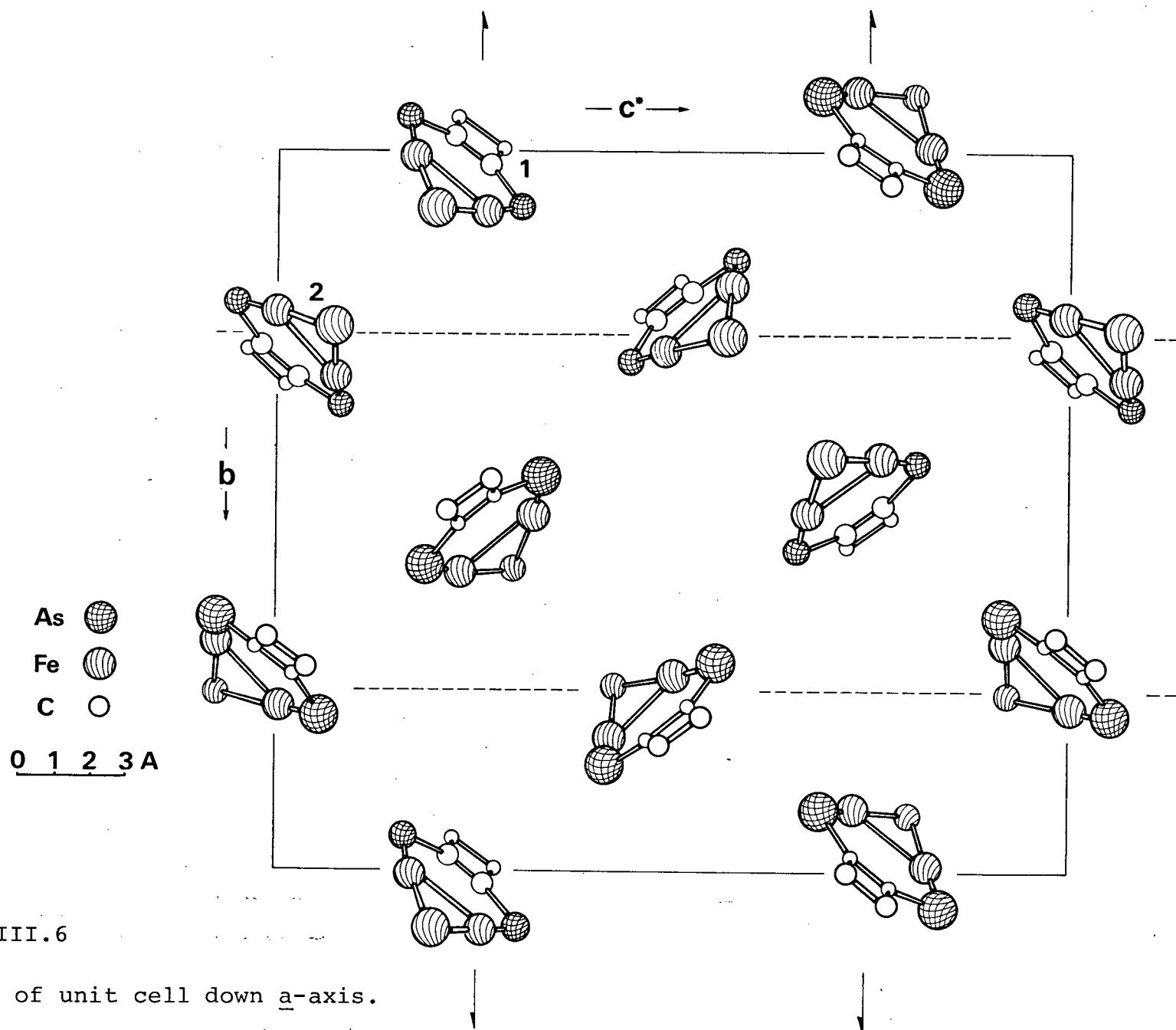
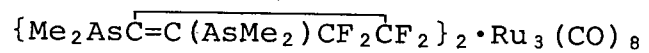


Figure III.6

Projection of unit cell down a-axis.

IV. THE STRUCTURE DETERMINATION OF



STRUCTURE ANALYSIS

The asymmetric unit contains half a molecule, requiring that the molecule be located on a crystallographic symmetry element. Since the molecule is not centrosymmetric (it contains three ruthenium atoms in a triangle), it was expected to lie on the two-fold axis at $(0, y, \frac{1}{4})$ of Pbcn. The structure was solved by the use of three dimensional direct methods. Sixteen sets of signs for 219 reflections having normalized structure factor $|E| > 1.50$ were determined by Long's computer program, in which Sayre relationships were applied in an iterative procedure.³⁴ The program uses a starting set of seven signs and applies Sayre's equation in conjunction with other conditions imposed on the E 's by space group symmetry. The first three E 's are chosen to specify the origin and can be arbitrarily assigned positive signs. The other four are allowed to take on both positive and negative signs in turn. The E 's are ordered in such a way that the starting set is at the beginning, followed by the remainder, sorted in order of decreasing $|E|$. From each of the starting sets, the program predicts the signs for reflections below on the list. Each new prediction is used to determine signs further down the list. When the bottom of the list is reached, the iteration is repeated, starting with the eighth reflection (the signs of the starting set are not allowed to change). The number of sign changes and the number of signs newly determined

are counted for each cycle and the iteration is said to have converged when there are no additions to or changes in the list of signs.

A consistency index, \underline{U} , is defined as³⁴

$$\underline{U} = \frac{\langle |\underline{E}_{\vec{h}_1} \sum \underline{E}_{\vec{h}_2} \underline{E}_{\vec{h}_3}| \rangle}{\langle |\underline{E}_{\vec{h}_1}| \sum |\underline{E}_{\vec{h}_2}| |\underline{E}_{\vec{h}_3}| \rangle} \quad (4.1)$$

where the sums are over all pairs \vec{h}_2 and \vec{h}_3 for which $\vec{h}_2 + \vec{h}_3 = \vec{h}_1$ and where $\langle \rangle$ means "average over all values of \vec{h}_1 ". The true solution will usually be the most consistent one, *i.e.* it will have the highest consistency index. Usually the correct solution requires fewer iterative cycles and converges to a set of signs which are approximately equally distributed between positive and negative. Table IV.I gives a comparison of the sixteen possible solutions generated for the present structure. Solution 9 was outstanding in that the iteration procedure converged in three cycles to a set of signs having the highest consistency index (0.95) and equal numbers of positive and negative signs. An E -map calculated with this set of signs indicated the positions of four independent atoms, one of which was situated on the two-fold rotation axis as expected. The positions and thermal parameters of these four atoms (assigned as two As and two Ru) were improved by two cycles of full-matrix least-squares refinement, with use of the scattering factors of ref. 26. The real part of the dispersion correction was applied. A difference synthesis

Table IV.I
 Comparison of the 16 solutions from
 Long's sign determination program

Set	Signs of starting set	Number of cycles	Number of pluses	Number of minuses	Consistency index <u>U</u>
1	++++++	7	109	110	0.539
2	+++++-	8	103	116	0.464
3	+++-+-	12	112	107	0.641
4	++--++	5	117	102	0.896
5	++-++-	12	116	103	0.588
6	++-+-+	6	108	111	0.638
7	++--++	5	108	111	0.691
8	++-+--	8	103	116	0.543
9	++-+--	3	109	110	0.954
10	++-+--	6	109	110	0.909
11	++-+--	5	110	109	0.684
12	++-+--	10	108	111	0.481
13	++-+--	7	106	113	0.899
14	++-+--	8	102	117	0.557
15	++-+--	7	110	109	0.680
16	++-+--	12	105	114	0.424

phased on the refined parameters revealed the positions of all twenty carbon, oxygen, and fluorine atoms.

Two cycles of full-matrix refinement, with minimization of $\sum_w (F_O - F_C)^2$, $w = \{A + B|F_O| + C|F_O|^2 + D|F_O|^3\}^{-1}$ for observed reflections (unobserveds were excluded from refinement but included in final structure factor calculation), reduced R to 0.124. A , B , C , and D were adjusted to give constant average values of $w(F_O - F_C)^2$ over the whole range of $|F_O|$, the final values being 37.32, 1.09, -0.0159, and 0.00008 respectively. At this stage a difference map showed small peaks and troughs around the positions of the ruthenium and arsenic atoms. Two further cycles of full-matrix refinement using anisotropic thermal parameters for the heavy atoms reduced R to 0.089. A difference map computed at this stage indicated the necessity of also treating the fluorine atoms anisotropically. Two final cycles of full-matrix refinement were carried out varying the positional parameters, anisotropic thermal parameters for the ruthenium, arsenic, and fluorine atoms, isotropic thermal parameters for the other atoms, and a single overall scale factor, for a total of 133 variables. At final convergence of the refinement, R and R_w were 0.078 and 0.098 respectively, for the 1507 observed reflections, and 0.088 and 0.114 respectively, for all data. Measured and calculated structure factors are listed in Table IV.II. A final difference map showed fluctuations around the heavy

Table IV.II

Final measured and calculated structure factors. Unobserved reflections have an asterisk after the $|F_O|$ value.

R	L	OBS CALC	R	L	OBS CALC	R	L	OBS CALC	R	L	OBS CALC	R	L	OBS CALC	R	L	OBS CALC	R	L	OBS CALC	R	L	OBS CALC													
**** H = 0****																																				
0	11	150	157	-10	10	22	17	4	6	222	218	14	8	8*	5	8	5	153	149	5	13	41	53	0	2	230	309									
0	4	98	37	-13	129	135	11	32	26	4	7	232	233	14	8	42	52	8	4	102	108	1	14	102	108	0	4	125	158							
0	6	145	159	-14	145	146	10	13	56	52	4	9	199	202	14	10	48	50	9	20	199	202	5	14	51	53	0	6	125	158						
0	8	94	109	-15	15	20	14	10	48	58	4	10	49	47	14	12	66	68	8	8	109	109	0	8	75	36	1	2	109	109						
0	10	145	145	-17	15	16	14	10	48	58	4	10	49	47	14	12	66	68	8	8	109	109	1	12	66	68	0	8	85	85						
0	12	111	127	-17	10	30	40	10	16	76	68	12	22	29	15	2	40	41	10	9	48	49	1	14	12	12	1	12	5	41	43					
0	14	333	354	-18	111	111	10	17	18	2	13	12	29	15	2	41	46	8	10	10	10	1	12	29	27	1	12	11	11	1	12	148	150			
0	16	172	125	-19	10	20	27	11	15	16	14	10	16	159	159	15	5	101	106	8	11	106	105	5	14	2	177	167	1	10	105	105	0	2	10	9
0	18	126	126	-20	10	20	27	11	15	16	14	10	16	159	159	15	5	101	106	8	11	106	105	5	14	2	177	167	1	10	105	105	0	2	10	9
0	20	112	112	-21	1	154	155	11	2	44	40	4	16	109	9	5	6	76	88	8	13	114	107	2	11	12	12	1	12	2	24	27				
2	0	456	437	-22	2	222	202	11	3	11	14	5	17	26	19	15	7	11*	15	6	4	6	137	137	1	12	3	62	60	1	12	132	132			
2	1	211	211	-23	2	222	202	11	3	11	14	5	17	26	19	15	7	11*	15	6	4	6	137	137	1	12	3	62	60	1	12	132	132			
2	2	103	104	-24	4	19	26	11	5	55	64	6	10	50	48	13	9	19	24	1	12	83	79	1	12	5	55	64	1	12	104	104				
2	3	27	29	-5	9	10	15	6	1	6	26	26	5	1	86	78	15	10	47	47	8	17	16	8	8	38	36	1	12	32	32					
2	4	97	97	-6	7	10	34	6	1	6	26	26	5	1	86	78	15	10	47	47	8	17	16	8	8	38	36	1	12	32	32					
2	6	290	307	-7	8	179	193	9	1	6	17	16	5	4	40	35	16	2	30	29	2	10	16	16	1	12	105	105								
2	7	224	231	-8	10	20	27	11	15	16	14	10	16	159	159	15	5	101	106	8	11	106	105	5	14	2	177	167								
2	9	10	9	-9	10	20	27	11	15	16	14	10	16	159	159	15	5	101	106	8	11	106	105	5	14	2	177	167								
2	9	162	162	-10	11	15	18	11	15	16	14	10	16	159	159	15	5	101	106	8	11	106	105	5	14	2	177	167								
2	10	266	291	-11	12	171	185	11	15	16	14	10	16	159	159	15	5	101	106	8	11	106	105	5	14	2	177	167								
2	11	207	207	-12	14	77	81	11	15	16	14	10	16	159	159	15	5	101	106	8	11	106	105	5	14	2	177	167								
2	13	159	177	-13	2	23	22	11	15	16	14	10	16	159	159	15	5	11	41	40	17	2	26	29	1	12	105	105								
2	14	174	195	-14	2	23	22	11	15	16	14	10	16	159	159	15	5	12	41	40	17	2	26	29	1	12	105	105								
2	16	152	152	-15	2	18	10*	6	1	6	23	29	12	15	9	14	41	42	9	12	53	49	5	3	195	190	2	12	105	105						
2	17	10*	9	-16	19	19	11	12	4	5	15	35	31	1	12	101	101	5	14	2	177	167	1	12	105	105	0	2	12	105						
2	19	31	31	-17	3	0	120	125	12	6	177	175	15	5	17	0*	17	2	26	29	12	15	9	14	2	177	167	1	12	105	105					
2	20	106	105	-18	5	121	103	7	2	71	15	16	12	26	26	0	2	50	49	9	16	60	60	7	16	5	17	16	16	2	12	105	105			
2	4	264	252	-19	5	121	103	7	2	71	15	16	12	26	26	0	2	50	49	9	16	60	60	7	16	5	17	16	16	2	12	105	105			
2	6	48	48	-20	3	122	125	12	6	15	55	58	6	1	106	40	8	47	3	3	216	216	5	10	90	90	2	12	105	105						
2	8	15	15	-21	3	122	125	12	6	15	55	58	6	1	106	40	8	47	3	3	216	216	5	10	90	90	2	12	105	105						
2	10	60	54	-22	5	14	24	24	11	15	21	12	17	12	61	55	7	16	57	57	16	55	61	55	7	16	57	57	2	12	105	105				
2	12	15	15	-23	5	14	24	24	11	15	21	12	17	12	61	55	7	16	57	57	16	55	61	55	7	16	57	57	2	12	105	105				
2	14	15	15	-24	5	14	24	24	11	15	21	12	17	12	61	55	7	16	57	57	16	55	61	55	7	16	57	57	2	12	105	105				
2	16	54	54	-25	5	14	24	24	11	15	21	12	17	12	61	55	7	16	57	57	16	55	61	55	7	16	57	57	2	12	105	105				
2	18	54	54	-26	5	14	24	24	11	15	21	12	17	12	61	55	7	16	57	57	16	55	61	55	7	16	57	57	2	12	105	105				
2	20	54	54	-27	5	14	24	24	11	15	21	12	17	12	61	55	7	16	57	57	16	55	61	55	7	16	57	57	2	12	105	105				
2	22	54	54	-28	5	14	24	24	11	15	21	12	17	12	61	55	7	16	57	57	16	55	61	55	7	16	57	57	2	12	105	105				
2	24	54	54	-29	5	14	24	24	11	15	21	12	17	12	61	55	7	16	57	57	16	55	61	55	7	16	57	57	2	12	105	105				
2	26	54	54	-30	5	14	24	24	11	15	21	12	17	12	61	55	7	16	57	57	16	55	61	55	7	16	57	57	2	12	105	105				
2	28	54	54	-31	5	14	24	24	11	15	21	12	17	12	61	55	7	16	57	57	16	55	61	55	7	16	57	57	2	12	105	105				
2	30	54	54	-32	5	14	24	24	11	15	21	12	17	12	61	55	7	16	57	57	16	55	61	55	7	16	57	57	2	12	105	105				
2	32	54	54	-33	5	14	24	24	11	15	21	12	17	12	61	55	7	16	57	57	16	55	61	55	7	16	57	57	2	12	105	105				
2	34	54	54	-34	5	14	24	24	11	15	21	12	17	12	61	55	7	16	57	57	16	55	61	55	7	16	57	57	2	12	105	105				
2	36	54	54	-35	5	14	24	24	11	15	21	12	17	12	61	55	7	16	57	57	16	55	61	55	7	16	57	57	2	12	105	105				
2	38	54	54	-36	5	14	24	24	11	15	21	12	17	12	61	55	7	16	57	57	16	55	61	55	7	16	57	57	2	12	105	105				
2	40	54	54	-37	5	14	24	24	11	15	21	12	17	12	61	55	7	16	57	57	16	55	61	55	7	16	57	57	2	12	105	105				
2	42	54	54	-38	5	14	24	24	11	15	21	12	17	12	61	55	7	16	57	57	16	55	61	55	7	16	57	57	2	12	105	105				
2	44	54	54	-39	5	14	24	24	11	15	21	12	17	12	61	55	7	16	57	57	16															

atoms of $\pm 1.5 \text{ e}/\text{\AA}^3$, which could not be attributed to any elements of the structure and were assumed to be a result of random experimental error.

Table IV.III gives the final positional and thermal parameters, with standard deviations calculated from the inverse matrix of the last cycle of refinement. Bond distances and valence angles are given in Table IV.IV. Standard deviations for these quantities include a contribution from the standard deviations of the lattice parameters. Table IV.V gives the equations of the weighted mean planes of the ruthenium triangle and the arsenic and carbon atoms of the di-(tertiary arsine) ligand. The magnitudes of the principal axes of anisotropic thermal vibration ellipsoids are in Table IV.VI.

Table IV.III
 Final positional (fractional, $\times 10^4$) and thermal parameters,
 with standard deviations in parentheses.

ATOM	<u>x</u>	<u>y</u>	<u>z</u>	<u>B</u> or <u>b</u> ₁₁	<u>b</u> ₂₂	<u>b</u> ₃₃	<u>b</u> ₁₂	<u>b</u> ₁₃	<u>b</u> ₂₃ [†]
Ru(1)	0	1014(1)	2500	1014(39)	101(8)	189(7)	0	- 68(12)	0
Ru(2)	0686(2)	-0329(1)	3071(1)	1013(29)	113(6)	187(5)	28(9)	- 44(9)	8(4)
As(1)	0189(3)	1847(1)	3340(1)	1386(41)	110(7)	245(7)	72(13)	-125(13)	- 35(5)
As(2)	2288(2)	0000(1)	3909(1)	1003(35)	162(8)	188(6)	66(13)	- 61(11)	- 15(5)
F(1)	2657(22)	2546(10)	4549(8)	3493(319)	267(79)	463(53)	-298(130)	-637(111)	- 7(53)
F(2)	0652(23)	2200(12)	4981(10)	3799(392)	623(94)	396(66)	617(163)	-107(136)	-158(66)
F(3)	1952(19)	1013(10)	5378(8)	4149(310)	414(72)	210(51)	181(120)	-122(100)	- 10(51)
F(4)	3968(22)	1332(11)	4931(9)	2783(363)	294(83)	571(58)	128(140)	-691(111)	- 91(56)
C(1)	2102(29)	0973(14)	2434(12)	4.5(6)					
C(2)	2281(25)	-0586(12)	2560(10)	3.6(5)					
C(3)	0225(28)	-1266(14)	3311(11)	4.3(5)					
C(4)	-0948(26)	0081(13)	3505(11)	3.8(5)					
C(5)	1275(25)	1560(12)	4054(10)	3.3(5)					
C(6)	1734(32)	1978(15)	4623(12)	5.4(6)					
C(7)	2003(23)	0956(12)	4265(10)	3.2(4)					
C(8)	2448(31)	1294(14)	4843(12)	5.2(5)					
Me(1)	1250(35)	2780(17)	3192(13)	6.2(7)					
Me(2)	-1618(39)	2147(20)	3771(16)	7.4(8)					
Me(3)	2171(29)	-0563(14)	4650(12)	4.6(6)					
Me(4)	4427(33)	0051(17)	3766(13)	6.0(7)					
O(1)	3360(22)	1028(10)	2400(8)	5.7(4)					
O(2)	3278(19)	-0782(9)	2276(8)	5.1(4)					
O(3)	-0111(22)	-1861(11)	3432(9)	6.5(5)					
O(4)	-1890(19)	0271(10)	3810(8)	5.2(4)					

[†]coefficients in the temperature expression: $\exp -10^{-5} (\underline{b}_{11}\underline{h}^2 + \underline{b}_{22}\underline{k}^2 + \underline{b}_{33}\underline{\ell}^2 + 2\underline{b}_{12}\underline{hk} + 2\underline{b}_{13}\underline{hl} + 2\underline{b}_{23}\underline{kl})$

Table IV.IV

Bond distances (\AA) and valence angles (degrees),
with standard deviations in parentheses.

Ru(1)-Ru(2)	2.853(3)	C(5)-C(7)	1.39(3)
Ru(1)-As(1)	2.401(3)	C(5)-C(6)	1.52(3)
Ru(1)-C(1)	1.91(3)	C(6)-C(8)	1.46(3)
		C(7)-C(8)	1.46(3)
Ru(2)-Ru(2')	2.785(4)		
Ru(2)-C(2)	1.89(2)	C(6)-F(1)	1.35(3)
Ru(2)-C(3)	1.86(3)	C(6)-F(2)	1.32(3)
Ru(2)-C(4)	1.92(2)	C(8)-F(3)	1.36(3)
Ru(2)-As(2)	2.413(3)	C(8)-F(4)	1.39(3)
As(1)-Me(1)	2.00(3)	C(1)-O(1)	1.15(3)
As(1)-Me(2)	1.97(4)	C(2)-O(2)	1.15(2)
As(1)-C(5)	1.92(2)	C(3)-O(3)	1.17(3)
		C(4)-O(4)	1.14(3)
As(2)-Me(3)	1.93(3)		
As(2)-Me(4)	1.97(3)		
As(2)-C(7)	1.95(2)		
C(1)-Ru(1)-Ru(2)	77.3(8)	Ru(2)-As(2)-C(7)	116.8(6)
C(1)-Ru(1)-Ru(2')	98.6(8)	Me(3)-As(2)-Me(4)	102.3(12)
C(1)-Ru(1)-As(1)	90.7(8)	Me(3)-As(2)-C(7)	98.6(10)
C(1)-Ru(1)-As(1')	92.3(8)	Me(4)-As(2)-C(7)	98.7(11)
C(1)-Ru(1)-C(1')	175.4(16)		
As(1)-Ru(1)-As(1')	100.0(1)	As(1)-C(5)-C(7)	137.9(17)
As(1)-Ru(1)-Ru(2)	102.3(1)	As(1)-C(5)-C(6)	131.5(17)
Ru(2)-Ru(1)-Ru(2')	58.42(9)	C(7)-C(5)-C(6)	90.6(18)
C(2)-Ru(2)-Ru(2')	79.3(7)	As(2)-C(7)-C(5)	131.9(17)
C(2)-Ru(2)-Ru(1)	97.4(7)	As(2)-C(7)-C(8)	134.0(17)
C(2)-Ru(2)-As(2)	92.8(7)	C(5)-C(7)-C(8)	94.1(19)
C(2)-Ru(2)-C(3)	95.9(10)		
Ru(2')-Ru(2)-Ru(1)	60.79(4)	C(5)-C(6)-F(1)	117.8(23)
Ru(2')-Ru(2)-C(3)	98.7(8)	C(5)-C(6)-F(2)	116.0(24)
Ru(2')-Ru(2)-C(4)	95.5(7)	C(5)-C(6)-C(8)	87.1(19)
C(3)-Ru(2)-As(2)	99.1(8)	F(1)-C(6)-C(8)	115.3(23)
C(3)-Ru(2)-C(4)	93.3(11)	F(1)-C(6)-F(2)	106.8(23)
C(4)-Ru(2)-As(2)	89.5(7)	F(2)-C(6)-C(8)	113.3(24)
C(4)-Ru(2)-Ru(1)	72.6(7)		
Ru(1)-Ru(2)-As(2)	104.0(1)	C(7)-C(8)-F(3)	119.0(22)
		C(7)-C(8)-F(4)	114.4(22)
Ru(1)-As(1)-Me(1)	117.8(8)	C(7)-C(8)-C(6)	88.2(19)
Ru(1)-As(1)-Me(2)	119.0(10)	F(3)-C(8)-C(6)	117.1(23)
Ru(1)-As(1)-C(5)	118.5(7)	F(3)-C(8)-F(4)	103.2(21)
Me(1)-As(1)-Me(2)	103.5(14)	C(6)-C(8)-F(4)	115.4(23)
Me(1)-As(1)-C(5)	97.1(11)		
Me(2)-As(1)-C(5)	96.8(12)	O(1)-C(1)-Ru(1)	172.5(23)
Ru(2)-As(2)-Me(3)	117.8(8)	O(2)-C(2)-Ru(2)	175.1(20)
Ru(2)-As(2)-Me(4)	119.1(9)	O(3)-C(3)-Ru(2)	176.1(23)
		O(4)-C(4)-Ru(2)	172.6(21)

Table IV.V

Equations of planes in the form $\underline{\ell}X + \underline{m}Y + \underline{n}Z = \underline{p}$, where X, Y, Z are coordinates in Å, referred to orthogonal axes $\underline{a}, \underline{b}, \underline{c}$.

	$\underline{\ell}$	\underline{m}	\underline{n}	\underline{p}	maximum displacement (Å)
Ruthenium triangle (3 Ru atoms)	0.8945	0	-0.4471	-2.4377	0
Di-(tertiary arsine) (2 As and 4C atoms)	0.8442	0.3112	-0.4364	-1.9683	0.04

Table IV.VI

Magnitudes (Å) of the principal axes of the thermal vibration ellipsoids

	Axis 1	Axis 2	Axis 3
Ru(1)	0.13	0.19	0.22
Ru(2)	0.14	0.20	0.22
As(1)	0.13	0.21	0.27
As(2)	0.16	0.19	0.23
F(1)	0.19	0.27	0.44
F(2)	0.24	0.32	0.45
F(3)	0.22	0.26	0.42
F(4)	0.22	0.24	0.45

DISCUSSION

The molecular stereochemistry is shown in Figure IV.1. The molecule is situated on a crystallographic two-fold axis, and is conveniently described as a derivative of $\text{Ru}_3(\text{CO})_{12}$ ³⁵ in which two carbonyl groups on one ruthenium and one carbonyl on each of the other two ruthenium atoms are replaced by the two bidentate di-(tertiary arsine) ligands, in such a way that each ligand bridges two ruthenium atoms, and one Ru-Ru bond remains unbridged.

The replacement of four carbonyl groups from $\text{Ru}_3(\text{CO})_{12}$ to form $\text{L}_2\text{Ru}_3(\text{CO})_8$ causes several structural changes. All Ru-Ru bond lengths are no longer equal. The distance between two ruthenium atoms which are linked by the four-membered bridge of the di-(tertiary arsine) ligand is 2.853(3) Å (standard deviation in parentheses), compared with 2.785(4) Å for the unbridged Ru-Ru distance and 2.849, 2.859, and 2.837 Å (each $\sigma = 0.006$ Å) for the three Ru-Ru distances in the parent molecule.³⁵ This significant shortening probably arises from differences in π -acceptor character of the di-(tertiary arsine) relative to carbonyl groups. This electronic difference has been used previously to explain the increase in isomer shift of $\text{LFe}_3(\text{CO})_{10}$ relative to $\text{Fe}_3(\text{CO})_{12}$.¹⁷ Several other ruthenium cluster compounds have been studied³⁶⁻⁴⁰ in which Ru-Ru bond lengths ranged from 2.853 to 2.956 Å, with one short distance of 2.782 reported for the Ru(2)-

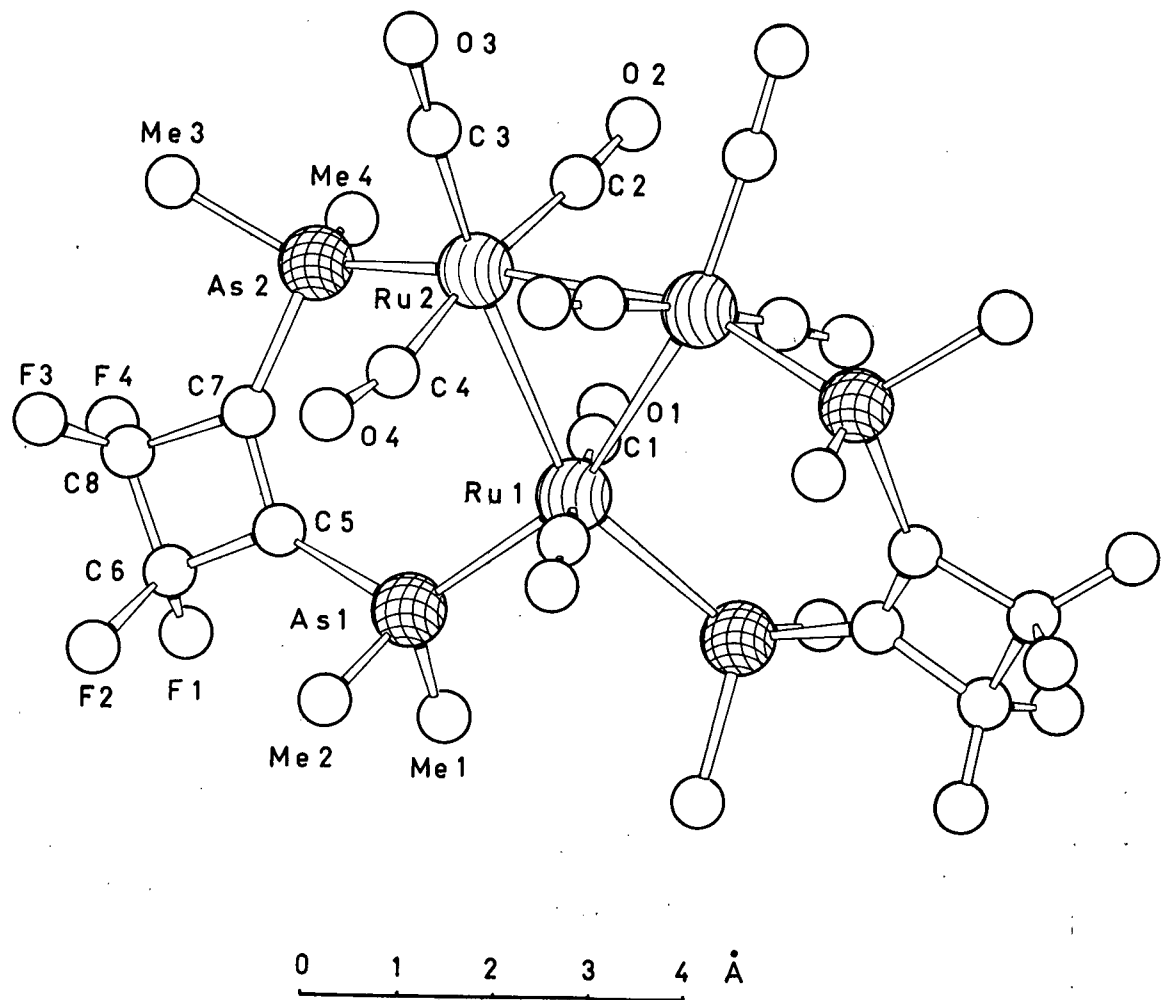
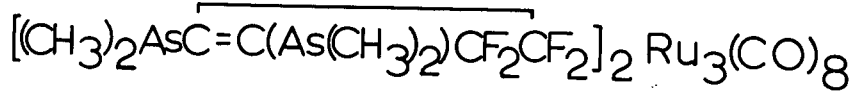


Figure IV.1 Molecular structure of $\text{L}_2\text{Ru}_3(\text{CO})_8$.

Ru(3) bond distance in bis(cyclo-octatetraene)triruthenium tetracarbonyl (Figure IV.2a).⁴⁰ The marked similarity between Figures IV.2a and IV.2b would suggest that C₈H₈ and the di-(tertiary arsine) are exerting the same effect on the bonding properties in the cluster. In both cases, Ru-Ru bonds involving the ruthenium atoms with the greatest number of carbonyl ligands are the shortest, reflecting the superiority of the carbonyl relative to the other ligands as an extractor of electron density from non-bonding d orbitals on the metal atom. In other words, the di-(tertiary arsine) and cyclo-octatetraene ligands are weaker π-acceptors than the carbonyl group.

As expected from n.m.r. observations and from the structure of LFe₃(CO)₁₀, the skeleton of the ligand does not differ significantly from exact planarity. The plane of the ligand is twisted 18.2° with respect to the plane of the ruthenium triangle and this twisting causes significant displacements of the carbonyl groups from their positions in the parent carbonyl. In Ru₃(CO)₁₂³⁵ axial carbonyl groups are very nearly perpendicular to the plane of the ruthenium triangle (angles vary from 88.0 to 89.9°), whereas in L₂Ru₃(CO)₈ the twisting of the ligand causes the carbonyl groups to be bent from axial positions, as shown in Figure IV.3. Nevertheless, ruthenium does retain an approximately octahedral co-ordination in the complex.

The arsenic atoms also suffer minor distortions

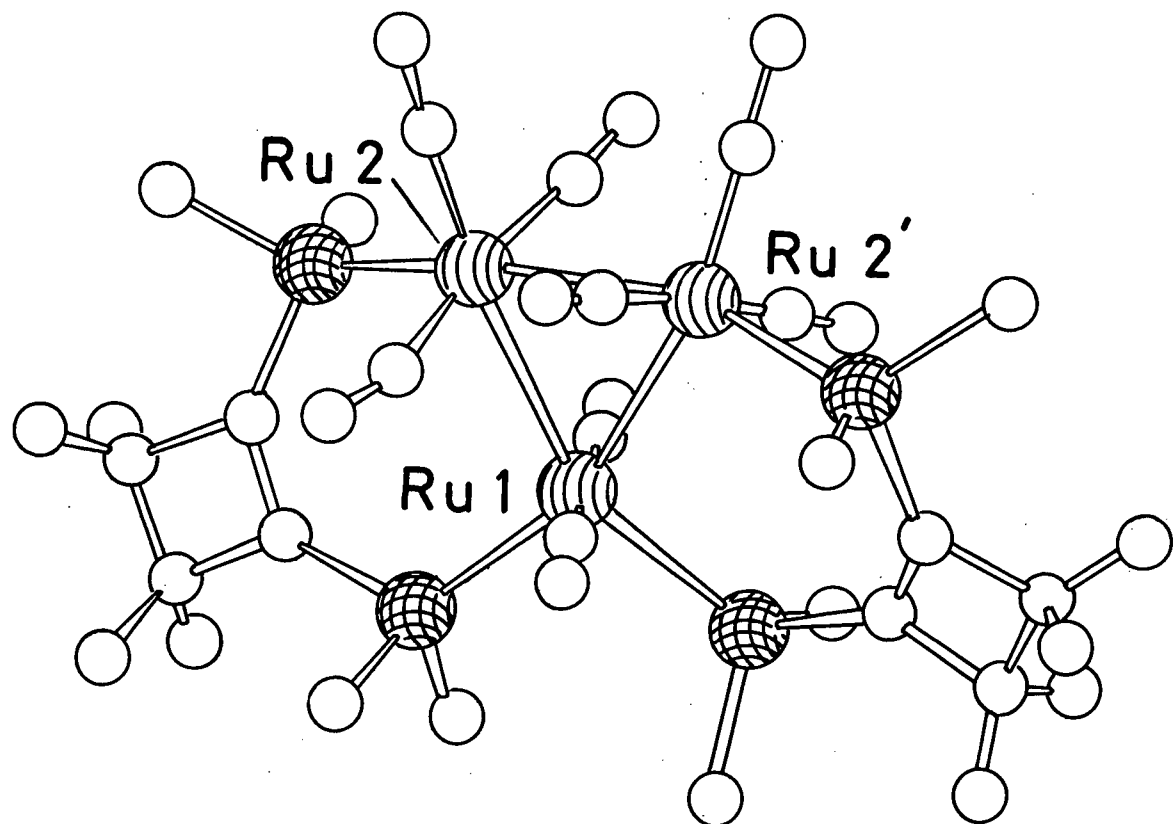
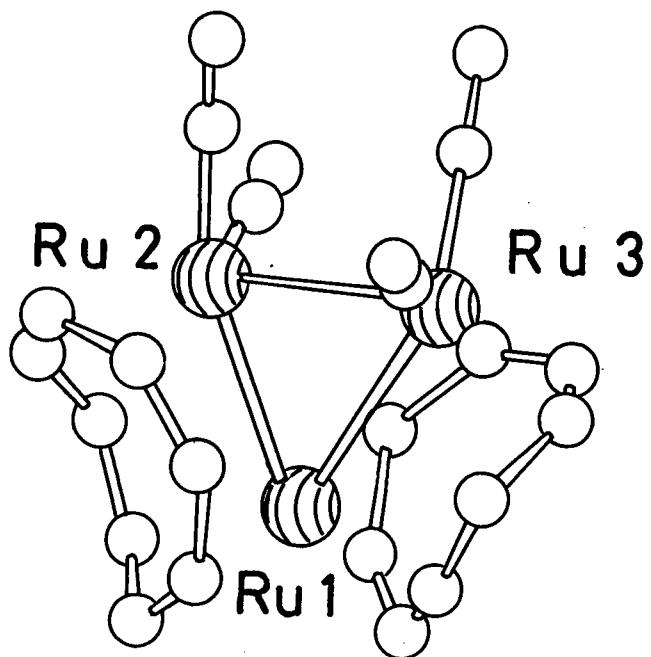
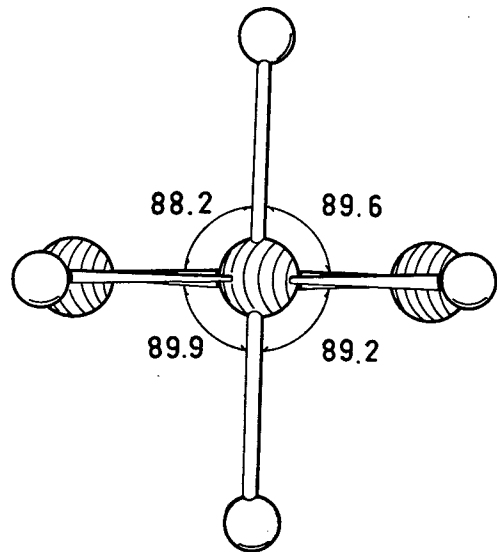
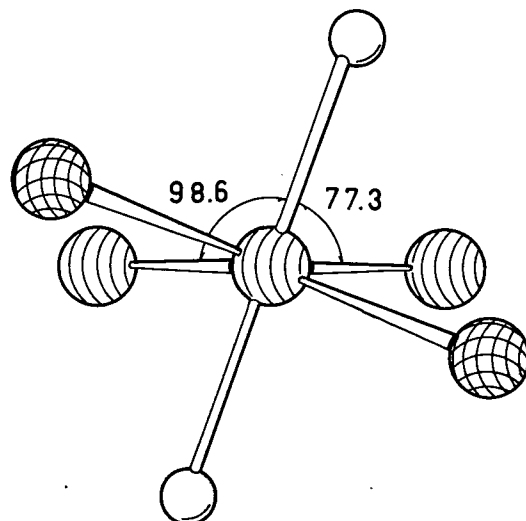


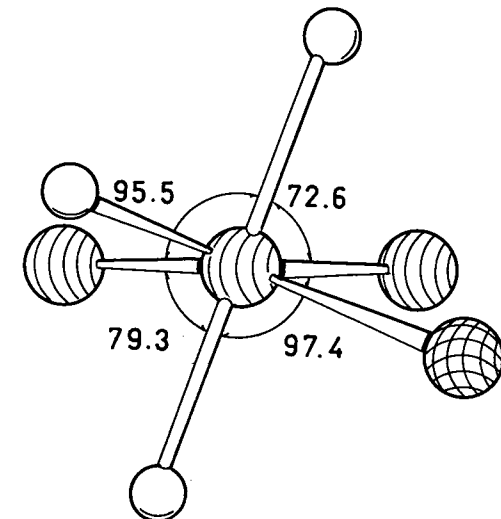
Figure IV.2 Comparison of $(C_8H_8)_2Ru_3(CO)_4$ and $L_2Ru_3(CO)_8$.



(a)



(b)



(c)

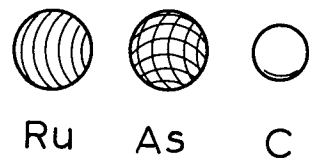


Figure IV.3 Co-ordination about ruthenium atoms (a) in parent compound and (b) Ru(1) and (c) Ru(2) of di-(tertiary arsine) complex.

of their co-ordination. As in $\text{LFe}_3(\text{CO})_{10}$, the large size of the metal atom causes Ru-As-C angles to be larger than C-As-C angles (averages 118.1 and 99.5° respectively; cf. Figure III.4). Ru-As bond distances are within the range $2.308 - 2.472 \text{ \AA}$ reported for $\text{Ru}\{\text{(Ph}_2\text{AsC}_6\text{H}_4)_3\text{As}\}\text{Br}_2$.⁴¹ Our mean value (2.407 \AA) is in accord with the distance which would be predicted from the Fe-As bond length, and from the difference of atomic radii of Ru and Fe; e.g. the Fe-As bond distance in $\text{LFe}_3(\text{CO})_{10}$ is 2.30 \AA , the Ru-Ru distance in $\text{Ru}_3(\text{CO})_{12}$ is 2.85 \AA ,³⁵ and the unbridged Fe-Fe distance in $\text{Fe}_3(\text{CO})_{12}$ is 2.65 \AA ¹⁸ giving a predicted Ru-As bond length of $\{2.30 + \frac{1}{2}(2.85 - 2.65)\} = 2.40 \text{ \AA}$.

None of the other structural parameters is particularly surprising. Average Ru-C and C-O distances are 1.89 and 1.15 \AA , as in the parent compound, and the Ru-C-O angles show the same slight deviations from linearity which are found in all the metal carbonyls.³¹ The retention of the double bond in the ligand between C(5) and C(7) is indicated by the short bond length of $1.39(3) \text{ \AA}$, not significantly different from the value for the sp^2 hybridization scheme. The compound $\text{LRu}_2(\text{CO})_6$ which forms during the preparation of the present derivative,²⁰ is assumed to be analogous to $\text{LFe}_2(\text{CO})_6$ ¹⁹ in which this double bond is broken to allow the involvement of the π -electrons in bonding to one of the iron atoms.

Intermolecular contacts range from 2.9 to 3.5 \AA

and are normal van der Waals interactions. The most important of these are shown in a projection of the structure (Figure IV.4).

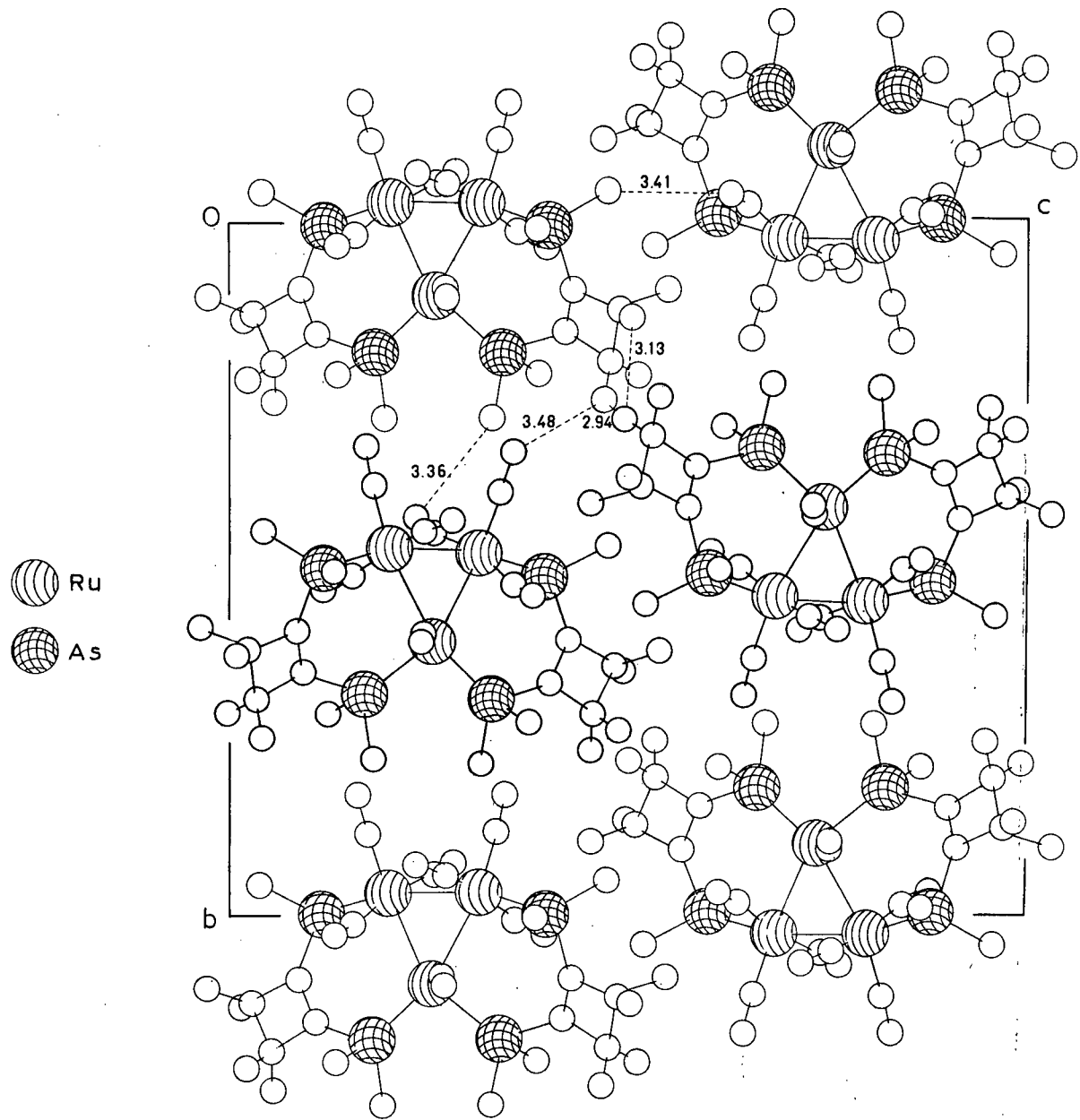
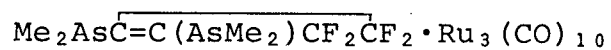


Figure IV.4 Projection of unit cell down a-axis.

V. THE STRUCTURE DETERMINATION OF



STRUCTURE ANALYSIS

The positions of the three ruthenium and two arsenic atoms in the asymmetric unit were determined from the Patterson function and improved with two cycles of full-matrix least-squares refinement using scattering factors from ref. 26. A difference synthesis phased on these refined parameters revealed the positions of all thirty-two carbon, oxygen, and fluorine atoms. One cycle of full-matrix refinement, varying an isotropic thermal parameter and three positional parameters for each of the thirty-two light atoms reduced \underline{R} to 0.126. At this point, all atoms were given anisotropic temperature factors which, along with positional parameters, were improved by six cycles of block-diagonal least-squares refinement, minimizing $\Sigma w(F_O - F_C)^2$. Reflections were given weights according to the following scheme.

$$\sqrt{w} = 1 \quad \text{if } |F_O| < F^*$$

$$\sqrt{w} = F^*/|F_O| \quad \text{if } |F_O| \geq F^*$$

$$\text{and } \sqrt{w} = 0.5 \quad \text{for unobserved}$$

For this data, a choice of $F^* = 70$ results in approximately constant values for $w(F_O - F_C)^2$ over the whole range of $|F_O|$. At final convergence, parameter shifts were small fractions of their corresponding standard deviations and \underline{R} and \underline{R}_w were 0.076 and 0.096 respectively for the 1828 observed reflections and 0.088 and 0.100 for

all data. Measured and calculated structure factors are given in Table V.I. A final difference map showed fluctuations around the heavy atoms of $\pm 1.8 \text{ e}/\text{\AA}^3$ which have been assumed to arise from random experimental error.

Table V.II lists the final positional and thermal parameters with standard deviations calculated from the inverses of the diagonal terms of the matrix of the final refinement cycle. Bond distances and valence angles are given in Table V.III. Standard deviations of these quantities contain a contribution from the standard deviations of the unit cell parameters. Table V.IV gives the equations of the weighted mean planes of the ruthenium triangle and of the arsenic and carbon atoms of the di-(tertiary arsine) ligand. The magnitudes of the principal axes of anisotropic thermal vibration are given in Table V.V for the three ruthenium and two arsenic atoms.

Table V.I

Final measured and calculated structure factors. Unobserved reflections have an asterisk after the $|F_o|$ value.

H	K	OBS CALC	H	K	OBS CALC	H	K	OBS CALC	H	K	OBS CALC	H	K	OBS CALC	H	K	OBS CALC	H	K	OBS CALC	H	K	OBS CALC				
**** L = 0****	9	4	10	19	7	13	17	57	6	12	30	26	4	0	20	32	8	7	63	66	9	0	16	17			
0	2	348	326	8	1	77	72	6	14	26	23	1	61	57	5	1	81	80	9	1	20	27	5	5	41	42	
0	4	26	42	**** L = 1****	2	8	23	36	6	15	22	24	3	51	48	5	9	66	59	5	2	62	59	5	7	36	35
0	6	38	29	0	2	0*	18	8	5	10*	8	7	2	38	92	6	5	72	67	5	11	12	12	5	8	71	66
0	10	38	39	0	3	112	118	8	6	54	53	7	3	61	62	6	7	78	78	6	12	42	43	5	5	15	15
0	12	53	50	0	4	10*	16	8	5	10*	8	7	2	38	92	6	6	63	83	5	5	65	63	5	5	15	15
0	14	51	51	0	5	40	45	8	6	54	53	7	3	61	62	6	7	78	78	6	12	42	43	5	5	15	15
0	16	83	83	0	6	85	79	8	7	20	25	9	8	25	25	6	9	100	9	5	15	12	12	5	8	71	66
0	18	33	29	0	7	143	146	8	9	63	61	7	0	54	51	6	10	82	87	5	14	24	23	5	10	26	25
0	20	52	48	0	8	10	10	9	10	72	76	7	1	31	34	6	11	100	97	5	13	12	12	5	8	71	66
0	22	40	37	0	9	211	223	9	1	37	36	7	8	37	36	6	12	102	108	6	1	75	71	5	12	44	42
1	2	136	77	0	10	56	60	9	1	37	36	7	9	19	22	6	13	40	42	6	2	34	35	6	13	37	36
1	3	56	54	0	11	49	51	9	2	36	57	7	10	41	43	6	16	72	76	6	3	34	35	6	13	37	36
1	4	29	28	0	12	40	45	9	3	37	36	7	11	38	37	6	4	31	33	5	15	40	42	6	13	37	36
1	5	77	74	0	13	49	56	9	4	12*	20	7	12	33	37	7	0	20	23	6	5	15	16	5	15	37	36
1	6	235	233	0	14	33	33	7	13	60	60	7	1	75	72	6	6	65	79	6	11	23	26	6	6	33	34
1	8	252	266	0	15	34	40	7	14	60	59	0	20	15	15	6	7	58	58	6	6	60	59	6	7	34	35
1	9	141	141	0	16	57	52	9	15	54	53	7	15	61	62	6	9	100	99	5	16	22	24	6	6	48	49
1	10	65	61	0	18	50	49	0	19	36	35	8	2	44	45	6	9	51	51	5	15	24	23	6	10	26	25
1	11	15	15	0	20	100	99	8	19	36	35	7	5	53	52	6	10	21	20	5	15	24	23	6	10	26	25
1	12	13	13	0	20	26	26	7	17	81	80	5	15	32	32	6	12	91	88	6	12	22	22	5	15	32	32
1	13	13	14	0	21	19	151	0	3	65	66	6	8	35	32	7	8	53	52	6	13	17	17	5	15	32	32
1	14	30	26	0	22	19	15	0	1	34	24	6	14	26	26	7	9	61	61	6	13	37	39	5	15	32	32
1	16	44	43	0	23	10	56	0	13	12	12	6	9	35	34	7	11	32	33	5	15	44	44	5	15	32	32
1	17	26	24	0	1	91	92	7	22	21	20	9	0	14	14	7	12	23	23	6	2	66	53	6	12	38	37
1	18	1	5	91	92	7	22	21	20	9	0	14	14	7	12	23	23	6	2	66	53	6	12	38	37		
1	19	25	22	0	9	148	140	9	2	33	29	8	1	119	123	7	4	45	45	6	13	41	41	5	15	32	32
1	20	61	54	0	21	20	19	0	11	20	19	9	4	19	18	8	2	103	102	7	5	29	24	6	13	37	36
1	20	55	42	0	22	19	15	0	12	19	15	9	5	10	10	7	1	103	102	7	4	45	45	6	13	37	36
1	21	123	124	0	23	10	55	0	13	17	22	5	5	37	37	7	8	11	11	7	2	133	130	7	4	45	45
1	23	26	24	0	1	11	12	0	14	12	10	10	2	22	22	2	1	103	102	7	4	45	45	6	13	37	36
1	24	9	11	0	12	9	102	0	15	15	15	0	1	15	14	8	3	37	34	7	4	45	45	6	13	37	36
1	25	65	66	0	16	55	51	0	17	36	36	9	8	36	37	7	11	52	51	5	15	44	44	6	13	37	36
1	26	62	220	0	17	55	51	0	18	55	52	9	0	37	41	8	9	11	11	7	2	131	130	7	4	45	45
1	27	99	92	0	18	55	51	0	19	55	52	9	0	37	41	8	9	11	11	7	2	131	130	7	4	45	45
1	28	32	30	0	19	55	51	0	20	55	52	9	0	37	41	8	9	11	11	7	2	131	130	7	4	45	45
1	29	12	12	0	20	55	51	0	21	55	52	9	0	37	41	8	9	11	11	7	2	131	130	7	4	45	45
1	30	10	12	0	21	55	51	0	22	55	52	9	0	37	41	8	9	11	11	7	2	131	130	7	4	45	45
1	31	10	12	0	22	55	51	0	23	55	52	9	0	37	41	8	9	11	11	7	2	131	130	7	4	45	45
1	32	11	12	0	23	55	51	0	24	55	52	9	0	37	41	8	9	11	11	7	2	131	130	7	4	45	45
1	33	12	12	0	24	55	51	0	25	55	52	9	0	37	41	8	9	11	11	7	2	131	130	7	4	45	45
1	34	12	12	0	25	55	51	0	26	55	52	9	0	37	41	8	9	11	11	7	2	131	130	7	4	45	45
1	35	12	12	0	26	55	51	0	27	55	52	9	0	37	41	8	9	11	11	7	2	131	130	7	4	45	45
1	36	12	12	0	27	55	51	0	28	55	52	9	0	37	41	8	9	11	11	7	2	131	130	7	4	45	45
1	37	12	12	0	28	55	51	0	29	55	52	9	0	37	41	8	9	11	11	7	2	131	130	7	4	45	45
1	38	12	12	0	29	55	51	0	30	55	52	9	0	37	41	8	9	11	11	7	2	131	130	7	4	45	45
1	39	12	12	0	30	55	51	0	31	55	52	9	0	37	41	8	9	11	11	7	2	131	130	7	4	45	45
1	40	12	12	0	31	55	51	0	32	55	52	9	0	37	41	8	9	11	11	7	2	131	130	7	4	45	45
1	41	12	12	0	32	55	51	0	33	55	52	9	0	37	41	8	9	11	11	7	2	131	130	7	4	45	45
1	42	12	12	0	33	55	51	0	34	55	52	9	0	37	41	8	9	11	11	7	2	131	130	7	4	45	45
1	43	12	12	0	34	55	51	0	35	55	52	9	0	37	41	8	9	11	11	7	2	131	130	7	4	45	45
1	44	12	12	0	35	55	51	0	36	55	52	9	0	37	41	8	9	11	11	7	2	131	130	7	4	45	45
1	45	12	12	0	36	55	51	0	37	55	52	9	0	37	41	8	9	11	11	7	2	131	130	7	4	45	45
1	46	12	12	0	37	55	51	0	38	55	52	9	0	37	41	8	9	11	11	7	2	131	130	7	4	45	45
1	47	12	12	0	38	55	51	0	39	55	52	9	0	37	41	8	9	11	11	7	2	131	130	7	4	45	45
1	48	12	12	0	39	55	51	0	40	55	52	9	0	37	41	8	9	11	11	7	2	131	130	7	4	45	45
1	49	12	12	0	40	55	51	0	41	55	52	9	0	37	41	8	9	11	11	7	2	131	130	7	4	45	45
1	50	12	12	0	41	55	51	0	42	55	52	9	0	37	41	8	9	11	11	7	2</td						

Table V.I (continued)

H	K	OBS CALC	H	K	IMN CALC	H	K	OBS CALC	H	K	OBS CALC	H	K	OBS CALC	H	K	OBS CALC	H	K	OBS CALC	H	K	OBS CALC																							
T	7	38	41	3	2	37	33		3	9	56	52	0	9	17	17	4	9	67	44	2	6	32	35	0	10	78	0	0	1	0*	23	0	3	22	34										
T	8	69	66	3	5	78	81	**** L-11*****	3	10	0*	10	0	10	50	47	4	10	38	39	2	8	29*	18	0	11	53	43	0	3	41	31	0	5	0*	20										
B	0	49	45	3	4	58	61		3	11	0*	11	0	11	54	52	4	11	49	42	2	8	25	17	0	12	48	5	0	3	41	31	0	5	0*	20										
B	1	30	23	3	10	83	80		3	12	18	16	0	12	57	55	4	12	30	28	2	9	24	27	1	0	49	41	0	4	18	23	0	6	0*	24										
B	2	51	47	3	11	37	32		3	13	20	19	0	13	57	55	4	13	32	30	2	10	37	30	1	1	50	41	0	3	41	31	0	5	0*	22										
B	3	10	12	3	13	23	20		3	14	25	25	0	14	57	55	4	14	32	30	2	11	37	30	1	1	50	41	0	3	41	31	0	5	0*	22										
B	4	97	85	3	13	23	20		3	14	26	25	0	14	57	55	4	14	32	30	2	11	37	30	1	1	50	41	0	3	41	31	0	5	0*	22										
B	5	146	122	3	14	47	42		3	15	25	28	0	15	47	42	4	15	55	66	5	8	47	46	3	6	32	33	1	9	19	21	1	1	50	41	0	3	41	31	0	5	0*	21		
B	6	65	65	3	15	18	16		3	16	11	11	0	16	79	78	6	16	69	85	5	9	30	32	3	5	24	22	1	10	27	27	1	2	64	38	1	6	61	47						
B	7	29	29	3	16	0*	16		3	17	25	26	0	17	79	78	6	17	64	85	5	10	30	32	3	5	24	22	1	10	27	27	1	2	64	38	1	6	61	47						
B	8	45	18	4	1	34	32		3	18	72	70	0	18	9	31	6	18	41	46	6	19	20	23	2	12	37	35	1	12	59	54	1	1	50	41	0	3	41	31	0	5	0*	22		
B	9	34	30	4	2	37	39		3	19	14	15	0	19	10	11	12	1	9	0*	16	6	1	34	23	3	8	77	7	2	20	1	15	12	1	1	50	41	0	3	41	31	0	5	0*	22
B	10	81	79	4	3	72	68		3	20	15	14	0	20	10	11	12	1	10	32	32	6	2	46	45	3	9	0*	8	2	20	1	15	12	1	1	50	41	0	3	41	31	0	5	0*	22
B	11	17	17	4	4	34	32		3	21	15	14	0	21	10	11	12	1	11	32	32	6	3	46	45	3	10	27	28	1	1	50	41	0	3	41	31	0	5	0*	22					
B	12	107	91	4	5	18	16		3	22	15	14	0	22	11	12	13	1	12	41	41	6	4	41	40	3	11	31	29	2	2	40	40	1	6	26	26	2	3	32	30					
B	13	0*	17	4	6	20	19		3	23	15	14	0	23	11	12	13	1	13	25	19	6	5	32	33	3	12	62	93	2	2	40	39	1	6	26	26	2	3	32	30					
B	14	52	44	4	7	21	20		3	24	15	14	0	24	11	12	13	1	14	25	35	6	7	0*	15	4	1	49	45	2	2	35	33	2	2	44	43	1	6	26	26	2	3	32	30	
B	15	69	62	4	9	25	25		3	25	16	15	0	25	11	12	13	1	15	24	34	6	8	32	32	2	2	7	7	2	2	44	43	1	6	26	26	2	3	32	30					
B	16	32	37	4	10	21	20		3	26	16	15	0	26	11	12	13	1	16	24	34	6	9	32	32	2	2	7	7	2	2	44	43	1	6	26	26	2	3	32	30					
B	17	49	43	4	11	31	30		3	27	16	15	0	27	11	12	13	1	17	24	34	6	10	32	32	2	2	7	7	2	2	44	43	1	6	26	26	2	3	32	30					
B	18	2	45	4	12	51	48		3	28	17	16	0	28	11	12	13	1	18	24	34	6	11	32	32	2	2	7	7	2	2	44	43	1	6	26	26	2	3	32	30					
B	19	123	137	4	13	27	22		3	29	18	17	0	29	11	12	13	1	19	24	34	6	12	32	32	2	2	7	7	2	2	44	43	1	6	26	26	2	3	32	30					
B	20	110	108	4	14	28	22		3	30	19	18	0	30	11	12	13	1	20	24	34	6	13	32	32	2	2	7	7	2	2	44	43	1	6	26	26	2	3	32	30					
B	21	86	97	4	15	41	36		3	31	20	19	0	31	11	12	13	1	21	24	34	6	14	32	32	2	2	7	7	2	2	44	43	1	6	26	26	2	3	32	30					
B	22	64	70	4	16	42	42		3	32	21	20	0	32	11	12	13	1	22	24	34	6	15	32	32	2	2	7	7	2	2	44	43	1	6	26	26	2	3	32	30					
B	23	48	56	4	17	23	23		3	33	22	21	0	33	11	12	13	1	23	24	34	6	16	32	32	2	2	7	7	2	2	44	43	1	6	26	26	2	3	32	30					
B	24	63	63	4	18	24	24		3	34	23	22	0	34	11	12	13	1	24	24	34	6	17	32	32	2	2	7	7	2	2	44	43	1	6	26	26	2	3	32	30					
B	25	31	31	4	19	24	24		3	35	24	23	0	35	11	12	13	1	25	24	34	6	18	32	32	2	2	7	7	2	2	44	43	1	6	26	26	2	3	32	30					
B	26	75	75	4	20	24	24		3	36	25	24	0	36	11	12	13	1	26	24	34	6	19	32	32	2	2	7	7	2	2	44	43	1	6	26	26	2	3	32	30					
B	27	39	39	4	21	24	24		3	37	26	25	0	37	11	12	13	1	27	24	34	6	20	32	32	2	2	7	7	2	2	44	43	1	6	26	26	2	3	32	30					
B	28	49	49	4	22	24	24		3	38	27	26	0	38	11	12	13	1	28	24	34	6	21	32	32	2	2	7	7	2	2	44	43	1	6	26	26	2	3	32	30					
B	29	69	69	4	23	24	24		3	39	28	27	0	39	11	12	13	1	29	24	34	6	22	32	32	2	2	7	7	2	2	44	43	1	6	26	26	2	3	32	30					
B	30	45	45	4	24	24	24		3	40	29	28	0	40	11	12	13	1	30	24	34	6	23	32	32	2	2	7	7	2	2	44	43	1	6	26	26	2	3	32	30					
B	31	24	24	4	25	24	24		3	41	30	29	0	41	11	12	13	1	31	24	34	6	24	32	32	2	2	7	7	2	2	44	43	1	6	26	26	2	3	32	30					
B	32	24	24	4	26	24	24		3	42	31	30	0	42	11	12	13	1	32	24	34	6	25	32	32	2	2	7	7	2	2	44	43	1	6	26	26	2	3	32	30					
B	33	32	32	4	27	24	24		3	43	32	31	0	43	11	12	13	1	33	24	34	6	26	32	32	2	2	7	7	2	2	44	43	1	6	26	26	2	3	32	30					
B	34	22	20	4	28	24	24		3	44	33	32	0	44	11	12	13	1	34	24	34	6	27	32	32	2	2	7	7	2	2	44	43	1	6	26	26	2	3	32	30					
B	35	75	86	4	29	24	24		3	45	34	33	0	45	11	12	13	1	35	24	34	6	28	32	32	2	2	7	7	2	2	44	43	1	6	26	26	2	3	32	30					
B	36	109	109	4	30	24	24		3	46	35	34	0	46	11	12	13	1	36	24	34	6	29	32	32	2	2	7	7	2	2	44	43	1	6	26	26	2	3	32	30					
B	37	56	60	4	31	24	24		3	47	36	35	0	47	11	12	13	1	37	24	34	6	30	32	32	2	2	7	7	2	2	44	43	1	6	26	26	2	3	32	30					
B	38	44	44	4	32																																									

Table V.II
 Final positional (fractional $\times 10^4$) and thermal parameters
 with standard deviations in parentheses

ATOM	<u>x</u>	<u>y</u>	<u>z</u>	<u>b</u> ₁₁	<u>b</u> ₂₂	<u>b</u> ₃₃	<u>b</u> ₁₂	<u>b</u> ₁₃	<u>b</u> ₂₃ [†]
Ru(1)	2495(3)	1378(1)	0800(2)	120(3)	23(1)	52(1)	-13(1)	- 4(2)	0(1)
Ru(2)	2190(2)	-0011(1)	1438(1)	72(2)	25(1)	43(1)	- 7(1)	- 1(2)	1(1)
Ru(3)	0295(2)	0432(1)	0121(1)	72(2)	21(1)	44(1)	- 3(1)	- 1(2)	0(1)
As(1)	-0713(3)	-0690(1)	-0359(2)	72(3)	22(1)	45(1)	- 1(1)	- 6(2)	- 1(1)
As(2)	0934(3)	-1098(2)	1860(2)	92(3)	29(1)	46(1)	-13(1)	- 6(2)	- 6(1)
F(1)	-3672(20)	-1923(11)	0440(15)	104(24)	53(7)	100(12)	-38(12)	-22(16)	5(9)
F(2)	-1941(23)	-2541(9)	-0158(10)	239(33)	35(5)	53(7)	-19(11)	6(15)	- 5(11)
F(3)	-2339(30)	-2315(12)	1849(16)	292(44)	53(7)	93(12)	-64(16)	11(24)	15(9)
F(4)	-0567(27)	-2873(9)	1204(14)	341(41)	37(5)	103(11)	-28(13)	-50(19)	9(7)
O(1)	-0400(35)	1991(14)	1631(20)	280(49)	61(9)	129(18)	73(17)	22(28)	-22(11)
O(2)	2162(38)	2506(14)	-0515(15)	339(56)	67(9)	84(11)	-40(21)	-16(23)	41(7)
O(3)	5391(22)	0701(12)	0031(12)	128(26)	70(8)	62(8)	-16(26)	11(28)	-16(14)
O(4)	4618(32)	2079(15)	1975(16)	285(45)	82(10)	74(12)	-57(18)	11(23)	-14(10)
O(5)	2703(26)	0368(18)	-1206(15)	127(30)	118(14)	63(10)	-48(20)	49(16)	-13(11)
O(6)	-1672(35)	1406(12)	-0908(15)	343(56)	43(7)	69(11)	34(19)	-48(22)	13(9)
O(7)	-2148(25)	0464(16)	1452(14)	120(30)	88(12)	62(10)	12(19)	35(16)	-13(11)
O(8)	0550(32)	0784(13)	2740(15)	276(51)	43(8)	61(11)	- 1(18)	26(22)	- 4(9)
O(9)	3814(26)	-0830(11)	0052(14)	214(35)	39(6)	94(11)	8(13)	25(18)	-22(14)
O(10)	5086(24)	-0163(16)	2460(16)	69(24)	102(13)	71(10)	11(18)	-43(14)	- 1(11)
C(1)	0631(59)	1713(18)	1350(26)	296(93)	15(10)	65(20)	47(27)	54(41)	- 1(13)
C(2)	2240(34)	2083(19)	-0043(17)	129(39)	82(14)	39(11)	-29(21)	-30(20)	-11(11)
C(3)	4218(35)	0904(16)	0355(18)	138(43)	39(9)	46(12)	-10(18)	-10(21)	14(9)
C(4)	3816(42)	1816(15)	1561(19)	285(54)	41(8)	48(13)	-91(16)	-21(26)	5(9)
C(5)	1905(31)	0391(16)	-0682(18)	56(35)	35(9)	44(13)	-24(17)	23(19)	- 5(10)
C(6)	-0834(30)	1053(13)	-0487(19)	202(35)	28(7)	106(14)	-19(13)	-56(18)	13(9)
C(7)	-1124(38)	0470(17)	1068(17)	176(48)	63(11)	44(10)	-18(22)	28(20)	-16(9)

Table V.II (continued)

ATOM	<u>X</u>	<u>Y</u>	<u>Z</u>	<u>b</u> ₁₁	<u>b</u> ₂₂	<u>b</u> ₃₃	<u>b</u> ₁₂	<u>b</u> ₁₃	<u>b</u> ₂₃
C(8)	1163(41)	0506(14)	2233(18)	284(56)	27(7)	55(12)	- 5(19)	2(25)	- 4(8)
C(9)	3080(35)	-0520(15)	0569(18)	163(43)	30(8)	57(12)	-42(18)	-71(19)	1(9)
C(10)	4002(42)	-0089(21)	2096(27)	100(51)	44(13)	60(21)	-59(25)	-19(31)	- 4(16)
C(11)	-1048(29)	-1417(14)	0429(16)	80(32)	35(8)	36(10)	- 8(32)	-13(33)	-24(16)
C(12)	-0510(29)	-1577(13)	1125(20)	68(32)	23(7)	76(14)	-21(13)	-21(19)	- 2(9)
C(13)	-2106(38)	-2062(14)	0439(22)	157(47)	21(7)	84(16)	-12(17)	13(26)	15(9)
C(14)	-1443(45)	-2249(19)	1196(27)	166(57)	38(11)	98(22)	-23(24)	13(34)	34(14)
Me(1)	-0484(44)	-1033(20)	2796(18)	254(60)	71(13)	36(12)	-36(25)	29(25)	-13(11)
Me(2)	2253(40)	-1881(18)	2084(26)	125(46)	40(11)	86(21)	3(22)	-13(31)	22(14)
Me(3)	-2629(33)	-0711(14)	-0924(23)	44(36)	37(12)	73(19)	-11(20)	-52(25)	6(14)
Me(4)	0547(35)	-1257(14)	-1083(19)	278(44)	29(7)	100(14)	10(17)	63(19)	0(9)

[†]Coefficients in the temperature expression: $\exp -10^{-4}(\underline{b}_{11}\underline{h}^2 + \underline{b}_{22}\underline{k}^2 + \underline{b}_{33}\underline{\ell}^2 + 2\underline{b}_{12}\underline{h}\underline{k}$
 $+ 2\underline{b}_{13}\underline{h}\underline{\ell} + 2\underline{b}_{23}\underline{k}\underline{\ell})$

Table V.III

Bond distances (\AA) and valence angles (degrees),
with standard deviations in parentheses

Ru(1)-Ru(2)	2.831(3)	C(13)-F(1)	1.37(4)
Ru(1)-Ru(3)	2.831(3)	C(13)-F(2)	1.35(4)
Ru(1)-C(1)	1.95(5)	C(14)-F(3)	1.34(5)
Ru(1)-C(2)	1.95(3)	C(14)-F(4)	1.39(4)
Ru(1)-C(3)	1.88(3)		
Ru(1)-C(4)	1.89(3)	C(1)-O(1)	1.13(6)
		C(2)-O(2)	1.12(4)
Ru(2)-Ru(3)	2.858(6)	C(3)-O(3)	1.21(4)
Ru(2)-As(2)	2.417(4)	C(4)-O(4)	1.09(4)
Ru(2)-C(8)	1.87(3)	C(5)-O(5)	1.11(4)
Ru(2)-C(9)	1.90(3)	C(6)-O(6)	1.21(4)
Ru(2)-C(10)	1.91(4)	C(7)-O(7)	1.09(4)
		C(8)-O(8)	1.13(4)
Ru(3)-As(1)	2.417(3)	C(9)-O(9)	1.22(4)
Ru(3)-C(5)	1.93(3)	C(10)-O(10)	1.12(5)
Ru(3)-C(6)	1.83(3)		
Ru(3)-C(7)	2.00(3)	C(11)-C(12)	1.29(4)
		C(11)-C(13)	1.52(4)
As(1)-C(11)	1.92(3)	C(12)-C(14)	1.50(4)
As(1)-Me(3)	1.90(3)	C(13)-C(14)	1.43(6)
As(1)-Me(4)	1.94(3)		
As(2)-C(12)	1.96(3)		
As(2)-Me(1)	1.98(3)		
As(2)-Me(2)	1.90(3)		
Ru(2)-Ru(1)-Ru(3)	60.64(11)	Ru(3)-As(1)-C(11)	117(1)
Ru(2)-Ru(1)-C(1)	93(1)	Ru(3)-As(1)-Me(3)	120(1)
Ru(2)-Ru(1)-C(3)	78(1)	Ru(3)-As(1)-Me(4)	119(1)
Ru(2)-Ru(1)-C(4)	102(1)	C(11)-As(1)-Me(3)	101(1)
Ru(3)-Ru(1)-C(1)	81(1)	C(11)-As(1)-Me(4)	97(1)
Ru(3)-Ru(1)-C(2)	94(1)	Me(3)-As(1)-Me(4)	99(1)
Ru(3)-Ru(1)-C(3)	94(1)		
C(1)-Ru(1)-C(2)	92(1)	Ru(2)-As(2)-C(12)	119(1)
C(1)-Ru(1)-C(4)	92(2)	Ru(2)-As(2)-Me(1)	117(1)
C(2)-Ru(1)-C(3)	97(1)	Ru(2)-As(2)-Me(2)	117(1)
C(2)-Ru(1)-C(4)	105(1)	C(12)-As(2)-Me(1)	98(1)
C(3)-Ru(1)-C(4)	90(1)	C(12)-As(2)-Me(2)	98(1)
		Me(1)-As(2)-Me(2)	105(2)
Ru(1)-Ru(2)-Ru(3)	59.68(9)		
Ru(1)-Ru(2)-C(8)	80(1)	As(1)-C(11)-C(12)	137(2)
Ru(1)-Ru(2)-C(9)	98(1)	As(1)-C(11)-C(13)	132(2)
Ru(1)-Ru(2)-C(10)	102(1)	C(12)-C(11)-C(13)	91(2)
Ru(3)-Ru(2)-As(2)	102.48(11)		

Table V.III (continued)

Ru(3)-Ru(2)-C(8)	97(1)	As(2)-C(12)-C(11)	133(2)
Ru(3)-Ru(2)-C(9)	78(1)	As(2)-C(12)-C(14)	132(3)
As(2)-Ru(2)-C(8)	91(1)	C(11)-C(12)-C(14)	94(3)
As(2)-Ru(2)-C(9)	89(1)		
As(2)-Ru(2)-C(10)	97(1)	F(1)-C(13)-F(2)	103(3)
C(8)-Ru(2)-C(10)	91(2)	F(1)-C(13)-C(11)	116(2)
C(9)-Ru(2)-C(10)	94(2)	F(1)-C(13)-C(14)	116(3)
		F(2)-C(13)-C(11)	118(3)
Ru(1)-Ru(3)-Ru(2)	59.67(9)	F(2)-C(13)-C(14)	116(3)
Ru(1)-Ru(3)-C(5)	80(1)	C(11)-C(13)-C(14)	88(2)
Ru(1)-Ru(3)-C(6)	100(1)		
Ru(1)-Ru(3)-C(7)	94(1)	F(3)-C(14)-F(4)	103(3)
Ru(2)-Ru(3)-As(1)	101.80(12)	F(3)-C(14)-C(12)	117(3)
Ru(2)-Ru(3)-C(5)	97(1)	F(3)-C(14)-C(13)	121(3)
Ru(2)-Ru(3)-C(7)	76(1)	F(4)-C(14)-C(12)	115(3)
As(1)-Ru(3)-C(5)	90(1)	F(4)-C(14)-C(13)	116(3)
As(1)-Ru(3)-C(6)	101(1)	C(12)-C(14)-C(13)	86(3)
As(1)-Ru(3)-C(7)	94(1)		
C(5)-Ru(3)-C(6)	91(1)	Mean Ru-C-O	173
C(6)-Ru(3)-C(7)	95(1)		

Table V.IV

Equations of planes in the form $\underline{\ell}X + \underline{m}Y + \underline{n}Z = \underline{p}$, where X, Y, Z are coordinates in Å, referred to orthogonal axes a, b, c .

	$\underline{\ell}$	\underline{m}	\underline{n}	\underline{p}	maximum displacement (Å)
Ruthenium triangle					
(3 Ru atoms)	0.6940	-0.3306	-0.6396	-0.2223	0
Di-(tertiary arsine)					
(2 As and 4 C atoms)	0.7490	-0.5311	-0.3961	0.4677	0.06

Table V.V

Magnitudes (Å) of the principal axes of the thermal vibration ellipsoids of the heavy atoms.

	Axis 1	Axis 2	Axis 3
Ru (1)	0.18	0.23	0.27
Ru (2)	0.16	0.21	0.25
Ru (3)	0.16	0.20	0.25
As (1)	0.16	0.20	0.25
As (2)	0.17	0.22	0.27

DISCUSSION

In the same way that $LFe_3(CO)_{10}$ is related to $Fe_3(CO)_{12}$,¹⁸ the complex $LRu_3(CO)_{10}$ is related to $Ru_3(CO)_{12}$.³⁵ As shown in Figure V.1, one carbonyl group on each of two ruthenium atoms is replaced by the arsenic atoms of the di-(tertiary arsine) ligand. Since ligands of lower acceptor strengths than the carbonyl group are less efficient at removing π -antibonding electron density from the metal cluster, metal-metal bonds between atoms having carbonyl groups replaced by these ligands would be expected to be longer than metal-metal bonds involving atoms having only carbonyl groups. This effect has been observed previously, and is in evidence in the present structure. The bond distances Ru(1)-Ru(2) and Ru(1)-Ru(3), (both 2.831(3) Å) are significantly shorter than Ru(2)-Ru(3), (2.858(6) Å).

Although both 1H and ^{19}F n.m.r. spectra consist of singlet resonances, the mean plane of the di-(tertiary arsine) ligand is in fact twisted 18.4° with respect to the plane of the ruthenium triangle. This implies either that this twist is a result of packing forces (the plane of the ligand being co-planar with the ruthenium triangle in solution), or that the ligand is flexing in solution and assumes a stationary configuration upon crystallization. As in $L_2Ru_3(CO)_8$, the twisting of the ligand again causes Ru-Ru-C angles for axial carbonyls to change from nearly 90° in $Ru_3(CO)_{12}$ to the severely skewed configurations shown

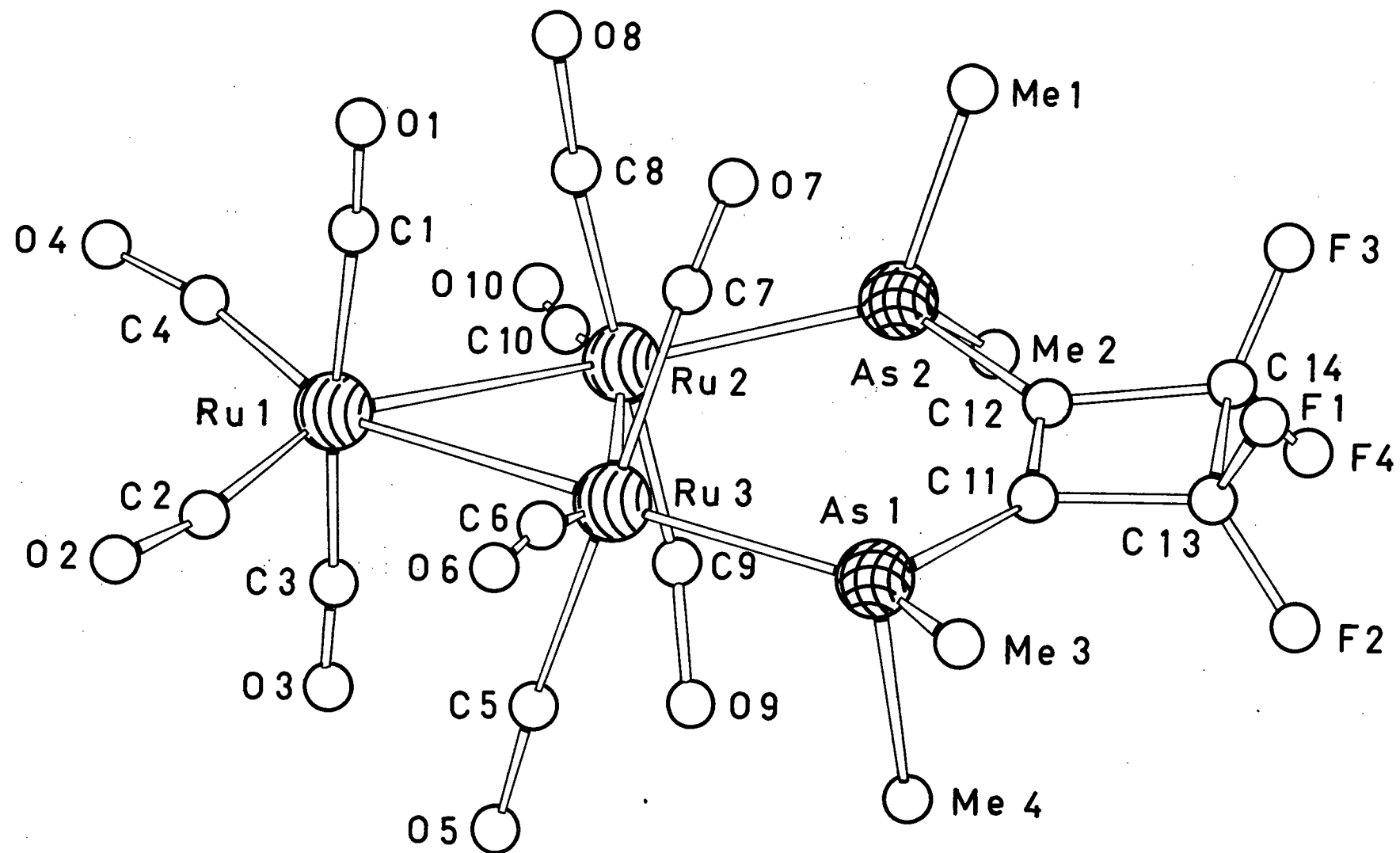


Figure V.1 Molecular structure of $\text{LRu}_3(\text{CO})_{10}$.

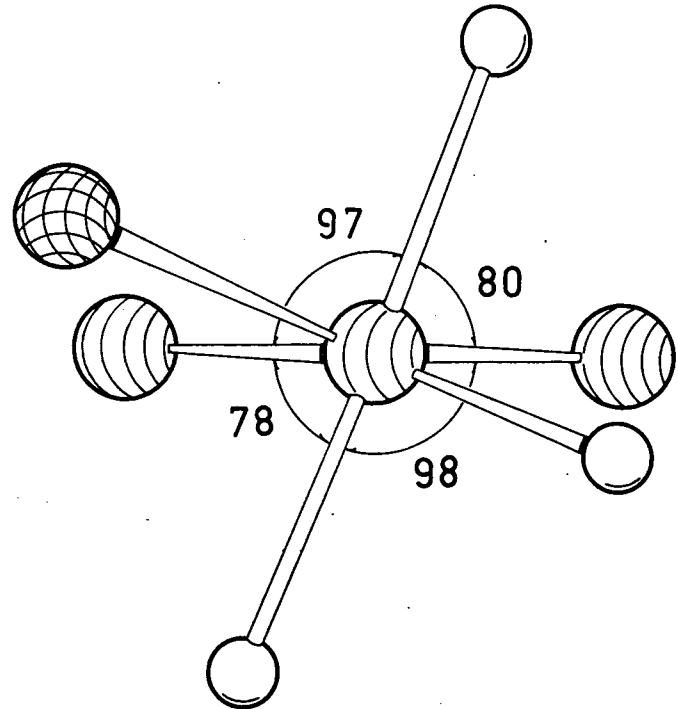
in Figure V.2. Mean Ru-C and C-O bond distances are in excellent agreement with previously reported values^{36-40,42,43} and Ru-C-O angles (mean 172.8°, σ(mean) 1.3°) are significantly non-linear as in most carbonyl complexes.

Ru-As bond distances (both 2.417 Å) are in good agreement with the values 2.401 and 2.413 Å found for L₂Ru₃(CO)₈ and are within the range 2.308 to 2.472 Å reported for Ru((Ph₂AsC₆H₄)₃As)Br₂.⁴¹ Ru-As-C angles are again larger than C-As-C angles (averages 118.2 and 99.7° respectively) due to the steric effect of the ruthenium atom (cf. Figure III.4).

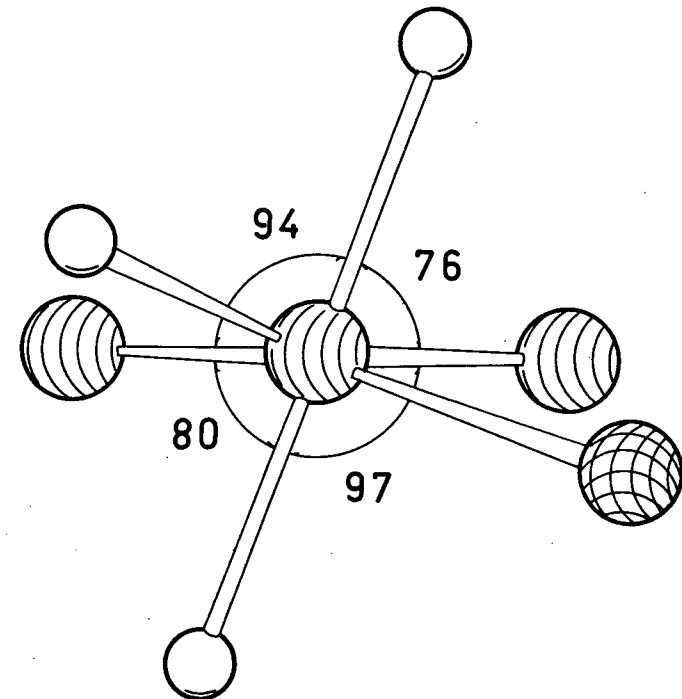
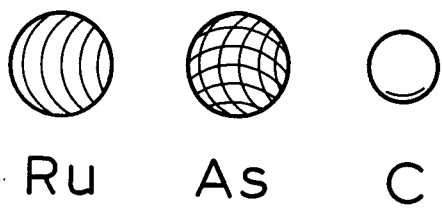
The dimensions of the di-(tertiary arsine) ligand are essentially identical to those in other similar structures.³² The double bond in the cyclobutene ring (1.29 Å) is retained and other carbon-carbon distances are reasonable. Carbon-fluorine bond distances (mean 1.36 Å) are also as expected.

The extent of anisotropy of the thermal vibrations of the heavy atoms is shown in Table V.V. The principal axes of vibration show no regularities in orientation with respect to intramolecular vectors.

Intermolecular van der Waals contacts ranging from 2.96 to 3.48 Å are shown in the a-axis projection of the structure in Figure V.3.



(a)



(b)

Figure V.2 Co-ordination around (a) Ru(2) and (b) Ru(3) of $\text{LRu}_3(\text{CO})_{10}$.

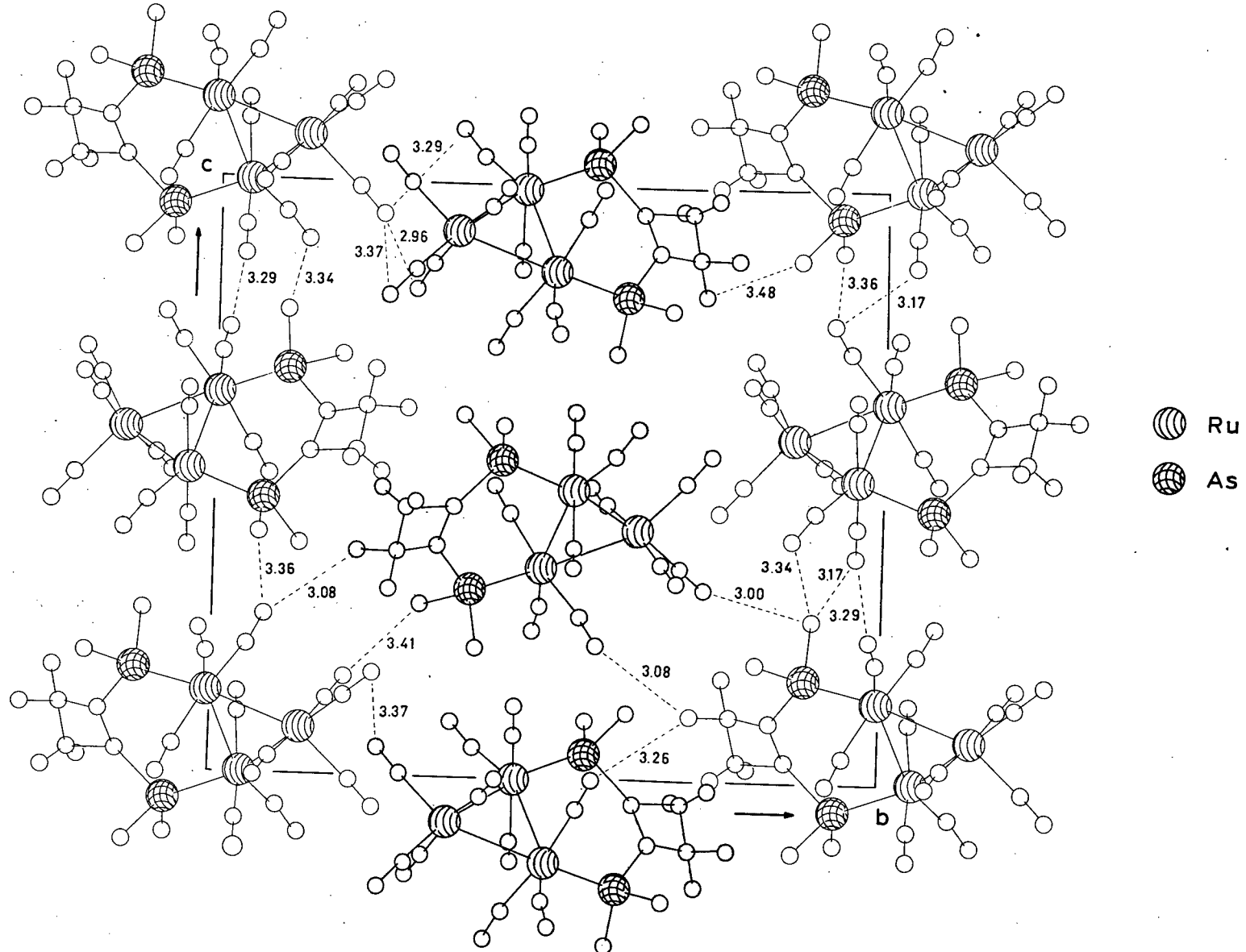
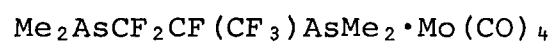


Figure V.3 Projection of unit cell down a-axis.

VI. THE STRUCTURE DETERMINATION OF



STRUCTURE ANALYSIS

The coordinates of the molybdenum and arsenic atoms in space group C2/c were derived from the Patterson function and improved with two cycles of full-matrix refinement, using scattering factors from ref. 26. A difference synthesis phased on the refined parameters revealed the positions of all twenty-one carbon, oxygen, and fluorine atoms.

One cycle of full-matrix least-squares refinement with minimization of $\Sigma w\Delta^2$ using unit weights for all observed reflections and isotropic thermal parameters for all atoms reduced R to 0.116. Converting to anisotropic temperature factors for molybdenum, arsenic, and fluorine atoms and refining for one cycle reduced R to 0.083. At this point, observed reflections were assigned weights from the following scheme.

$$w = \{A + B|F_O| + C|F_O|^2 + D|F_O|^3\}^{-1}$$

where A, B, C, and D are calculated by least-squares treatment to give best fit to constant $w\Delta^2$ over all $|F_O|$. Two cycles of refinement (142 variables) using this weighting scheme with A, B, C, and D equal to 7.1341, 1.5458, -0.0186 and 0.00008 respectively (unobserved reflections are excluded from refinement but included in final structure factor calculation), reduced R and R_w to 0.073 and 0.094 for observed reflections and 0.085 and 0.148 for all data. At final convergence, all parameter shifts were small

fractions of their standard deviations. A final difference Fourier revealed residuals of $\pm 1.5 \text{ e}/\text{\AA}^3$ around the heavy atoms which can only be explained as random experimental error. Measured and calculated structure factors are given in Table VI.I. Table VI.II gives the final positional and thermal parameters with standard deviations calculated from the inverse matrix of the last refinement cycle. Bond distances and valence angles are in Table VI.III; standard deviations of these quantities take into account the standard deviations of the unit cell parameters. Table VI.IV shows the extent of anisotropy of the thermal motion of the molybdenum, arsenic, and fluorine atoms. The anisotropy is large for the fluorine atoms, particularly those of the trifluoromethyl group, and the bond distances should be increased somewhat by corrections for libration. However, since the carbon and oxygen atoms were refined isotropically, no corrections were made. Although bond length comparisons within the present molecule are valid, detailed comparisons with distances in other molecules should take account of possible libration corrections.

Table VI.I

Final measured and calculated structure factors. Unobserved reflections have an asterisk after the $|F_O|$ value.

H	K	OBS CALC	H	K	OBS CALC	H	K	OBS CALC	H	K	OBS CALC	H	K	OBS CALC	H	K	OBS CALC	H	K	OBS CALC	H	K	OBS CALC	H	K	OBS CALC	
***	L = 0****	-2	71	70	-2	10	20	17	3	163	184	-13	3	45	43	-18	8	77	71	-4	6	105	96	0	4	113	111
4	0	501	639	-2	2	121	150	2	18	49	49	-19	3	154	151	-9	3	99	98	-10	8	91	81	-2	6	22	15
4	7	47	40	-2	2	46	29	4	16	45	45	-20	4	10	10	-10	3	141	134	-11	3	81	78	-12	6	203	201
10	12	57	75	-2	2	76	65	6	15	44	42	-20	4	10	10	-10	3	141	134	-11	3	81	78	-12	6	203	201
10	12	57	75	-2	2	76	65	6	15	44	42	-20	4	10	10	-10	3	141	134	-11	3	81	78	-12	6	203	201
12	3	226	240	0	2	9	11	0	10	10	10	-10	3	29	16	-10	6	49	42	-1	3	81	78	-12	6	203	201
14	6	234	253	10	2	184	199	12	20	22	22	-14	12	11	11	-11	3	207	197	-10	5	55	56	-12	6	126	120
14	6	234	253	10	2	184	199	12	20	22	22	-14	12	11	11	-11	3	207	197	-10	5	55	56	-12	6	126	120
14	6	234	253	10	2	184	199	12	20	22	22	-14	12	11	11	-11	3	207	197	-10	5	55	56	-12	6	126	120
14	6	234	253	10	2	184	199	12	20	22	22	-14	12	11	11	-11	3	207	197	-10	5	55	56	-12	6	126	120
14	6	234	253	10	2	184	199	12	20	22	22	-14	12	11	11	-11	3	207	197	-10	5	55	56	-12	6	126	120
14	6	234	253	10	2	184	199	12	20	22	22	-14	12	11	11	-11	3	207	197	-10	5	55	56	-12	6	126	120
20	11	111	110	16	3	31	27	-9	11	55	54	-6	6	65	63	9	3	94	95	-10	2	132	129	12	6	20	19
20	12	30	23	16	3	70	73	10	10	104	104	-6	6	65	63	9	3	94	95	-10	2	132	129	12	6	20	19
13	1	55	66	16	4	41	41	-6	10	45	45	-10	11	11	11	-11	3	147	147	-6	6	65	63	9	3	132	129
5	1	66	71	22	2	3	9	-3	11	168	180	-2	6	45	45	10	3	151	151	-10	2	132	129	12	6	20	19
5	1	66	71	22	2	3	9	-3	11	168	180	-2	6	45	45	10	3	151	151	-10	2	132	129	12	6	20	19
5	1	66	71	22	2	3	9	-3	11	168	180	-2	6	45	45	10	3	151	151	-10	2	132	129	12	6	20	19
5	1	66	71	22	2	3	9	-3	11	168	180	-2	6	45	45	10	3	151	151	-10	2	132	129	12	6	20	19
5	1	66	71	22	2	3	9	-3	11	168	180	-2	6	45	45	10	3	151	151	-10	2	132	129	12	6	20	19
5	1	66	71	22	2	3	9	-3	11	168	180	-2	6	45	45	10	3	151	151	-10	2	132	129	12	6	20	19
5	1	66	71	22	2	3	9	-3	11	168	180	-2	6	45	45	10	3	151	151	-10	2	132	129	12	6	20	19
5	1	66	71	22	2	3	9	-3	11	168	180	-2	6	45	45	10	3	151	151	-10	2	132	129	12	6	20	19
5	1	66	71	22	2	3	9	-3	11	168	180	-2	6	45	45	10	3	151	151	-10	2	132	129	12	6	20	19
5	1	66	71	22	2	3	9	-3	11	168	180	-2	6	45	45	10	3	151	151	-10	2	132	129	12	6	20	19
5	1	66	71	22	2	3	9	-3	11	168	180	-2	6	45	45	10	3	151	151	-10	2	132	129	12	6	20	19
5	1	66	71	22	2	3	9	-3	11	168	180	-2	6	45	45	10	3	151	151	-10	2	132	129	12	6	20	19
5	1	66	71	22	2	3	9	-3	11	168	180	-2	6	45	45	10	3	151	151	-10	2	132	129	12	6	20	19
5	1	66	71	22	2	3	9	-3	11	168	180	-2	6	45	45	10	3	151	151	-10	2	132	129	12	6	20	19
5	1	66	71	22	2	3	9	-3	11	168	180	-2	6	45	45	10	3	151	151	-10	2	132	129	12	6	20	19
5	1	66	71	22	2	3	9	-3	11	168	180	-2	6	45	45	10	3	151	151	-10	2	132	129	12	6	20	19
5	1	66	71	22	2	3	9	-3	11	168	180	-2	6	45	45	10	3	151	151	-10	2	132	129	12	6	20	19
5	1	66	71	22	2	3	9	-3	11	168	180	-2	6	45	45	10	3	151	151	-10	2	132	129	12	6	20	19
5	1	66	71	22	2	3	9	-3	11	168	180	-2	6	45	45	10	3	151	151	-10	2	132	129	12	6	20	19
5	1	66	71	22	2	3	9	-3	11	168	180	-2	6	45	45	10	3	151	151	-10	2	132	129	12	6	20	19
5	1	66	71	22	2	3	9	-3	11	168	180	-2	6	45	45	10	3	151	151	-10	2	132	129	12	6	20	19
5	1	66	71	22	2	3	9	-3	11	168	180	-2	6	45	45	10	3	151	151	-10	2	132	129	12	6	20	19
5	1	66	71	22	2	3	9	-3	11	168	180	-2	6	45	45	10	3	151	151	-10	2	132	129	12	6	20	19
5	1	66	71	22	2	3	9	-3	11	168	180	-2	6	45	45	10	3	151	151	-10	2	132	129	12	6	20	19
5	1	66	71	22	2	3	9	-3	11	168	180	-2	6	45	45	10	3	151	151	-10	2	132	129	12	6	20	19
5	1	66	71	22	2	3	9	-3	11	168	180	-2	6	45	45	10	3	151	151	-10	2	132	129	12	6	20	19
5	1	66	71	22	2	3	9	-3	11	168	180	-2	6	45	45	10	3	151	151	-10	2	132	129	12	6	20	19
5	1	66	71	22	2	3	9	-3	11	168	180	-2	6	45	45	10	3	151	151	-10	2	132	129	12	6	20	19
5	1	66	71	22	2	3	9	-3	11	168	180	-2	6	45	45	10	3	151	151	-10	2	132	129	12	6	20	19
5	1	66	71	22	2	3	9	-3	11	168	180	-2	6	45	45	10	3	151	151	-10	2	132	129	12	6	20	19
5	1	66	71	22	2	3	9	-3	11	168	180	-2	6	45	45	10	3	151	151	-10	2	132	129	12	6	20	19
5	1	66	71	22	2	3	9	-3	11	168	180	-2	6	45	45	10	3	151	151	-10	2	132	129	12	6	20	19
5	1	66	71	22	2	3	9	-3	11	168	180	-2	6	45	45	10	3	151	151	-10	2	132	129	12	6	20	19
5	1	66	71	22	2	3	9	-3	11	168	180	-2	6	45	45	10	3	151	151	-10	2	132	129	12	6	20	19
5	1	66	71	22	2	3	9	-3	11	168	180	-2	6	45	45	10	3	151	151	-10	2	132	129	12	6	20	19
5	1	66	71	22	2	3	9	-3	11	168	180	-2	6	45	45	10	3	151	151	-10	2	132	129	12	6	20	19
5	1	66	71	22	2	3	9	-3	11	168	180	-2	6	45	45	10	3	151	151	-10	2	132	129	12	6	20	19
5	1	66	71	22	2	3	9	-3	11	168	180	-2	6	45	45	10	3	151	151	-10	2	132	129	12	6	20	19
5	1	66	71	22	2	3	9	-3	11	168	180	-2	6	45	45	10	3	151	151	-10	2	132	129	12	6	20	19
5	1	66	71	22	2	3	9	-3	11	168	180	-2	6	45	45	10	3	151	151	-10	2	132	129	12	6	20	19
5	1	66	71	22	2	3	9	-3	11	168	180	-2	6	45	45	10	3	151	151	-10	2	132	129	12	6	20	19
5	1	66	71	22	2	3																					

Table VI.II
Final positional (fractional $\times 10^4$) and thermal parameters,
with standard deviations in parentheses

ATOM	<u>X</u>	<u>Y</u>	<u>Z</u>	<u>B</u> or <u>b</u> ₁₁	<u>b</u> ₂₂	<u>b</u> ₃₃	<u>b</u> ₁₂	<u>b</u> ₁₃	<u>b</u> ₂₃
Mo	1503(1)	1128(2)	1863(2)	22(1)	66(2)	77(2)	0(1)	8(1)	1(1)
As(1)	1563(1)	2939(2)	2675(2)	28(1)	63(2)	83(3)	-1(1)	6(1)	-3(2)
As(2)	0840(1)	1960(2)	0112(2)	24(1)	81(2)	73(3)	0(1)	4(1)	7(2)
F(1)	0328(9)	3159(16)	1540(21)	47(6)	159(20)	299(32)	19(8)	78(12)	25(20)
F(2)	0396(9)	3916(15)	-0236(17)	59(6)	139(17)	171(21)	46(9)	-27(10)	39(15)
F(3)	1460(7)	3969(13)	0505(17)	36(4)	113(14)	216(23)	6(6)	35(8)	71(15)
F(4)	1441(10)	5343(14)	2357(29)	50(7)	81(13)	512(56)	14(9)	2(15)	-48(22)
F(5)	0775(13)	5515(17)	0955(24)	86(10)	118(18)	286(35)	29(11)	17(15)	42(21)
F(6)	0680(13)	4909(17)	2533(28)	102(11)	115(18)	455(51)	24(12)	156(22)	-5(25)
C(1)	2134(12)	1379(22)	1161(25)	6.9(6)					
C(2)	2014(11)	0691(21)	3245(25)	6.3(6)					
C(3)	1430(9)	-0220(19)	1193(20)	5.1(6)					
C(4)	0917(11)	0826(21)	2679(24)	6.3(6)					
C(5)	0682(15)	3327(28)	0663(32)	8.8(8)					
C(6)	1109(13)	3859(23)	1399(28)	7.6(7)					
C(7)	1010(16)	4916(29)	1860(33)	8.5(8)					
Me(1)	0073(14)	1565(27)	-0416(29)	8.7(8)					
Me(2)	1055(13)	2251(25)	-1364(29)	8.4(8)					
Me(3)	1333(15)	3248(29)	4113(34)	9.9(9)					
Me(4)	2249(14)	3645(26)	2903(31)	8.9(8)					
O(1)	2529(9)	1517(18)	0749(20)	9.4(6)					
O(2)	2331(9)	0453(18)	4112(21)	9.5(6)					
O(3)	1372(8)	-1066(16)	0848(19)	8.2(5)					
O(4)	0572(10)	0590(18)	3206(21)	9.8(6)					

[†]Coefficients in the temperature expression: $\exp -10^{-4} (b_{11}h^2 + b_{22}k^2 + b_{33}\ell^2 + 2b_{12}hk + 2b_{13}h\ell + 2b_{23}k\ell)$

Table VI.III

Bond distances (\AA) and valence angles (degrees),

with standard deviations in parentheses

Mo-C(1)	1.96 (3)	C(1)-O(1)	1.20 (3)
Mo-C(2)	1.90 (3)	C(2)-O(2)	1.18 (3)
Mo-C(3)	1.94 (3)	C(3)-O(3)	1.19 (3)
Mo-C(4)	1.96 (3)	C(4)-O(4)	1.20 (3)
Mo-As(1)	2.573 (4)		
Mo-As(2)	2.569 (7)	C(5)-C(6)	1.40 (4)
		C(6)-C(7)	1.54 (4)
As(1)-Me(3)	1.92 (4)	C(5)-F(1)	1.50 (4)
As(1)-Me(4)	1.92 (3)	C(5)-F(2)	1.37 (4)
As(1)-C(6)	2.06 (3)	C(6)-F(3)	1.51 (4)
As(2)-Me(1)	1.95 (3)	C(7)-F(4)	1.24 (4)
As(2)-Me(2)	1.94 (3)	C(7)-F(5)	1.34 (4)
As(2)-C(5)	1.99 (4)	C(7)-F(6)	1.26 (4)
C(1)-Mo-As(1)	90 (1)	As(2)-C(5)-F(1)	106 (2)
C(1)-Mo-As(2)	92 (1)	As(2)-C(5)-F(2)	113 (2)
C(1)-Mo-C(2)	87 (1)	As(2)-C(5)-C(6)	118 (3)
C(1)-Mo-C(3)	90 (1)	F(1)-C(5)-F(2)	108 (3)
C(4)-Mo-As(1)	90 (1)	F(1)-C(5)-C(6)	99 (3)
C(4)-Mo-As(2)	93 (1)	F(2)-C(5)-C(6)	112 (3)
C(4)-Mo-C(2)	88 (1)		
C(4)-Mo-C(3)	89 (1)	As(1)-C(6)-C(7)	113 (2)
As(1)-Mo-C(2)	90 (1)	As(1)-C(6)-F(3)	104 (2)
As(1)-Mo-As(2)	82.1 (2)	As(1)-C(6)-C(5)	111 (2)
As(2)-Mo-C(3)	95 (1)	C(7)-C(6)-F(3)	108 (3)
C(3)-Mo-C(2)	92 (1)	C(7)-C(6)-C(5)	121 (3)
		F(3)-C(6)-C(5)	97 (3)
Mo-As(1)-Me(3)	121 (1)		
Mo-As(1)-Me(4)	119 (1)	C(6)-C(7)-F(4)	113 (3)
Mo-As(1)-C(6)	108 (1)	C(6)-C(7)-F(5)	110 (3)
Me(3)-As(1)-C(6)	106 (1)	C(6)-C(7)-F(6)	113 (3)
Me(3)-As(1)-Me(4)	102 (2)	F(4)-C(7)-F(5)	106 (3)
Me(4)-As(1)-C(6)	98 (1)	F(4)-C(7)-F(6)	110 (3)
		F(5)-C(7)-F(6)	105 (3)
Mo-As(2)-Me(1)	123 (1)		
Mo-As(2)-Me(2)	122 (1)	Mo-C(1)-O(1)	178 (3)
Mo-As(2)-C(5)	106 (1)	Mo-C(2)-O(2)	178 (3)
Me(1)-As(2)-C(5)	95 (1)	Mo-C(3)-O(3)	176 (2)
Me(1)-As(2)-Me(2)	103 (1)	Mo-C(4)-O(4)	176 (2)
Me(2)-As(2)-C(5)	102 (1)		

Table VI.IV

Magnitudes (\AA) of the principal axes of the thermal vibration ellipsoids of anisotropic atoms.

	Axis 1	Axis 2	Axis 3
Mo	0.22	0.24	0.26
As(1)	0.23	0.24	0.30
As(2)	0.21	0.27	0.28
F(1)	0.26	0.37	0.49
F(2)	0.19	0.38	0.51
F(3)	0.24	0.32	0.42
F(4)	0.25	0.39	0.61
F(5)	0.29	0.44	0.53
F(6)	0.26	0.37	0.65

DISCUSSION

The molecule 1,2-bis(dimethylarsino)hexafluoropropanemolybdenum tetracarbonyl (Figure VI.1) is derived from molybdenum hexacarbonyl^{44,45} by replacement of two carbonyl groups by the arsenic atoms of the chelating di-(tertiary arsine) ligand. The co-ordination around molybdenum remains essentially octahedral. The five atoms C(2), C(3), Mo, As(1) and As(2) are situated in the least-squares plane given in Table VI.V with C(1) and C(4) equally spaced above and below this plane. The As-Mo-As angle is 82.1°, and the other angles at molybdenum are in the range 87-95° (Table VI.III). The Mo-C bond distances, 1.90-1.96(3), mean 1.94 Å, and the C-O bond lengths, 1.18-1.20(3), mean 1.19 Å, are similar to values reported previously.⁴⁶⁻⁵² The Mo-C-O groupings are almost exactly linear, 176-178(3)°.

The Mo-As bond distance appears to be measured for the first time, the mean value being 2.572(4) Å. This distance is close to that which would be predicted from a knowledge of other metal-arsenic bond lengths, and from differences in covalent radii; e.g. the Fe-As bond distance is 2.30 Å, the Mo-Mo distances in various compounds⁴⁹⁻⁵² average 3.25 Å, and the unbridged Fe-Fe distance in $\text{Fe}_3(\text{CO})_{12}$ is 2.65 Å,¹⁸ giving a predicted Mo-As bond length of $(2.30 + \frac{1}{2}(3.25 - 2.65)) = 2.60$ Å.

The As-Me bond lengths are 1.92-1.95(3), mean 1.93 Å, and the As-C (fluorocarbon) bond distances are 1.99(4)

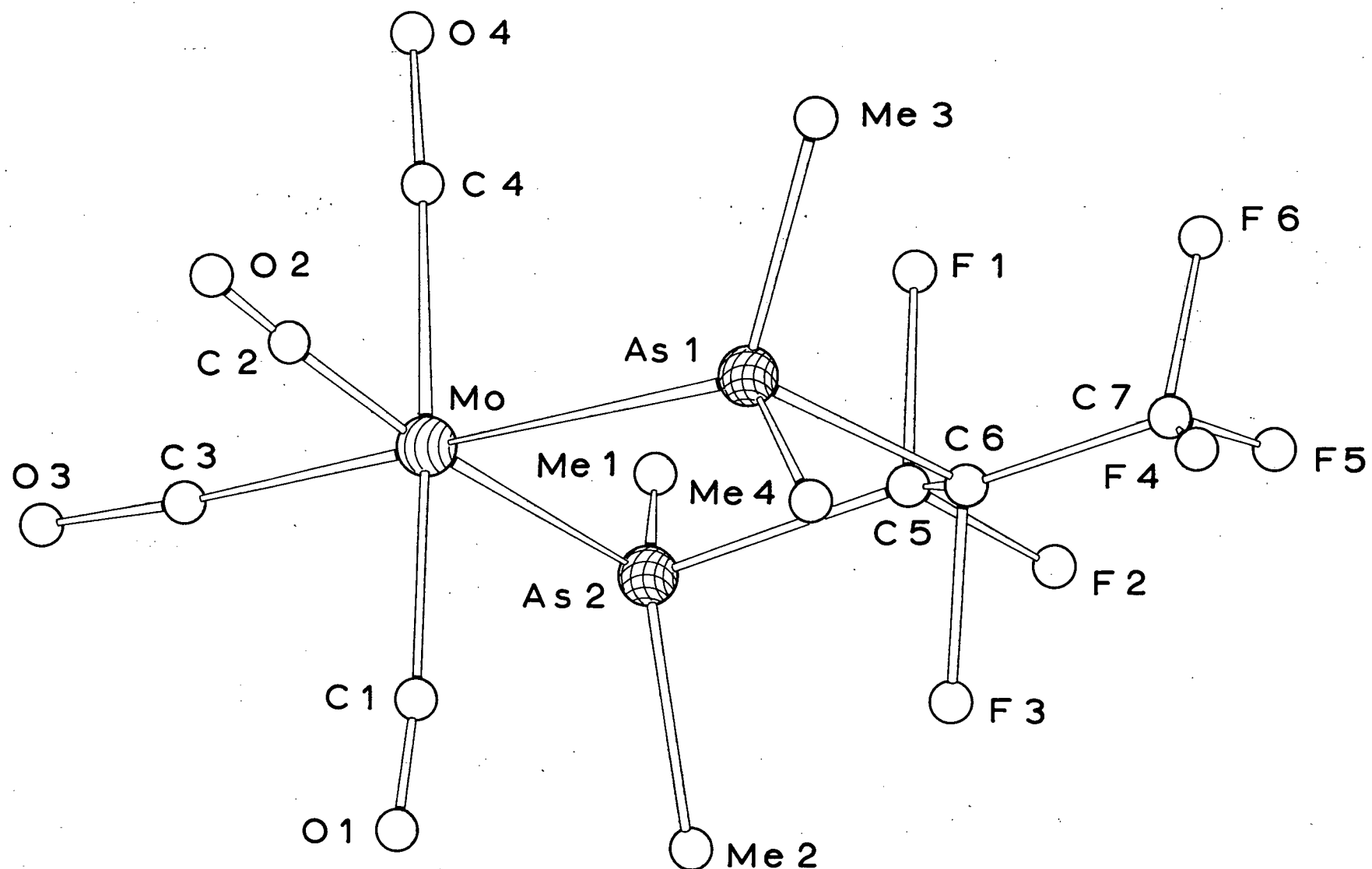


Figure VI.1 Molecular structure of $L'Mo(CO)_4$.

Table VI.V

(a.) Equation of weighted mean plane of Mo, As(1), As(2), C(2) and C(3) in the form $\underline{\ell}X' + \underline{m}Y + \underline{n}Z' = \underline{p}$ where X', Y, Z' are coordinates in Å, referred to the orthogonal axes a, b, c^* .

$\underline{\ell}$	\underline{m}	\underline{n}	\underline{p}	maximum displacement (Å)
0.8801	0.1876	-0.4361	2.2605	0.03

(b.) Direction cosines of the vector C(5)-C(6) referred to the orthogonal axes a, b, c^* .

$$(0.6333, 0.5014, 0.5895)$$

and 2.06(3), mean 2.03 Å; the mean values of the two types of As-C bond are significantly different. The angles at arsenic which involve the molybdenum atom are larger than the angles involving only carbon atoms. The Mo-As-C(fluorocarbon) angles, 106 and 108(1)°, are probably influenced by their presence in the five-membered ring, but the Mo-As-Me angles, 119-123 mean 121°, are all significantly larger than the tetrahedral angle, presumably as a result of the steric influence of the $\text{Mo}(\text{CO})_4$ group. There are two distinct Me-As-C(fluorocarbon) angles at each arsenic atom, 98 and 106(1)° at As(1), and 95 and 102(1)° at As(2), probably as a result of differing steric interactions between the two methyl groups at each arsenic and the fluorocarbon.

A table of α (the dihedral angle between the plane

containing the ring carbon atoms and the metal atom and the plane containing the ring nitrogen atoms and the metal atom) and β (the angle between the nitrogen atoms as one looks down the carbon-carbon bond) has been compiled for a number of $M(en)_3$ complexes. Average values of α and β are 24.8 and 48.6° respectively.⁵³ The five-membered ring in $L'Mo(CO)_4$ is non-planar with C(5) and C(6) displaced by -0.40 and 0.14 Å respectively from the As-Mo-As plane, so that the C-C bond is twisted 23.2° with respect to the central plane of the molybdenum octahedron (cf. 24.8° average of values from ref. 53). A view along the C-C bond is shown in Figure VI.2. The arrangement is staggered, with the *trans* dihedral angles all being close to 180° (178, 175, and 179°). The As-C-C-As dihedral angle (47° , cf. 48.6° , average from ref. 53) is reduced from an ideal 60° as a result of the formation of the chelate ring. The one trifluoromethyl and three fluorine substituents of the C-C bond may be classified as axial or equatorial with respect to the chelate ring; the bulkier trifluoromethyl group occupies a less sterically-hindered equatorial position (Figures VI.1 and VI.2).

The bond distances and valence angles in the fluorocarbon group (Table VI.III) show some unusual and interesting features. The C-F(axial) bond distances are 1.50 and 1.51(4), mean 1.51(3) Å, the C-F(equatorial) bond length is 1.37(4) Å, and the C-F(trifluoromethyl) bonds

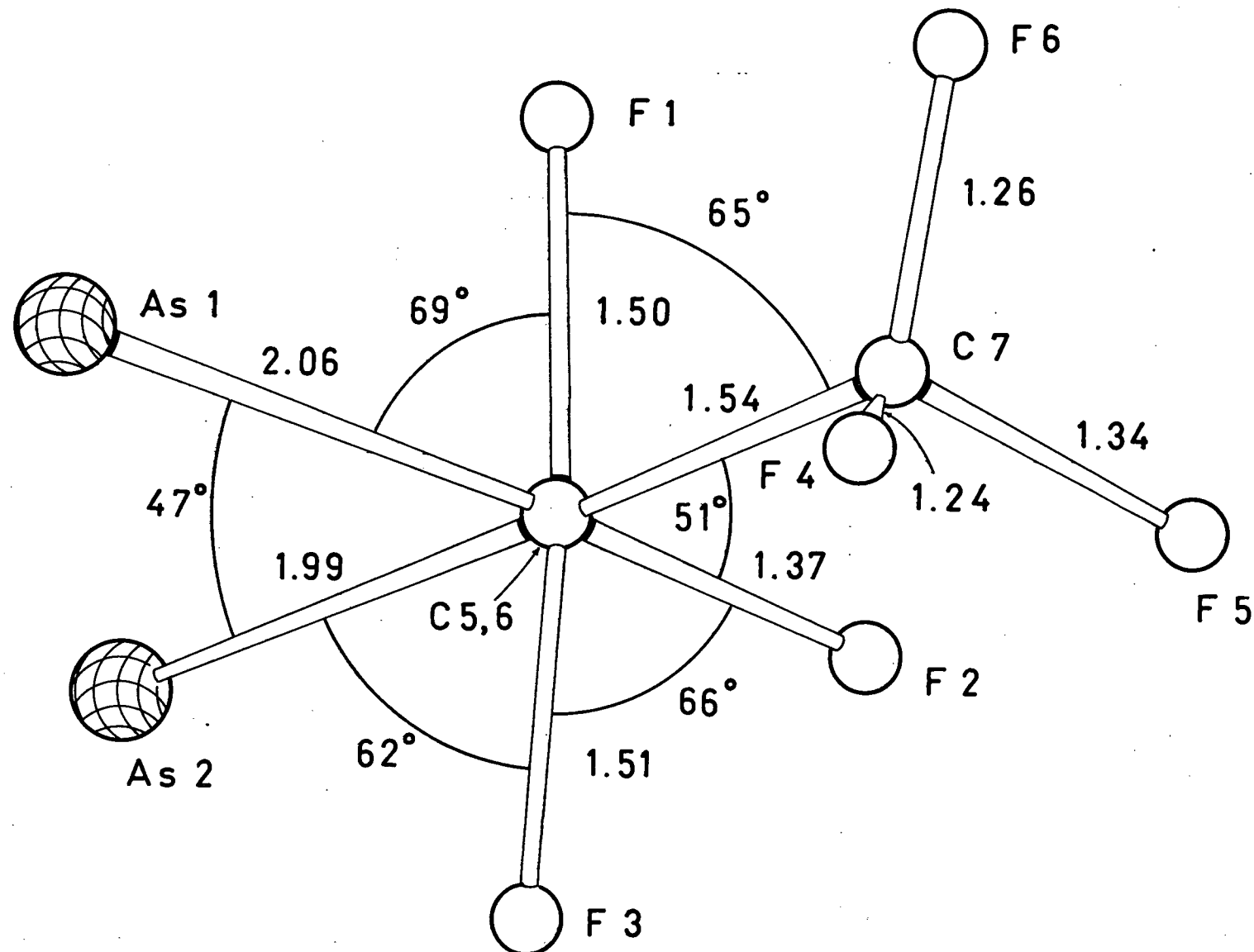
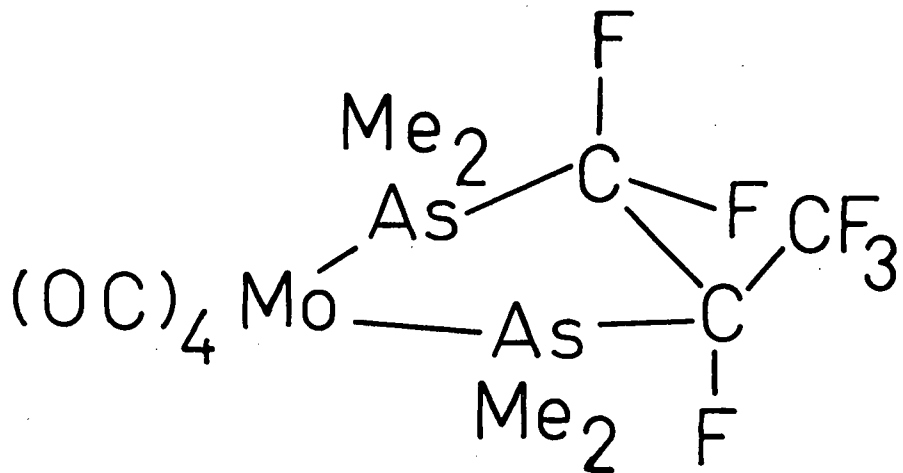


Figure VI.2 View of bond distances and dihedral angles around C(5)-C(6) bond.

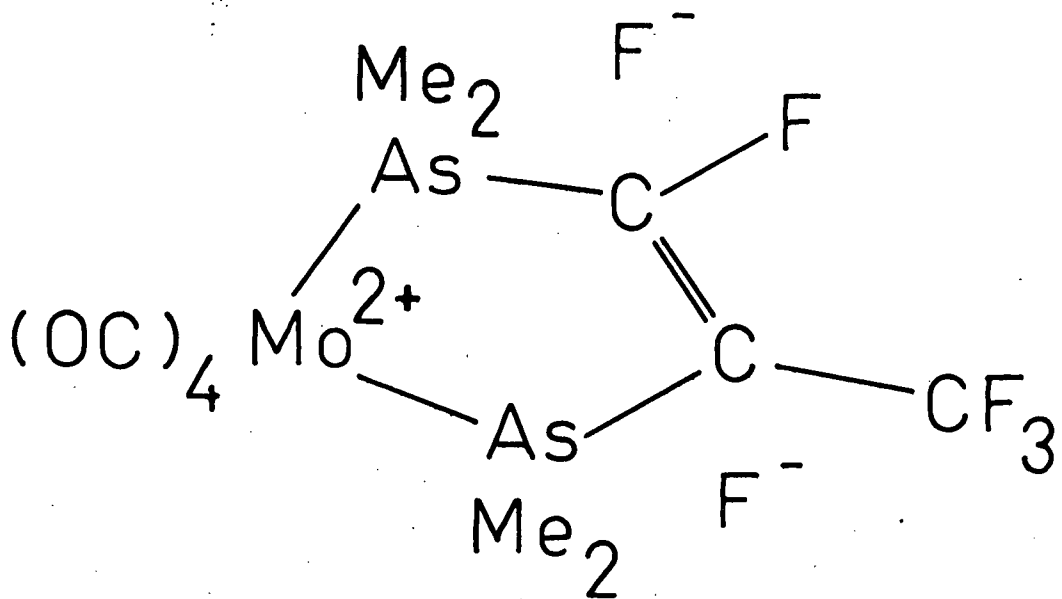
measure 1.24, 1.26, and 1.34(4), mean 1.28(2) Å. The normal C-F bond distance⁵⁴ is 1.33 Å. The equatorial and trifluoromethyl C-F bond lengths do not differ significantly from the normal value; the equatorial C-F bond cannot be claimed to be significantly longer than the trifluoromethyl bonds, as it differs from the mean trifluoromethyl length by only 2σ and from the longest observed trifluoromethyl bond by only 0.5σ. The C-F(axial) bonds are however very significantly longer than a normal C-F bond (by 6σ), than the C-F(equatorial) bond (by 2.8σ), and than the mean of the C-F(trifluoromethyl) bonds (by 6σ).

The C-C bond distance is 1.40(4) Å, significantly shorter (by 3.5σ) than a normal C-C single bond (1.54 Å). The valence angles at C(5) and C(6) are also informative. Those angles not involving the axial fluorine atoms are all greater than the tetrahedral value, range 111-121(3), mean 115°; the angles involving the axial fluorines are correspondingly less than the tetrahedral value, with the C-C-F(axial) angles being 97 and 99(3)°.

All of these unusual features are explicable in terms of a bonding system which, in valence bond language, contains a contribution not only from the normal structure Ia (Figure VI.3), but also from the structure Ib, which involves donation of molybdenum non-bonding d-electrons, via the arsenic 4d orbitals, into orbitals of the fluorocarbon group. The molecular dimensions are best explained by an equal contribution of the two canonical forms Ia and



I a



I b

Figure VI.3 Proposed bonding scheme to account for anomalous observations.

Ib to the resonance hybrid; the C-C bond thus has 50% double bond character, in agreement with the observed distance of 1.40 Å, and the angles not involving F(axial) would be expected to be about midway between the tetrahedral (110°) and trigonal (120°) values, as observed (mean 115°). The C-F(axial) bond distance would be predicted to be considerably longer than a normal single bond (1.33 Å) as a result of the contribution of the no-bond structure, Ib, again as observed (1.51 Å). In molecular orbital terminology, the chelate ring contains a delocalized π-bond system, which involves a filled molybdenum 4d orbital, empty arsenic 4d orbitals, and an orbital on each carbon atom which approximates a p orbital, normal to an approximate sp^2 σ-bonding system.

It is difficult to predict what distance would be expected for the C-F(axial) bonds on the basis of the above bonding scheme. However, since the bonds have a predicted total bond order of 0.5, the distance would be longer than the single bond distance (1.33 Å) by approximately 0.14 Å, which is the shortening noted in the C-C bond for a related change in bond order. This is in agreement with the observed value of 1.51 Å.

More reliable comparison may be made with $\text{CHF}=\text{CF}\cdot\text{Mn}(\text{CO})_5$, in which long C-F bonds, 1.48(2) Å, have been observed.⁵⁵ These long bonds have been rationalized in terms of structures involving $\text{Mn}^{+}=\overset{\text{II}}{\text{C}} \text{F}^{-}$. Another comparable structure is $\text{Mn}(\text{CO})_5\text{CF}_3$, where i.r. spectra have been interpreted⁵⁶ in terms of weak

C-F bonds resulting from resonance structures of the type $Mn^+ = CF_2 \quad F^-$. Contributions from structures of this type have been supported by the observance of a short Mo-C₃F₇ in $\pi\text{-C}_5\text{H}_5\text{Mo}(\text{CO})_3\text{C}_3\text{F}_7$,⁴⁷ although no related abnormalities were found in the C-F bonds. The situation in the present compound is similar, but with the added feature that the carbon atom is not directly bonded to the metal, so that any effect must be transmitted through the arsenic atoms.

It is well known that in a metal complex, the metal atom tends to reduce a high formal negative charge by back-donation of electrons into non-bonding or anti-bonding orbitals of the ligands. It would appear that the ligand in the present compound is able to function in this back-donation by virtue of the presence of the C-F bonds in the axial positions. Such bonding appears to be able to force C-F bonds into a favourable axial position even in compounds where steric factors favour an equatorial position for the fluorine atom. In $\text{Me}_2\text{AsCHFC}_2\text{AsMe}_2 \cdot \text{Cr}(\text{CO})_4$ for example, n.m.r. studies⁵⁷ indicate an axial fluorine atom.

At first glance, this model appears to have the undesirable feature that the positive charge on the molybdenum might be expected to cause Mo-C bonds to be longer and C-O bonds to be shorter than those of Mo(CO)₆ as a result of the unavailability of non-bonded metal electrons for back-bonding. Corresponding shifts of C-O stretching

frequencies to higher wavenumbers might also be expected. However, the charge distribution pictured in Figure VI.3.Ib can also be interpreted as a mechanism for increasing the π -acceptor strength of the di-(tertiary arsine) ligand to the level of the carbonyl group, in which case, no difference between the Mo-C and C-O bond lengths in $\text{Mo}(\text{CO})_6$ and those in $\text{L}'\text{Mo}(\text{CO})_4$ would be expected.

The C-CF₃ bond in the present compound, 1.54(4) Å, is a normal single bond, the C-C-F angles, 110-113(3) $^\circ$, are slightly larger, and the F-C-F angles, 105-110(3) $^\circ$ slightly smaller than the tetrahedral value.

The thermal vibration ellipsoids for those atoms treated anisotropically (Table VI.IV) are in general oriented so that the maximum vibrations are in directions of least steric restraint, *i.e.* between or perpendicular to bonds.

The intermolecular packing appears to be governed solely by van der Waals interactions. A projection of the structure, with the shorter intermolecular distances, is shown in Figure VI.4.

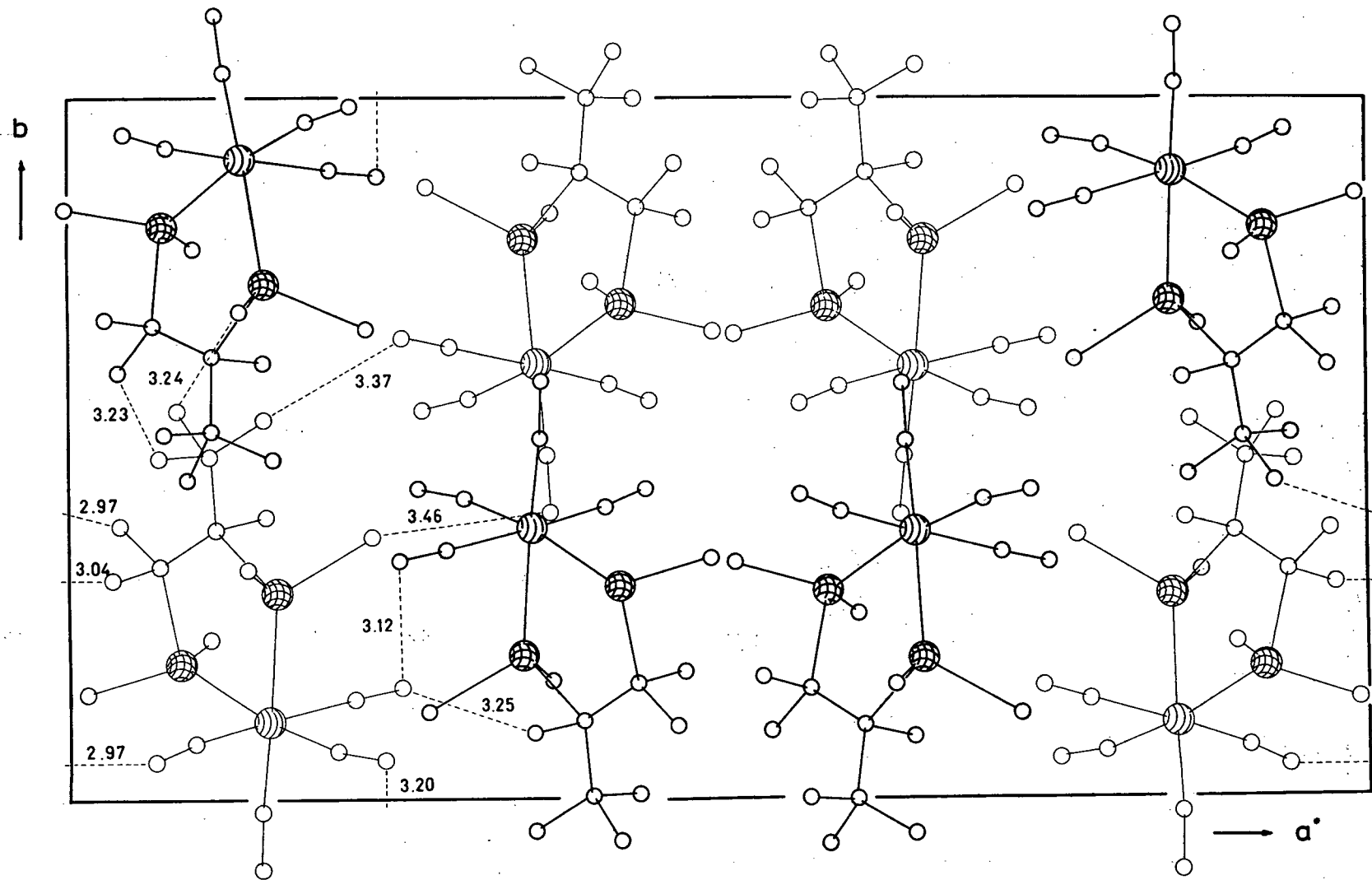


Figure VI.4 Projection of the unit cell down the c-axis.

VII. COMPUTER PROGRAMMING

A. PROGRAM "UPDATE"

During refinement by our full-matrix least-squares program, the residual quantity being minimized is $\sum w\Delta^2$ where $\Delta = |\underline{F}_O - \underline{F}_C|$ and $w = k/\sigma_F^2$ (k is a constant and σ_F is the standard deviation in \underline{F}). The program can be made to assign standard deviations in \underline{F} 's from Cruickshank's equation⁵⁸

$$\sigma_F^2 = A + B|\underline{F}_O| + C|\underline{F}_O|^2 + D|\underline{F}_O|^3 \quad (7.1)$$

A correct weighting scheme requires that $\sum w\Delta^2$ be constant over local ranges of $|\underline{F}_O|$. Since all ranges can be made to have equal numbers of reflections, $\sum w\Delta^2$ for a range is proportional to the mean $w\Delta^2$, $\langle w\Delta^2 \rangle$, of the range and we can say that the $\langle w\Delta^2 \rangle$ for all ranges must be equal and make them all equal to $\langle \Delta^2 \rangle$ of the first range.

$$\langle w\Delta^2 \rangle_i = \langle \Delta^2 \rangle_1 \quad (7.2)$$

$$\text{but since } w = k/\sigma_F^2 \quad (7.3)$$

$$\left(\frac{\langle \Delta^2 \rangle}{\sigma_F^2} \right)_i = \frac{\langle \Delta^2 \rangle_1}{k} \quad (7.4)$$

where σ_F^2 is calculated for the mean $|\underline{F}_O|$ of the range.

Therefore, by transposing,

$$\left(\sigma_F^2 \right)_i = k \langle \Delta^2 \rangle_1 / \langle \Delta^2 \rangle_i \quad (7.5)$$

and we must calculate A , B , C , and D for the best least-squares fit of

$(\sigma_F^2)_{ij}$ to $k \langle \Delta^2 \rangle_i / \langle \Delta^2 \rangle_1$ over NGRP ranges, where NGRP is input to the program from cards.

This leads to the familiar normal equations

$$\frac{\partial}{\partial A, B, C, D} \sum_{i=1}^{NGRP} \{ A + B \langle |F_O| \rangle_i + C \langle |F_O|^2 \rangle_i + D \langle |F_O|^3 \rangle_i - \frac{k \langle \Delta^2 \rangle_i}{\langle \Delta^2 \rangle_1} \}^2 = 0 \quad (7.6)$$

or in matrix notation,

$$\begin{pmatrix} NGRP & \sum_i \langle |F_O| \rangle_i & \sum_i \langle |F_O|^2 \rangle_i & \sum_i \langle |F_O|^3 \rangle_i \\ \sum_i \langle |F_O| \rangle_i & \sum_i \langle |F_O|^2 \rangle_i & \sum_i \langle |F_O|^3 \rangle_i & \sum_i \langle |F_O|^4 \rangle_i \\ \sum_i \langle |F_O|^2 \rangle_i & \sum_i \langle |F_O|^3 \rangle_i & \sum_i \langle |F_O|^4 \rangle_i & \sum_i \langle |F_O|^5 \rangle_i \\ \sum_i \langle |F_O|^3 \rangle_i & \sum_i \langle |F_O|^4 \rangle_i & \sum_i \langle |F_O|^5 \rangle_i & \sum_i \langle |F_O|^6 \rangle_i \end{pmatrix} \begin{pmatrix} A \\ B \\ C \\ D \end{pmatrix} =$$

$$k \begin{pmatrix} \sum_i \langle \Delta^2 \rangle_i / \langle \Delta^2 \rangle_1 \\ \sum_i \langle |F_O| \rangle_i \langle \Delta^2 \rangle_i / \langle \Delta^2 \rangle_1 \\ \sum_i \langle |F_O|^2 \rangle_i \langle \Delta^2 \rangle_i / \langle \Delta^2 \rangle_1 \\ \sum_i \langle |F_O|^3 \rangle_i \langle \Delta^2 \rangle_i / \langle \Delta^2 \rangle_1 \end{pmatrix} \quad (7.7)$$

$$\text{or } \underline{T} \underline{W}/k = \underline{S} \quad (7.8) \quad \text{and } \underline{W}/k = \underline{T}^{-1} \underline{S} \quad (7.9)$$

and we solve for A/k , B/k , C/k , and D/k by inverting \underline{T} and multiplying by \underline{S} .

The best choice of weights, which gives the lowest standard deviations in the derived parameters is $\underline{w} = 1/\sigma_F^2$ so that if we can evaluate the constant k in (7.3) we can achieve the best weighting scheme by multiplying the

solution of the normal equations by k. It can be shown theoretically that the constant k is

$$\text{ERROR} = \sum w \Delta^2 / (\text{NREF}-\text{NV}) \quad (7.10)$$

where NREF is the number of reflections and NV is the number of variables in the least-squares crystal structure refinement.

The program "UPDATE" can now be formulated in six stages (*cf.* Table VII.I).

i) read structure factor data and sort in order of increasing magnitude of $|F_O|$. Subroutine ASORT(A,I,N,M,K) is an assembler-language routine which sorts the M by K fragment of the array A (which is dimensioned N by K) according to one-word keys located in the first column of the array. Each row is moved with its first element. For adaptation to this program, A is dimensioned 10,000 by 2 and M is set to NREF, the number of reflections read from the structure factor data. The array elements A(J,1) and A(J,2) contain $|F_O|$ and $|F_C|$, respectively, for the Jth reflection. At the completion of this stage of the program, we have an array A(NREF,2) which is sorted in order of increasing $|F_O|$.

ii) determine the number of reflections in each range. The number of ranges desired (NGRP) is input to the program from cards. Each range is given NREF/NGRP reflections with additional single reflections added to the first few ranges if NREF/NGRP is not an integer.

Table VII.I

Listing of the program "UPDATE"

```

1      REAL MOLSO,MEANFD,MARFD,MOLSDO,MINDS
2      REAL A(10),C(10),Y(10),SIGD(1),YC(1),ST(1),AC(10),AS(10)
3      DIMENSION SUM(1),NUM(1),X(1),A(1),C(1)
4      DIMENSION HJ(10),HJ(1),HJ(1),FSCALE(1),WEIN(10),T(10),Y(10)
5      REAL X(1),Y(1),SUM(1)
6      INTEGER T(2),HJ(10),HJ(1),FSCALE(1),REFN
7      FORMAT(1X,'THIS DATA SET CANNOT BE FITTED TO A FOUR PARAMETER CURV')
8
9      527 FORMAT(IX,'BY LEAST SQUARES METHODS (WITHOUT NEGATIVE WEIGHTS)')
10     FORMAT(1X,' A = ',F15.5,' B = ',F15.5,' C = ',F15.5,' Q = ',F15.5)
11     528 FORMAT(1X,' FSCALE = ',F15.5)
12     529 FORMAT(1X,' SUM = ',I1)
13     530 FORMAT(1X,' ')
14     531 FORMAT(1X,' ')
15     532 FORMAT(1F10.1,I2,15)
16     533 FORMAT(1F10.1,I2,15)
17     534 FORMAT(1F10.1,I2,15)
18     535 FORMAT(1F10.1,I2,15)
19     536 FORMAT(1F10.1,I2,15)
20     537 FORMAT(1X,' R MEAN FD PW MEAN ERROR NREF=46')
21     538 FORMAT(1X,' ')
22     539 FORMAT(1X,'WEIGHTING PARAMETERS CORRECTED FOR F SQUARED')
23     540 FORMAT(1X,'WOLSDO=1.01')
24     541 FORMAT(1X,'REFN=NGRP')
25     542 FORMAT(1X,'JKP=1')
26     543 FORMAT(1X,'DO 20 I=1,10')
27     544 FORMAT(1X,'SUM(I)=0')
28     545 FORMAT(1X,'NREF=4')
29     546 C READ STRUCTURE FACTOR DATA AND SORT IN ORDER OF INCREASING
30     547 C MAGNITUDE OF FDOS
31     548 C
32     549 DO 1 J=1,1000
33     550 READ(1,END=99) (Y(IK),SIGIK),YC(K),ST(K),AC(K),AS(K),K=1,100
34     551 (HJ(1),HJ(1),HJ(1),FSCALE(1),REFN),L=1,10
35     552 DO 1 I=1,10
36     553 (Y(I),SIGD(I),Y(I)),I=1,10
37     554 IF(Y(10).LT.0.0) GO TO 90
38     555 NRFF=NRFF+1
39     556 4234 NRFF=NRFF+1
40     557 2 AINREF(1)=Y(1)
41     558 1 CONTINUE
42     559 CALL ASORT(A(1,1),NRFF,NRFF,2)
43     560 C DETERMINE NUMBER OF REFLECTIONS IN EACH RANGE
44     561 C
45     562 XNRFF=NRFF
46     563 TNRFF=NREF/NGRP
47     564 JX=NRFF-NGRP+1
48     565 DO 5 I=1,1000
49     566 IF(JX.LT.1) GO TO 5
50     567 5 NUM(I)=INREF
51     568 GU TO 3
52     569 4 NUM(I)=INREF+1
53     570 1 CONTINUE
54     571 C CALCULATE WEIGHTING ANALYSIS INFORMATION
55     572 C
56     573 SSOLTA = 0.0
57     574 SSUMFD=0.0
58     575 DO 6 J=1,NGRP
59     576 SUMFD=0.
60     577 SDELTAFD=0.
61     578 DELTA=0.
62     579 DELTA=0.
63     580 K0=NUM(I)
64     581 DO 7 I=1,KP
65     582 DELTA=AS(1)(JKP+I)+A(JKP+I,2)
66     583 DLTASC=DELTA*DELTA
67     584 DLSDO=MOLSO*DLTASC
68     585 SUMFD=SUMFD+DLSDO
69     586 SDELTAFD=SDELTAFD+DLSDO
70     587 SUMFD=SUMFD+A(JKP+I,1)
71     588 WRITE(1,1) DLTASC,A(JKP+I,1),
72     589 TFI,FU(1),MINFD,A(JKP+I,1)
73     590 TFI,FU(0),NUM(I)) MAYBE=A(JKP+I,1)
74     591 MOLSO=MOLSO+NUM(I)
75     592 K1=K0+1
76     593 MAFNFD=MAFNFD+MOLSO
77     594 P=SDELTAFD/SUMFD
78     595 MOLSD=MOLSO/MINDS
79     596 SSUMFD=SSUMFD+SUMFD
80     597 SSOLTA=SSOLTA+SDELTAFD
81     598 JK=1
82     599 6 WRITE(1,1) MINFD,MAFNF,MANFD,MOLSO,TFI,FU(0),MOLSD,TFI,FU(1)
83     600 ENDIF,3
84     601 C
85     602 C CALCULATE MATRIX ELEMENTS FOR LEAST SQUARES CALCULATION AND SOLVE
86     603 C FOR WEIGHTING SCHEME PARAMETERS
87     604 C
88     605 DO 8 J=1,NGRP
89     606 READ(1,END=161) E,F,H,G,AN
90     607 T(1)=R
91     608 SUM(1)=SUM(1)+T(1)
92     609 DO 15 J=2,6
93     610 JH(1)=R
94     611 T(1)=T(1)+R
95     612 SUM(1)=SUM(1)+T(1)
96     613 15 CONTINUE
97     614 T(7)=AN
98     615 SUM(7)=SUM(7)+T(7)
99     616 DO 16 I=1,6
100    617 LM=I+1
101    618 T(1)=T(1)+R
102    619 SUM(1)=SUM(1)+T(1)
103    620 16 CONTINUE
104    621 8 CONTINUE
105    622 16 CONTINUE
106    623 REWIND 3
107    624 X(1,1)=RNGRP
108    625 DO 19 K=2,4
109    626 KM=K-1
110    627 18 X(1,K)=SUM(KM)
111    628 DO 20 I=1,K
112    629 X(1,I)=SUM(K)
113    630 X(1,1)=SUM(1)
114    631 X(3,1)=SUM(5)
115    632 X(4,1)=SUM(6)
116    633 DO 21 I=2,4
117    634 IM=I-1
118    635
119    636 202 202 C SUBROUTINE SOLN(A,R,N,M,DET,>)
120    637 203 203 C SUBROUTINE TO SOLVE MATRIX EQUATION
121    638 204 204 C
122    639 205 205 C
123    640 206 206 C
124    641 207 207 C
125    642 208 208 C
126    643 209 209 C
127    644 210 210 C
128    645 211 211 C
129    646 212 212 C
130    647 213 213 C
131    648 214 214 C
132    649 215 215 C
133    650 216 216 C
134    651 217 217 C
135    652 218 218 C
136    653 219 219 C
137    654 220 220 C
138    655 221 221 C
139    656 222 222 C
140    657 223 223 C
141    658 224 224 C
142    659 225 225 C
143    660 226 226 C
144    661 227 227 C
145    662 228 228 C
146    663 229 229 C
147    664 230 230 C
148    665 231 231 C
149    666 232 232 C
150    667 233 233 C
151    668 234 234 C
152    669 235 235 C
153    670 236 236 C
154    671 237 237 C
155    672 238 238 C
156    673 239 239 C
157    674 240 240 C
158    675 241 241 C
159    676 242 242 C
160    677 243 243 C
161    678 244 244 C
162    679 245 245 C
163    680 246 246 C
164    681 247 247 C
165    682 248 248 C
166    683 249 249 C
167    684 250 250 C
168    685 251 251 C
169    686 252 252 C
170    687 253 253 C
171    688 254 254 C
172    689 255 255 C
173    690 256 256 C
174    691 257 257 C
175    692 258 258 C
176    693 259 259 C
177    694 260 260 C
178    695 261 261 C
179    696 262 262 C
180    697 263 263 C
181    698 264 264 C
182    699 265 265 C
183    700 266 266 C
184    701 267 267 C
185    702 268 268 C
186    703 269 269 C
187    704 270 270 C
188    705 271 271 C
189    706 272 272 C
190    707 273 273 C
191    708 274 274 C
192    709 275 275 C
193    710 276 276 C
194    711 277 277 C
195    712 278 278 C
196    713 279 279 C
197    714 280 280 C
198    715 281 281 C
199    716 282 282 C
200    717 283 283 C
201    718 284 284 C
202    719 285 285 C
203    720 286 286 C
204    721 287 287 C
205    722 288 288 C
206    723 289 289 C
207    724 290 290 C
208    725 291 291 C
209    726 292 292 C
210    727 293 293 C
211    728 294 294 C
212    729 295 295 C
213    730 296 296 C
214    731 297 297 C
215    732 298 298 C
216    733 299 299 C
217    734 300 300 C
218    735 301 301 C
219    736 302 302 C
220    737 303 303 C
221    738 304 304 C
222    739 305 305 C
223    740 306 306 C
224    741 307 307 C
225    742 308 308 C
226    743 309 309 C
227    744 310 310 C
228    745 311 311 C
229    746 312 312 C
230    747 313 313 C
231    748 314 314 C
232    749 315 315 C
233    750 316 316 C
234    751 317 317 C
235    752 318 318 C
236    753 319 319 C
237    754 320 320 C
238    755 321 321 C
239    756 322 322 C
240    757 323 323 C
241    758 324 324 C
242    759 325 325 C
243    760 326 326 C
244    761 327 327 C
245    762 328 328 C
246    763 329 329 C
247    764 330 330 C
248    765 331 331 C
249    766 332 332 C
250    767 333 333 C
251    768 334 334 C
252    769 335 335 C
253    770 336 336 C
254    771 337 337 C
255    772 338 338 C
256    773 339 339 C
257    774 340 340 C
258    775 341 341 C
259    776 342 342 C
260    777 343 343 C
261    778 344 344 C
262    779 345 345 C
263    780 346 346 C
264    781 347 347 C
265    782 348 348 C
266    783 349 349 C
267    784 350 350 C
268    785 351 351 C
269    786 352 352 C
270    787 353 353 C
271    788 354 354 C
272    789 355 355 C
273    790 356 356 C
274    791 357 357 C
275    792 358 358 C
276    793 359 359 C
277    794 360 360 C
278    795 361 361 C
279    796 362 362 C
280    797 363 363 C
281    798 364 364 C
282    799 365 365 C
283    800 366 366 C
284    801 367 367 C
285    802 368 368 C
286    803 369 369 C
287    804 370 370 C
288    805 371 371 C
289    806 372 372 C
290    807 373 373 C
291    808 374 374 C
292    809 375 375 C
293    810 376 376 C
294    811 377 377 C
295    812 378 378 C
296    813 379 379 C
297    814 380 380 C
298    815 381 381 C
299    816 382 382 C
300    817 383 383 C
301    818 384 384 C
302    819 385 385 C
303    820 386 386 C
304    821 387 387 C
305    822 388 388 C
306    823 389 389 C
307    824 390 390 C
308    825 391 391 C
309    826 392 392 C
310    827 393 393 C
311    828 394 394 C
312    829 395 395 C
313    830 396 396 C
314    831 397 397 C
315    832 398 398 C
316    833 399 399 C
317    834 400 400 C
318    835 401 401 C
319    836 402 402 C
320    837 403 403 C
321    838 404 404 C
322    839 405 405 C
323    840 406 406 C
324    841 407 407 C
325    842 408 408 C
326    843 409 409 C
327    844 410 410 C
328    845 411 411 C
329    846 412 412 C
330    847 413 413 C
331    848 414 414 C
332    849 415 415 C
333    850 416 416 C
334    851 417 417 C
335    852 418 418 C
336    853 419 419 C
337    854 420 420 C
338    855 421 421 C
339    856 422 422 C
340    857 423 423 C
341    858 424 424 C
342    859 425 425 C
343    860 426 426 C
344    861 427 427 C
345    862 428 428 C
346    863 429 429 C
347    864 430 430 C
348    865 431 431 C
349    866 432 432 C
350    867 433 433 C
351    868 434 434 C
352    869 435 435 C
353    870 436 436 C
354    871 437 437 C
355    872 438 438 C
356    873 439 439 C
357    874 440 440 C
358    875 441 441 C
359    876 442 442 C
360    877 443 443 C
361    878 444 444 C
362    879 445 445 C
363    880 446 446 C
364    881 447 447 C
365    882 448 448 C
366    883 449 449 C
367    884 450 450 C
368    885 451 451 C
369    886 452 452 C
370    887 453 453 C
371    888 454 454 C
372    889 455 455 C
373    890 456 456 C
374    891 457 457 C
375    892 458 458 C
376    893 459 459 C
377    894 460 460 C
378    895 461 461 C
379    896 462 462 C
380    897 463 463 C
381    898 464 464 C
382    899 465 465 C
383    900 466 466 C
384    901 467 467 C
385    902 468 468 C
386    903 469 469 C
387    904 470 470 C
388    905 471 471 C
389    906 472 472 C
390    907 473 473 C
391    908 474 474 C
392    909 475 475 C
393    910 476 476 C
394    911 477 477 C
395    912 478 478 C
396    913 479 479 C
397    914 480 480 C
398    915 481 481 C
399    916 482 482 C
400    917 483 483 C
401    918 484 484 C
402    919 485 485 C
403    920 486 486 C
404    921 487 487 C
405    922 488 488 C
406    923 489 489 C
407    924 490 490 C
408    925 491 491 C
409    926 492 492 C
410    927 493 493 C
411    928 494 494 C
412    929 495 495 C
413    930 496 496 C
414    931 497 497 C
415    932 498 498 C
416    933 499 499 C
417    934 500 500 C
418    935 501 501 C
419    936 502 502 C
420    937 503 503 C
421    938 504 504 C
422    939 505 505 C
423    940 506 506 C
424    941 507 507 C
425    942 508 508 C
426    943 509 509 C
427    944 510 510 C
428    945 511 511 C
429    946 512 512 C
430    947 513 513 C
431    948 514 514 C
432    949 515 515 C
433    950 516 516 C
434    951 517 517 C
435    952 518 518 C
436    953 519 519 C
437    954 520 520 C
438    955 521 521 C
439    956 522 522 C
440    957 523 523 C
441    958 524 524 C
442    959 525 525 C
443    960 526 526 C
444    961 527 527 C
445    962 528 528 C
446    963 529 529 C
447    964 530 530 C
448    965 531 531 C
449    966 532 532 C
450    967 533 533 C
451    968 534 534 C
452    969 535 535 C
453    970 536 536 C
454    971 537 537 C
455    972 538 538 C
456    973 539 539 C
457    974 540 540 C
458    975 541 541 C
459    976 542 542 C
460    977 543 543 C
461    978 544 544 C
462    979 545 545 C
463    980 546 546 C
464    981 547 547 C
465    982 548 548 C
466    983 549 549 C
467    984 550 550 C
468    985 551 551 C
469    986 552 552 C
470    987 553 553 C
471    988 554 554 C
472    989 555 555 C
473    990 556 556 C
474    991 557 557 C
475    992 558 558 C
476    993 559 559 C
477    994 560 560 C
478    995 561 561 C
479    996 562 562 C
480    997 563 563 C
481    998 564 564 C
482    999 565 565 C
483    999 566 566 C
484    999 567 567 C
485    999 568 568 C
486    999 569 569 C
487    999 570 570 C
488    999 571 571 C
489    999 572 572 C
490    999 573 573 C
491    999 574 574 C
492    999 575 575 C
493    999 576 576 C
494    999 577 577 C
495    999 578 578 C
496    999 579 579 C
497    999 580 580 C
498    999 581 581 C
499    999 582 582 C
500    999 583 583 C
501    999 584 584 C
502    999 585 585 C
503    999 586 586 C
504    999 587 587 C
505    999 588 588 C
506    999 589 589 C
507    999 590 590 C
508    999 591 591 C
509    999 592 592 C
510    999 593 593 C
511    999 594 594 C
512    999 595 595 C
513    999 596 596 C
514    999 597 597 C
515    999 598 598 C
516    999 599 599 C
517    999 600 600 C
518    999 601 601 C
519    999 602 602 C
520    999 603 603 C
521    999 604 604 C
522    999 605 605 C
523    999 606 606 C
524    999 607 607 C
525    999 608 608 C
526    999 609 609 C
527    999 610 610 C
528    999 611 611 C
529    999 612 612 C
530    999 613 613 C
531    999 614 614 C
532    999 615 615 C
533    999 616 616 C
534    999 617 617 C
535    999 618 618 C
536    999 619 619 C
537    999 620 620 C
538    999 621 621 C
539    999 622 622 C
540    999 623 623 C
541    999 624 624 C
542    999 625 625 C
543    999 626 626 C
544    999 627 627 C
545    999 628 628 C
546    999 629 629 C
547    999 630 630 C
548    999 631 631 C
549    999 632 632 C
550    999 633 633 C
551    999 634 634 C
552    999 635 635 C
553    999 636 636 C
554    999 637 637 C
555    999 638 638 C
556    999 639 639 C
557    999 640 640 C
558    999 641 641 C
559    999 642 642 C
560    999 643 643 C
561    999 644 644 C
562    999 645 645 C
563    999 646 646 C
564    999 647 647 C
565    999 648 648 C
566    999 649 649 C
567    999 650 650 C
568    999 651 651 C
569    999 652 652 C
570    999 653 653 C
571    999 654 654 C
572    999 655 655 C
573    999 656 656 C
574    999 657 657 C
575    999 658 658 C
576    999 659 659 C
577    999 660 660 C
578    999 661 661 C
579    999 662 662 C
580    999 663 663 C
581    999 664 664 C
582    999 665 665 C
583    999 666 666 C
584    999 667 667 C
585    999 668 668 C
586    999 669 669 C
587    999 670 670 C
588    999 671 671 C
589    999 672 672 C
590    999 673 673 C
591    999 674 674 C
592    999 675 675 C
593    999 676 676 C
594    999 677 677 C
595    999 678 678 C
596    999 679 679 C
597    999 680 680 C
598    999 681 681 C
599    999 682 682 C
510    999 683 683 C
511    999 684 684 C
512    999 685 685 C
513    999 686 686 C
514    999 687 687 C
515    999 688 688 C
516    999 689 689 C
517    999 690 690 C
518    999 691 691 C
519    999 692 692 C
520    999 693 693 C
521    999 694 694 C
522    999 695 695 C
523    999 696 696 C
524    999 697 697 C
525    999 698 698 C
526    999 699 699 C
527    999 700 700 C
528    999 701 701 C
529    999 702 702 C
530    999 703 703 C
531    999 704 704 C
532    999 705 705 C
533    999 706 706 C
534    999 707 707 C
535    999 708 708 C
536    999 709 709 C
537    999 710 710 C
538    999 711 711 C
539    999 712 712 C
540    999 713 713 C
541    999 714 714 C
542    999 715 715 C
543    999 716 716 C
544    9
```

iii) the following five quantities are calculated for each range and stored temporarily on a data file.

MINFO, MAXFO, and MEANFO, the minimum, maximum and mean $|F_O|$ in the range.

R, the discrepancy index $\sum |\Delta| / \sum |F_O|$ for the range.

MDLSQ, the ratio $\langle \Delta^2 \rangle_i / \langle \Delta^2 \rangle_1$

iv) the quantities MEANFO and MDLSQ are used to set up the matrix of normal equations and the system is solved for A/k, B/k, C/k, and D/k. SOLTN is a subroutine for solving matrix equations.

v) using these values for A, B, C, and D, the constant ERROR is evaluated and each of the four weighting scheme parameters is multiplied by this value. Using these corrected values of A, B, C, and D, a table of MINFO, MAXFO, R, MEANFO, WTDR, MWDLSQ, ERROR, and NUM(J) is compiled and printed for each range.

$$WTDR = \{ \sum w\Delta^2 / \sum wF_O^2 \}^{1/2}$$

$$MWDLSQ = \langle w\Delta^2 \rangle$$

NUM(J) = number of reflections in the Jth range.

vi) w and σ^2 are calculated and printed as a function of F_O in steps of FIN1 from FIN1 to FLIM and in steps of FIN2 from FLIM to FMAX where FIN1, FLIM, FIN2, and FMAX are input to the program from cards. Sometimes because of bad fit, the values of σ^2 are negative and should be adjusted by small changes to the weighting parameters before being used in structure refinement.

B. PROGRAM "ORTEP"

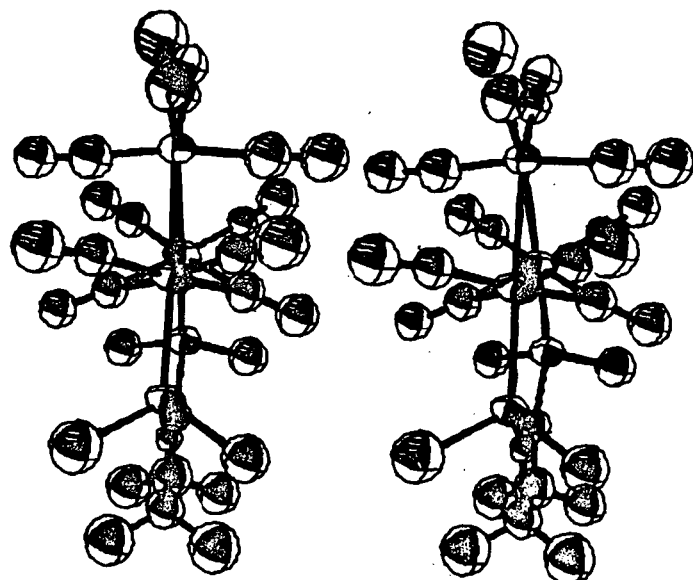
During the course of the work for this thesis, the Oak Ridge National Laboratory thermal ellipsoid plot program, ORTEP,⁵⁹ was made compatible with our existing programs and implemented on the IBM 360/67 by the author.

Stereo views of the four structures in this thesis are given in Figure VII.1 as plotted by ORTEP. Atoms are represented by 50% probability ellipsoids of thermal vibration.

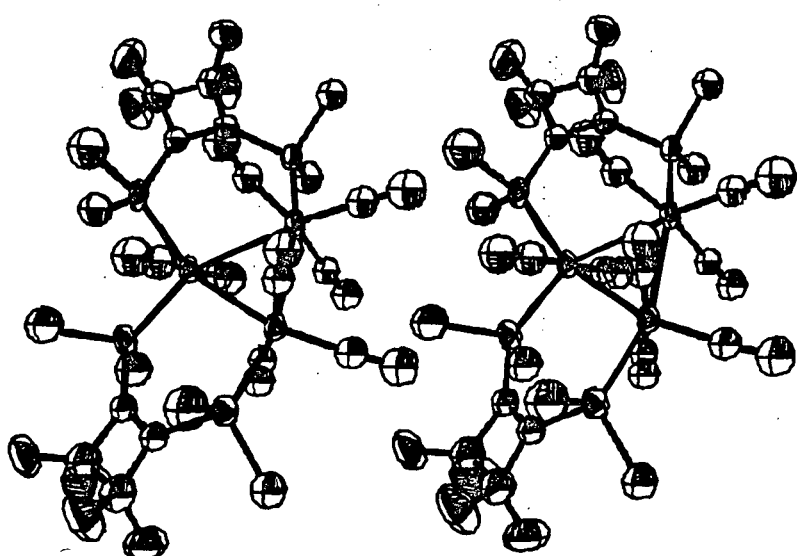
Figure VII.1

Stereo views of

- (a) $LFe_3(CO)_{10}$ (c) $LRu_3(CO)_{10}$
(b) $L_2Ru_3(CO)_8$ (d) $L'Mo(CO)_4$

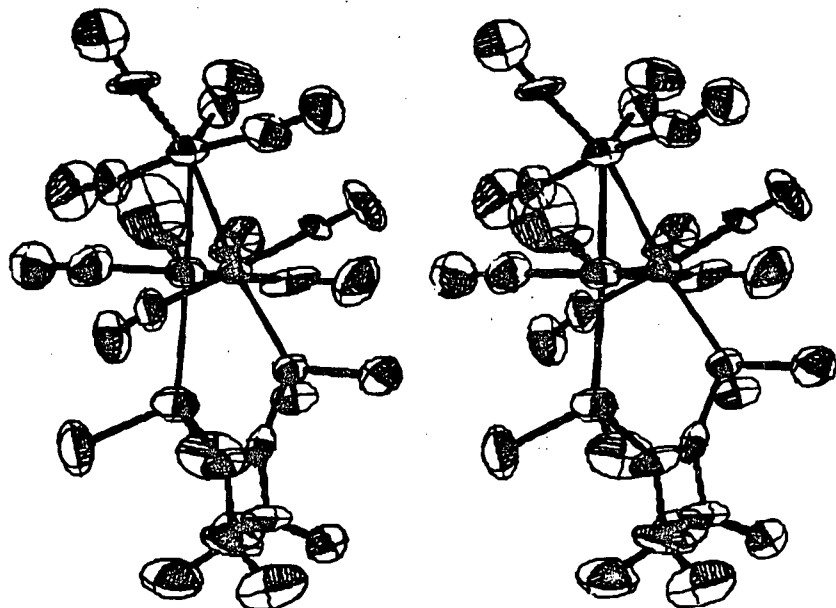


(a)

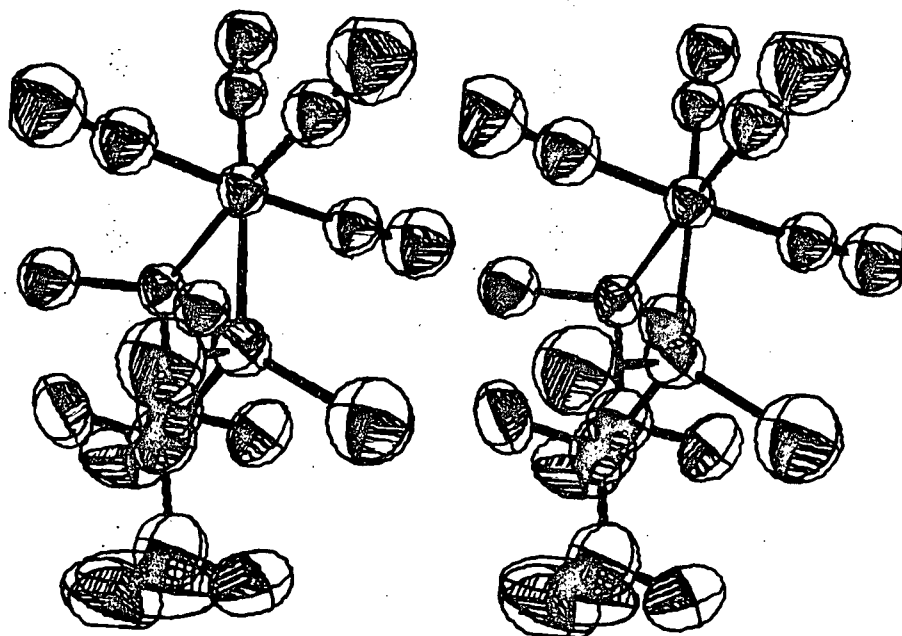


(b)

Figure VII.1 (continued)



(c)



(d)

VIII. REFERENCES

1. A. L. Patterson, Z. Krist., 1935, A90, 517.
2. A. J. C. Wilson, Nature, 1942, 150, 152.
3. D. Sayre, Acta Cryst., 1952, 5, 60.
4. J. Karle and H. Hauptmann, Acta Cryst., 1950, 3, 181.
5. E. W. Abel, Quart. Rev., 1963, 17, 133.
6. E. W. Abel and F. G. A. Stone, Quart. Rev., 1969, 23, 325.
7. J. W. Richardson, in "Organometallic Chemistry", H. Zeiss ed., Reinhold, 1960, p.1.
8. J. Chatt, P. L. Pauson, and L. M. Venanzi, *ibid.*, p. 468.
9. F. Calderazzo, R. Ercoli, and G. Natta, in "Organic Syntheses via Metal Carbonyls", I. Wender and P. Pino eds., Interscience, 1968, p. 1.
10. B. R. Penfold, in "Perspectives in Structural Chemistry", J. D. Dunitz and J. A. Ibers eds., Wiley, 1968, 2, 71.
11. L. M. Bower and M. H. B. Siddard, Inorg. Chim. Acta, 1967, 1, 231.
12. G. R. Dobson, I. W. Stoltz, and R. K. Sheline, Advan. Inorg. Chem. Radiochem., 1966, 8, 1.
13. G. Booth, *ibid.*, 1964, 6, 1.
14. T. A. Manuel, Advan. Organometallic Chem., 1965, 3, 181.
15. N. V. Sidgwick and R. W. Bailey, Proc. Roy. Soc., 1934, 144, 521.
16. F. A. Cotton and R. M. Wing, Inorg. Chem., 1965, 4, 314.
17. W. R. Cullen, D. A. Harbourne, B. V. Liengme, and J. R. Sams, J. Amer. Chem. Soc., 1968, 90, 3293.
18. C. H. Wei and L. F. Dahl, J. Amer. Chem. Soc., 1966, 88

- 1821; 1969, 91, 1351.
19. F. W. B. Einstein and J. Trotter, J. Chem. Soc. (A), 1967, 824.
 20. W. R. Cullen and D. A. Harbourne, Inorg. Chem., 1970, 9, 1839.
 21. W. R. Cullen, D. A. Harbourne, B. V. Liengme, and J. R. Sams, Inorg. Chem., 1969, 8, 1469.
 22. J. E. H. Ward and W. R. Cullen, unpublished results.
 23. S. H. Whitlow, Ph. D. Thesis, University of British Columbia, 1969.
 24. a) R. Hoge, Ph. D. Thesis, University of British Columbia, 1969.
b) R. Hoge and J. Trotter, J. Chem. Soc. (A), 1969, 2165.
 25. M.M. Woolfson, "Direct Methods in Crystallography", Clarendon Press, 1961, (a) pp. 101-106, (b) pp 94-100.
 26. "International Tables for X-ray Crystallography", Kynoch Press, 1962, vol. III.
 27. D. J. Dahm and R. A. Jacobson, J. Amer. Chem. Soc., 1968, 90, 5106.
 28. W. S. McDonald *et. al.*, Chem. Comm., 1969, 1295.
 29. E. H. Braye *et. al.*, J. Amer. Chem. Soc., 1962, 84, 4633.
 30. J. F. Blount *et. al.*, J. Amer. Chem. Soc., 1966, 88, 292.
 31. S. F. A. Kettle, Inorg. Chem., 1965, 4, 1661.
 32. J. P. Crow *et. al.*, in press, J. Amer. Chem. Soc., 1970.
 33. B. M. Gatehouse, Chem. Comm., 1969, 948.
 34. R. E. Long, Ph. D. Thesis, University of California, Los Angeles, 1965.

35. R. Mason and A. I. M. Rae, J. Chem. Soc. (A), 1968, 778.
36. R. Mason and W. R. Robinson, *ibid.*, 1968, 468.
37. F. A. Cotton and W. T. Edwards, J. Amer. Chem. Soc., 1968, 90, 5412.
38. F. A. Cotton, A. Davison and A. Musco, *ibid.*, 1967, 89, 6796.
39. M. J. Bennett, F. A. Cotton and P. Legzdins, *ibid.*, 1967, 89, 6797.
40. M. J. Bennett, F. A. Cotton and P. Legzdins, *ibid.*, 1968, 90, 6335.
41. R. H. B. Mais and H. M. Powell, J. Chem. Soc., 1965, 7471.
42. L. F. Dahl and D. L. Wampler, Acta Cryst., 1962, 15, 946.
43. F. A. Cotton and R. Eiss, J. Amer. Chem. Soc., 1969, 91, 6593.
44. W. Rudorff and U. Hofmann, Z. Physik. Chem. (B), 1935, 28, 351.
45. L. D. Brockway, R. V. G. Ewens and M. W. Lister, Trans. Faraday Soc., 1938, 34, 1350.
46. M. J. Bennett and R. Mason, Proc. Chem. Soc., 1963, 273.
47. M. R. Churchill and J. P. Fennessey, Inorg. Chem., 1967, 6, 1213.
48. P. Bird and M. R. Churchill, Chem. Comm., 1967, 705.
49. F. C. Wilson and D. P. Shoemaker, J. Chem. Phys., 1957, 27, 809.
50. R. J. Doedens and L. F. Dahl, J. Amer. Chem. Soc., 1965, 87, 2576.

51. M. R. Churchill and P. Bird, Chem. Comm., 1967, 746.
52. J. S. McKechnie and I. C. Paul, Chem. Comm., 1967, 747.
53. K. N. Raymond, P. W. R. Corfield, J. A. Ibers, Inorg. Chem., 1968, 7, 842.
54. "Tables of Interatomic Distances and Configuration in Molecules and Ions", Chem. Soc. Special Publ. Nos. 11 and 18, 1958 and 1965.
55. F. W. B. Einstein, H. Luth, and J. Trotter, J. Chem. Soc., 1967, 89.
56. F. A. Cotton and J. A. McCleverty, J. Organometallic Chem., 1965, 4, 490.
57. W. R. Cullen, L. D. Hall, and J. E. H. Ward, Chem. Comm., 1970, 625.
58. a) D. W. J. Cruickshank *et. al.*, in "Computing Methods and the Phase Problem in X-ray Crystallography", R. Pepinsky, J. M. Robertson, and J. C. Speakman eds., Pergamon, 1961, p. 45.
b) D. W. J. Cruickshank in "Computing Methods in Crystallography", J. S. Rollett ed., Pergamon, 1965, p. 114.
59. C. K. Johnson, ORTEP, ORNL-3794, Oak Ridge National Laboratory, Oak Ridge, Tennessee, U. S. A.